

Macrodispersion and Concentration Fluctuations in Three-Dimensionally Heterogeneous Aquifers

by

VIVEK KAPOOR

B. E. Civil Engineering
Delhi College of Engineering, 1987

M. S. Civil Engineering
University of Mississippi, 1989

Submitted to the
Department of Civil and Environmental Engineering
in partial fulfillment of the
requirements for the degree of

DOCTOR OF SCIENCE

at the

MASSACHUSETTS INSTITUTE OF TECHNOLOGY

© Massachusetts Institute of Technology, 1993
All rights reserved

Signature of Author.....
Department of Civil and Environmental Engineering
September 1993

Certified by.....
Lynn W. Gelhar
Professor of Civil and Environmental Engineering
Thesis Supervisor

Accepted by.....
Eduardo Kausel
Chairman, Departmental Committee on Graduate Studies

MASSACHUSETTS INSTITUTE
OF TECHNOLOGY

1

OCT 14 1993

ARCHIVED

LIBRARIES

MACRODISPERSION AND CONCENTRATION FLUCTUATIONS IN THREE-DIMENSIONALLY HETEROGENEOUS AQUIFERS

by

VIVEK KAPOOR

Submitted to the Department of Civil and Environmental Engineering
at the Massachusetts Institute of Technology

September 1993

in partial fulfillment of the requirements for the degree of
Doctor of Science

ABSTRACT

The spatial second moments of a plume in a heterogeneous aquifer do not quantify contaminant concentrations, as evident from the insensitivity of the longitudinal spatial second moment to the exclusion of local dispersion. The mean squared concentration fluctuations, *i.e.*, concentration variance, determines the extent to which the observed and theorized enhanced rates of growth of spatial second moments are accompanied by a commensurate drop of point contaminant concentrations. The product of the macrodispersion coefficient and the squared gradient of the mean concentration field determines the rate of production of concentration variance. Its dissipation rate is determined by the product of the local dispersion coefficient and the mean squared derivatives of the concentration perturbation. The fluctuation dissipation due to local dispersion is represented as a first order decay with the decay coefficient equal to twice the local dispersion coefficient divided by the squared concentration microscale. For an advection dominated hydraulic conductivity microscale, the concentration microscale is an increasing function of the conductivity microscale, consequently, the larger the conductivity microscale, the slower is the dissipating action of local dispersion, and vice versa. A relative increase in the high wave number component of the hydraulic conductivity fluctuations enhances the dissipating action of local dispersion and a relative increase in the low wave number component inhibits the rate of destruction of fluctuations. The dominant transport mechanism for the concentration variance field is a correlation between squared concentration perturbations and velocity perturbations. The square root of the concentration variance divided by its mean, increases with time initially. Due to the dissipating action of local dispersion this fluctuation measure decreases with time at large times. The Cape Cod bromide tracer exhibited this predicted decrease in the relative magnitude of fluctuations with time. For the hypothetical zero local dispersion case, this fluctuation measure grows unboundedly with time. To determine the efficacy of the dissipating action of local dispersion on concentration variance, the hydraulic conductivity field microscale needs to be measured.

The correlation coefficient between a correlated stochastic process and its integral over a time period, is proven to decrease with the time period, asymptotically to a value of zero. This is a rationale for Corrsin's conjecture of independence between a particle's velocity and position, in a correlated velocity field. The conjecture yields a nonlinear formulation for the macrodispersivities, which is solved for the isotropic case. The longitudinal macrodispersivity remains unchanged from the linear theory. The transverse macrodispersivity shows a correlation scale dependence.

Thesis Supervisor: Dr. Lynn W. Gelhar

Title: Professor of Civil and Environmental Engineering

ACKNOWLEDGMENTS

Support of the National Science Foundation, grant CES-8814615, is gratefully acknowledged. Ippen travel fellowship provided the valuable opportunity to attend the 1992 Fall meeting of AGU.

Lynn W. Gelhar's critical observations contributed to the unraveling of the mystery of mean squared concentration fluctuations in three dimensionally heterogeneous aquifers. Dennis McLaughlin generously shared with me his experience in dealing with concentration fluctuations. E. Eric Adams's insight on advection-diffusion phenomenon helped clarify some of the findings.

Sudeshna's companionship during this work was a source of joy.

TABLE OF CONTENTS

Abstract	2
Acknowledgments	3
Table of Contents	4
List of Figures	7
1. Local Dispersion, Macrodispersion, and the Prediction of Contaminant Exposure Levels	9
2. Advection-Diffusion in Three Dimensionally Heterogeneous Aquifers: Dynamics of Concentration Variance	16
2.1 Introduction	17
2.2 Concentration Variance Conservation Equation	21
2.3 Macrodispersive Flux of Concentration Variance	28
2.3.1 Zero local dispersion case	28
2.4 Destruction of Concentration Variance by Local Dispersion	34
2.4.1 Variance Sink Term	34
2.4.2 Variance Decay Coefficient	38
2.4.3 Concentration Microscale	39
2.5 Conclusions	46
3. Advection-Diffusion in Three Dimensionally Heterogeneous Aquifers: Concentration Variance for a Finite Impulse Input	50
3.1 Introduction	51
3.2 Concentration Variance for a Multidimensional Finite-Size Impulse Input in Three-Dimensionally Heterogeneous Aquifers (Incorporating Fluctuation Dissipating Action of Local Dispersion)	53
3.2.1 Solution	54
3.2.2 Spatial-Temporal Characteristics of Concentration Fluctuations	61
3.3 Hypothetical, Hyperbolic, Non-Dissipative, Zero Local Dispersion Case	71
3.3.1 Solution	71
3.3.2 Exploding Hyperbolic Plumes	73
3.4 Concentration Fluctuations in the Bromide Tracer at Cape Cod, MA	75

3.4.1 Theoretical Predictions of Coefficient of Variation	77
3.4.2 Estimation of Coefficient of Variation From Bromide Sampling Data	80
3.4.3 Comparison of Theory and Observations	82
3.5 Summary and Discussion	88
4. The Hydraulic Conductivity Microscale	95
4.1 Introduction	95
4.2 The Microscale	97
4.2.1 Estimation of the Microscale	100
4.3 Limitation of Darcy's 'law' in Computing Velocity Strain Rates	106
4.3.1 The Darcy-Brinkman 'law'	109
4.3.2 Examples	109
4.3.3 Velocity Spectrum with Brinkman Smoothing	116
4.4 Conclusions	117
5. Nonlinear Computation of Macrodispersivities in Three Dimensionally Heterogeneous Aquifers via Corrsin's Conjecture	119
5.1 Theorem	120
5.1.1 Examples	123
5.2 Mean Squared Displacement of a Particle in a Correlated Velocity Field	127
5.3 Computation of Lagrangian Velocity Statistics From Eulerian Velocity Statistics	128
5.3.1 Corrsin's [1962] Conjecture	129
5.3.2 Large Displacement Condition on the Applicability of Corrsin's Conjecture	130
5.3.3 Nonlinear Formulation for Macrodispersivities using Corrsin's Conjecture	130
5.4 Nonlinear Computation of Macrodispersivities	132
5.4.1 Isotropic Case	132
5.4.2 Anisotropic Case	136
6. Summary of Findings	139

References	147
Appendix-I On the High Wave Number Sensitivity of Fluctuation Dissipation Phenomenon	152
Appendix-II Transport in Heterogeneous Aquifers: On the Critical Role of Local Dispersion	154
Appendix-III Cross-Sectional Concentration Profile in Rectilinear Ducts: A Variational Characteristic of G. I. Taylor's Solution	168
Appendix-IV Stochastic Description of the Heterogeneous Hydraulic Conductivity and Velocity Continuum	175
Appendix-V Characteristic Vorticity of the Flow Field	190
Appendix-VI Macrodispersivity Integrals for Statistically Isotropic Media with Anisotropic Local Dispersivities	192

LIST OF FIGURES

2.1	Are the concentration fluctuations a large multiple of the mean, or, a small fraction of it?	20
3.1	Standard deviation of concentration.	66
3.2	Coefficient of variation of concentration.	67
3.3	Breakthrough coefficient of variation of concentration.	68
3.4	Coefficient of variation at the center of mass: Comparison of large time analytical solution with numerical integration of time integral (3.17) for a ratio of $\ln K$ microscale to correlation scale of 0.4.	79
3.5	Sensitivity of the coefficient of variation to Δ/λ , the ratio of $\ln k$ microscale to correlation scale.	81
3.6	Estimated coefficient of variation for the bromide tracer at Cape Cod, MA.	83
3.7	Comparison of estimated coefficient of variation with theoretical predictions.	84
3.8	Peak sampled bromide concentrations at Cape Cod, MA.	86
4.1	$\ln k$ measurements by Ringrose and Pickup [1993].	
4.2	Upward convexity of $\ln k$ correlation function at the origin.	104
4.3	Root mean square estimation error.	105
4.4	Bakr's [1976] spectral analysis.	107
4.5	Shear in sinusoidally varying permeability: Importance of the Brinkman term at small wavelengths.	112
4.6	Discharge through a column of porous media.	115
5.1	Correlation coefficient between position and velocity: Example 1.	124

5.2	Correlation coefficient between position and velocity:	
	Example 2.	126
5.3	Nonlinear computation of longitudinal macrodispersivity in isotropic medium.	134
5.4	Nonlinear computation of transverse macrodispersivity in isotropic medium.	135
A-II.1	Bounded aquifer.	157
A-II.2	High wave number sensitivity of fluctuation dissipation function.	166
A-III.1.	Unidirectional flow in a rectilinear duct.	169
A-III.2	Minimum dissipation cross-sectional concentration profile.	173
A-IV.1a,b	Distribution of spectral energy over nondimensional wave number.	178
A-IV.2	Ratio of the $\ln K$ microscale and correlation scale.	181
A-IV.3a,b,c	Standard deviation of the velocity field.	184
A-IV.4a,b,c	Characteristic principal strain rate of velocity field.	187
A-VI.1	Longitudinal macrodispersivity.	196
A-VI.2	Transverse macrodispersivity.	197

CHAPTER 1

LOCAL DISPERSION, MACRODISPERSION, AND THE PREDICTION OF CONTAMINANT EXPOSURE LEVELS

Solute, in a homogeneous laboratory sand column with a hydraulic gradient across it, undergoes an advective flux and a local dispersive flux. The local dispersive flux manifests itself as the smearing of the breakthrough concentration at the end of the column. The breakthrough is a cross section averaged concentration, therefore averaged over a large number of pores. The breakthrough exhibits a diminished peak concentration and an enhanced spatial second moment, compared to what would be if there were no local dispersive flux. The mechanism of the local dispersive flux is that the sub-continuum (*i.e.*, pore scale) variations of advective velocities of the solute particles tends to flatten out continuum scale solute concentration gradients. In referring to pore scale variations as sub-continuum, it is being acknowledged that practical measurements involve averaging over a large number of pore scales, and typically there is no easy way of knowing or modeling the pore-scale velocity distribution, let alone modeling transport incorporating these variations. This description of transport in a sand column is quite unambiguously borne out in laboratory experiments. Breakthroughs are relatively smooth curves with small noise. Peak concentrations are found to be inversely proportional to breakthrough radii of gyration. Therefore by measuring a local dispersion coefficient one can model transport, by delineating boundary conditions and even porous material heterogeneities. In such a modeling effort one can expect to reproduce detailed solute distributions and peak concentrations quite well. The term *local dispersion* is used as a synonym for *diffusion*, as it embodies the effect of the Laplacian term in the advection-diffusion equation.

That advective heterogeneities can create larger spatial second moments of a solute distribution, than what would result by the local diffusive flux alone, excluding advective heterogeneities, is well known [Taylor, 1921 and 1953; Richardson, 1926; *etc.*]. For example, in Taylor's [1953] work on solute transport in a capillary tube, the cross section averaged concentration can be shown to be governed by an advection-dispersion equation with a large longitudinal dispersion coefficient, which is a popular engineering formula. The actual concentration distribution (a fourth order polynomial in Taylor's [1953] approximations) is certainly not constant over the cross section (see Appendix-III). As the longitudinal mean concentration gradients weaken, at time scales larger than the squared tube diameter divided by the transverse diffusion coefficient, the variation of the actual concentration distribution over the cross section tends to weaken. What if the diameter of the capillary tube was of the order of meters, and the measurement scale is less than a centimeter, over which the velocity does not vary much? Firstly, there is little use of knowing a cross section averaged concentration if scales pertinent to sampling and exposure are small. Secondly, the time scale governing the cross-sectional homogenization would become large. The peak point concentration at any cross-section will of course be larger than the cross-section averaged concentration. If the scale of the advective heterogeneities that are giving rise to large 'effective dispersion coefficients' is large, and exposure to solute does not involve large scale spatial averaging, one has to be concerned about concentration deviations around the cross-sectional mean, about which, nothing can be said by the effective dispersion formulae alone.

Each time a large effective dispersion coefficient is computed and recommended as an input to a numerical transport modeling code, it needs to be kept in mind that it implies a smaller peak (mean) concentration. Effective media modeling using large effective dispersion coefficients is certainly an attractive proposition because it seems to take away the need to delineate advective heterogeneities and model the detailed

advective diffusive transport. However, even for modeling the 'mean concentration' that is misleading. The effective dispersion coefficients can only be computed after delineating the advective heterogeneity ('deterministically' or 'stochastically'). Numerical modelers affinity for large dispersion coefficients is easily explained by the numerical grid Peclet number. Theoreticians have performed computations of 'effective dispersion coefficients', 'mean squared displacement of a particle (or two)' in more ways than one. In light of this convergence of interests, and the implied enhanced *dilution* by using a large dispersion coefficient, it can not be over stressed that *a priori*, nothing can be said about contamination exposure levels at a point, after knowing some ensemble averaged value (other than that the contamination exposure level will be less than or equal to the injection concentration and greater than or equal to zero). The viability of using effective dispersivities to 'model transport' in heterogeneous velocity fields can be judged only after estimating how poor the 'average concentration' or 'plume volume' is going to be in predicting the levels of contaminant exposure. The current practice is to merely assert that the "spatial second moments determines dilution". In principle, effective dispersivities (if they exist) can be experimentally found from field tracer tests. The effort involved in characterizing the advective heterogeneities to enable a reliable computation of a dispersivity has not been shown to be less than the effort in fitting one to a tracer test. The characterization of the advective heterogeneities to compute effective dispersion coefficients or spatial second moments of plumes, also creates the opportunity to understand and describe concentration fluctuations, that will give information about the nature of solute concentration distribution not contained in the mere bulk dimensions of a plume.

An approach to understanding transport processes in a heterogeneous aquifer is to consider it to be a sample realization of a three dimensional stochastic process, which is described by its spectrum or covariance function, unto second moments. The work of Bakr [1976], Bakr *et al.* [1978] and Gutjahr *et al.* [1978] produced a valuable

understanding of fluid flow phenomenon in (heterogeneous) aquifers in the form of a flow spectrum (see Appendix-IV). An ensemble of hydraulic conductivity and flow field realizations, related by Darcy's law (approximately) at each point, with the flow field obeying conservation of fluid mass (as the spectrum of the divergence is identically zero) is embodied in the spectral description. This remarkable description of the flow field set the stage for understanding the effects of hydraulic conductivity variations on contaminant transport. Gelhar and Axness [1983] computed the ensemble averaged concentration under the explicit assumptions of a scale disparity between the mean concentration field and the hydraulic conductivity field, and weak temporal gradients of the mean concentration field. It is under these two conditions that the ensemble averaged concentration may be governed by an effective advection dispersion equation with a constant macrodispersivity. These conditions impose a relaxation time, beyond which an effective dispersion-advection equation can be expected to model the mean concentration field. An explicitly time dependent macrodispersivity is sometimes computed to relax these assumptions. However it creates additional ambiguities; What is the significance of time = 0? Is it the time the solute was introduced? If so, what if we start with the solute initial conditions that result after N days of transport with different initial conditions? With explicitly time dependent dispersivities we would have the situation that if we started a simulation, stopped it, and started it again, it would yield an answer different than if we performed the simulation for the same cumulative time. An explicitly (injection) time dependent dispersivity violates the *belief* that constitutive equations should be independent of the frame of reference. The notion of a dispersivity depending on the mean concentration profiles can however be understood without violating this "principle of material frame indifference", and applied in an advection dispersion equation. Of course, as the mean concentration varies with time, the resulting macrodispersivity will be a function of time, however no matter what the 'time' is, for a particular mean concentration distribution, a unique macrodispersivity (field) can be

specified. This is not to say that the rate of change of the mean squared deviation of a particle (as computed by Taylor [1921]; Dagan [1984]) or that of the spatial second moment of a plume in a heterogeneous velocity field cannot be time dependent. However, the interpretation of that rate of change as implying a time-varying dispersion coefficient, to be plugged in an effective constitutive equation is not without ambiguities. The effect of the limitation on low frequency variations sampled due to a finite plume scale, described by Richardson [1926], and recently for the case of three dimensionally anisotropic heterogeneous aquifers by Rajaram [1991], is valuable in interpreting the developing dispersion problem, as the dispersive flux is related to a plume scale, and the meandering of the plume center of mass is separated from the growth of its dimensions around its center of mass. However, the law of large numbers tells us when a plume volume is much larger than the hydraulic conductivity correlation volume, the meandering of its center of mass cannot be significant. Of course one can entertain larger and larger correlation scales and add on more low wave number energy to our description of logarithm of hydraulic conductivity ($\ln K$) to claim that such a meandering effect is ever important. However in these circumstances one can expect no spatially-temporally local formulation of transport to describe the mean concentration field. Recently, Adams and Gelhar [1992] have shown the importance of explicitly recognizing large scale features and its implications for the plume moments. A spatially and temporally non-local model of transport for the mean concentration, as analyzed by Graham and McLaughlin [1989], provides a description of the ensemble averaged concentration even when the plume scale and the correlation scale overlap and the concentration temporal gradients may be significant.

The current work on transport in saturated heterogeneous aquifers constitutes of incremental theories that are increasingly ornate in their formulation of the spatial second moment of plumes. One such theory is also presented in Chapter 5. In contrast, little has been done to understand the usefulness of knowing the ensemble mean concentration or

the spatial second moment of the plume. There is another trend to include increasingly large scale features into the low wave number part of the hydraulic conductivity spectrum and compute a larger macrodispersivity. Neuman [1990] fit 'universal' *regression* lines to *empirical* log-'apparent longitudinal dispersivity' versus log-'apparent length scale' data. Of course, larger the dispersivity employed in an effective advection dispersion equation, smaller is the peak mean concentration. Is this peak mean concentration a good predictor of the sample peak concentration? Are these enhanced rates of attenuation of contaminant concentrations implied by these large dispersivities real? Is there some trade off to including large scale features into the random process and computing yet a larger dispersivity (one particle or two particle) that implies a smaller peak concentrations?

Consider a plume large enough so that the scale disparity assumptions of Gelhar and Axness [1983], apply over a range of correlation scales. And also consider the measurement scale always much smaller than the correlation scale. Is the smoothing effect of local dispersion going to be the same over the range of correlation scales? How large are the concentration fluctuations? How do they depend on the $\ln K$ description? How large a fraction of the mean concentration are the concentration fluctuations? Are the fluctuations increasing relative to the mean, or are they decreasing fraction of the mean, with time? The conditions most suited for the mean concentration theory in predicting the mean concentration are taken to apply. It is then asked how do concentrations in a sample plume vary around this mean. Chapters 2 and 3 are on the formulation and approximate analytical solution to the problem of mean squared concentration fluctuations, *i.e.*, concentration variance. In the literature, the word (plume) variance is sometimes used while referring to the spatial second moment or squared radius of gyration of the plume. In this work the word concentration variance refers to the ensemble average of squared concentration perturbations.

Chapter 4 is on the high wave number characteristics of the hydraulic conductivity field and an assessment of the applicability of Darcy's law in describing the

details of the velocity field in heterogeneous medium. In Chapter 5 a rationale is provided for Corrsin's [1962] conjecture of statistical independence between the position and velocity of a particle being transported in correlated velocity field. Applying the conjecture in computing Lagrangian velocity statistics from Eulerian ones and a nonlinear computation of macrodispersivities is presented. In Chapter 6 the findings of this work are enumerated.

The first three Appendices present aspects of fluctuation dissipation mechanism in simpler settings (than three dimensionally stochastic hydraulic conductivity fields). Appendix-I and II demonstrate the singularly important role of the interaction of local dispersion and the high wave number component of the $\ln K$ fluctuations in determining concentration levels in heterogeneous aquifers. Appendix-III reports a variational characteristic of Taylor's [1953] solution for the cross-sectional concentration profile in a tube. Appendix-IV and V describe the flow field in a heterogeneous aquifer. Appendix VI presents evaluations of macrodispersivity integrals.

Analytical studies in the groundwater literature, critically influencing this work, or, pertinent to the following analytical developments, are cited. A few numerical studies that can be related to the key conclusions made here are cited. The applied mathematics and fluid mechanics literature that has influenced this work due to similarities with various aspects of this work are also cited. That this work is not an exhaustive review of groundwater flow and transport literature is also reflected in the citations.

A note on the organization of the thesis. After each chapter and appendix title is presented a synopsis of the results developed therein. Reading these synopsis and the summary of findings in Chapter 6 constitutes a quick overview of this work. Chapter 2 and 3 are a pair and may be read in that order. Chapter 4 and 5 may be read independently. Appendices I-II- III constitute a simple introduction to the key ideas on fluctuation dissipation pursued in Chapter 2.

CHAPTER 2

ADVECTION-DIFFUSION IN THREE-DIMENSIONALLY HETEROGENEOUS AQUIFERS: DYNAMICS OF CONCENTRATION VARIANCE

The concentration variance, *i.e.*, mean squared concentration fluctuations, undergoes mean advection, a local dispersive flux, and a macrodispersive flux due to a correlation between squared concentration perturbations and velocity perturbations. The products of the macrodispersion coefficient and the squared gradient of the mean concentration field determine the rate of production of concentration variance. The rate of dissipation of concentration variance is determined by the products of the local dispersion coefficient and the mean squared gradient of the concentration perturbation field. Variance dissipation is represented as a first-order decay with the decay coefficient equal to twice the sum of the local dispersion coefficient divided by the squared concentration microscale. The concentration microscale, estimated for an advection dominated log-hydraulic conductivity microscale, is an increasing function of the log-conductivity microscale. Thus, the larger the log-conductivity microscale is, the slower is the rate of dissipation of concentration fluctuations by local dispersion and vice-versa. The wave number squared dependence of fluctuation dissipation is a fundamental property of advection-diffusion phenomenon. Hence, intensive sampling will be required to realistically model the log-conductivity spectrum and determine its microscale, which determines the rate of dissipation of concentration fluctuations by the action of local dispersion. There is no mechanism of destroying concentration fluctuations without the action of local dispersion.

2.1 INTRODUCTION

The spatially varying velocity field, resulting when a saturated porous medium with a spatially varying hydraulic conductivity is subjected to a hydraulic head difference, creates rates of growth of the spatial second moments of plumes that are greater than what would occur by local dispersion alone in the uniform mean velocity field. Theoretical studies [e.g., Gelhar and Axness, 1983; Dagan, 1984; Winter *et al.*, 1984; Gelhar, 1987] have related this enhanced rate of growth of spatial second moments to the characteristics of the velocity field and thus to the hydraulic conductivity field properties. An effective advection dispersion equation containing an effective dispersion coefficient is used to model the ensemble averaged concentration field. The rate of growth of the spatial second moments of the ensemble averaged concentration field is determined by the effective dispersion coefficient. This requires that there be a scale disparity between the smoothly varying mean concentration field and the rapidly varying hydraulic conductivity. Depending on the heterogeneity encountered, the spatial second moment will show fluctuations around the growing mean [Smith and Schwartz, 1980; Frind *et al.*, 1987; Tompson and Gelhar, 1990]. Rajaram [1991] has shown that the fluctuations in the spatial second moment, as a fraction of its mean value, die out in time. The ensemble averaged equation applies under conditions of sufficient smoothness of the mean concentration field, insofar as it predicts the field-scale spatial second moments of plumes.

However, *a priori*, the spatial second moment of a contaminant plume, in a heterogeneous hydraulic conductivity field, contains precious little information about the actual distribution of solute in space. Indeed the results on longitudinal macrodispersivities are insensitive to the exclusion of local dispersion, when local dispersivities are much smaller than the correlation scale of the log-hydraulic conductivity ($\ln K$) field. Thus, the spatial second moment has nothing to offer to

distinguish between plumes in which there is absolutely no attenuation of original concentrations, *i.e.*, the zero local dispersion case, and plumes in which there will be a decrease in solute concentration due to the action of local dispersion. *A priori*, the spatial second moment is not a predictor of 'dilution'. The use of large effective dispersivities, obtained from stochastic theories, or, from fitting observed spatial second moments in field experiments, may result in a large underestimation of point concentrations, if the solute is 'spreading' and breaking up into separate fragments without enhanced attenuation of concentrations, instead of 'mixing' and resulting in enhanced 'dilution'. While there is an abundance of studies that seek incremental refinements for the mean concentration and/or better predictions of the spatial second moments of the concentration distribution, rare are analytical evaluations of the deviations of solute concentrations from the mean value [Gelhar *et al.*, 1981; Dagan, 1982, 1984 and 1990; Vomvoris, 1986; Vomvoris and Gelhar, 1990].

A major applied motivation of stochastic analysis of transport in heterogeneous porous medium has been to derive an effective equation for the concentration that may be used to make decisions in real life contamination events which may require the assessment of the concentration at a 'point' in space and time. The spatial extent of this 'point' may indeed be small (*e.g.*, a well may sample an area not much larger than the Darcy continuum scale; human exposure to contaminated water may occur over scales smaller than the correlation scale of the $\ln K$ field), thus spatial averaging of the concentration field may not be pertinent in practical situations. Furthermore, for spatial averaging to result in a considerable reduction of the variance of concentration, averaging would have to occur over tens of correlation volumes (*i.e.*, the product of the three correlation scales). It does not seem prudent to rely on large-scale spatial averaging for the attenuation of high concentrations, in assessing risk of exposure to toxic substances. In any case, the statistics of spatial averages of the concentration field can only be computed after the second order statistics of point concentrations are determined.

The complex distribution of solute, due to the complexity of the velocity field, manifests itself as 'uncertainty' in the prediction associated with the mean concentration field (Figure 2.1). How good is the ensemble averaged concentration, a predictor of the concentration at a point in a plume in a sample realization of the hydraulic conductivity field? Do enhanced second moments of plumes translate into enhanced 'dilution', *e.g.*, attenuation of peak point concentration? What are the mechanisms and scales controlling these concentration deviations from the mean concentration? Do they become smaller in time relative to the mean concentration, or do they become arbitrarily large multiples of the mean and result in a fragmentation and ultimately an 'explosion' of the plume? A description of the ensemble average of the squared concentration fluctuations, *i.e.*, the concentration variance, and an enumeration of controlling mechanisms, to answer such questions, is the objective of this study.

The conservation equation for the concentration variance is derived in Section 2.2. The variance undergoes mean advection, a local dispersive flux, and a macrodispersive flux, just like the mean concentration field does. In Section 2.3 the macrodispersive flux term for the variance is estimated for the zero local dispersion case to get a Fickian flux term, in the variance equation. In addition to the transport terms in the variance conservation equation, there is a source term and sink term describing the processes of creation and destruction of fluctuations. The source term is twice the sum of the products of the macrodispersion coefficient and the squared gradient of the mean concentration field. The variance sink/dissipation term, is twice the sum of the products of the local dispersion coefficient and the mean squared gradients of the concentration perturbation field.

The variance dissipation term is represented as a first order decay term with the decay coefficient equal to twice the sum of the local dispersion coefficient divided by the squared concentration microscale, in three dimensions. The fact that the sink term is proportional to the variance of the *derivatives* of the concentration perturbation field

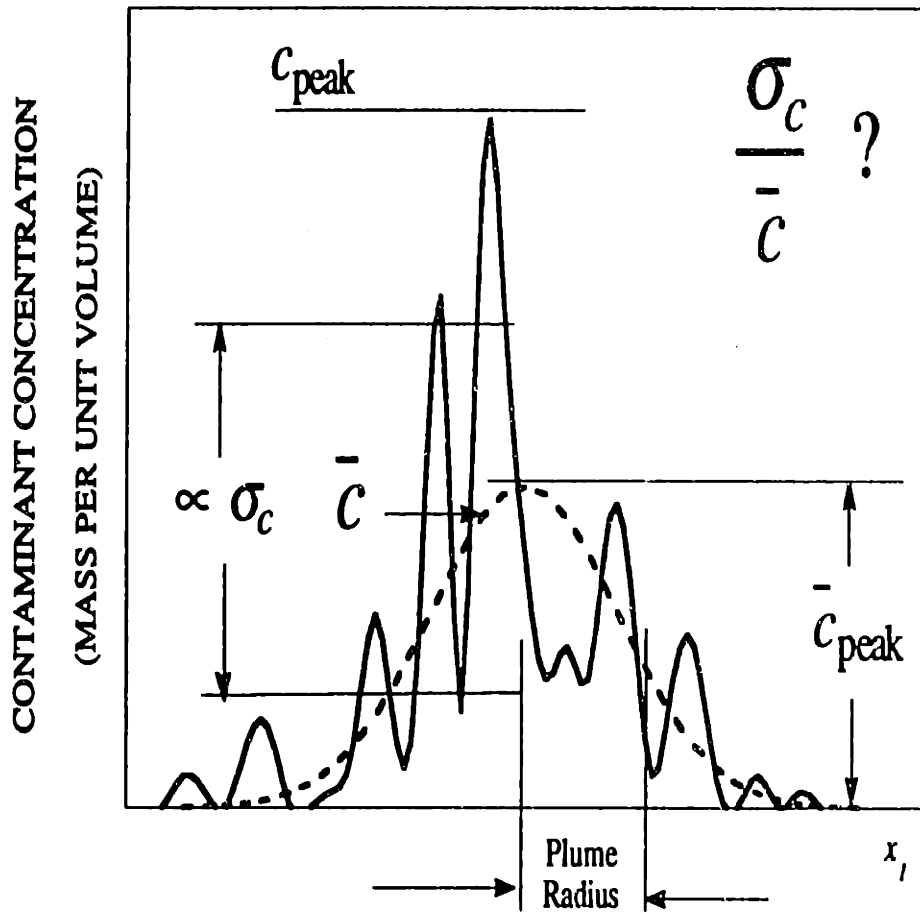


Figure 2.1

Are the concentration fluctuations a large multiple of the mean,
or, a small fraction of it ?

directly indicates the sensitivity of the dissipation mechanism to the rapidly fluctuating (*i.e.*, high wave number) content of the concentration field. Indeed diffusion acts rapidly on fine scale features than smoothly varying ones. In Section 2.4 the microscale of the concentration fluctuations is estimated by subjecting a small spot of the solute to the opposing effects of local dispersion and characteristic value of the principal convective compression (after Batchelor, 1959; Tennekes and Lumley, 1972), which is strongly dependent on the high wave number content of the velocity field. When the transport is advection dominated at the $\ln K$ microscale, the concentration microscale is an increasing function of the $\ln K$ microscale. Therefore, the variance decay coefficient is a decreasing function of the $\ln K$ microscale. Equivalently, the variance 'residence-time' (the inverse of the decay coefficient) is an increasing function of the $\ln K$ microscale.

Nondifferentiable $\ln K$ fields with zero microscales, result in infinite vorticity, infinite convective compression, and infinite shear in the velocity field, and are not entertained here. In deriving the results on variance dissipation, it is explicitly assumed that the $\ln K$ microscales are greater than the local dispersivities. In Appendix-IV is presented a differentiable spectrum for the $\ln K$ and the characteristic principal strain rate of the velocity field in statistically isotropic and anisotropic porous material. The role of the $\ln K$ microscale in controlling the rate of dissipation of concentration variance, points to the need for intensive characterization of the hydraulic conductivity in order to predict concentration variance.

2.2 CONCENTRATION VARIANCE CONSERVATION EQUATION

The transport of a passive scalar, undergoing local dispersion and advection in a velocity field with a mean v in the x_1 direction, and a zero mean-three dimensional -divergence free-spatially varying component v_i' , is governed by the parabolic equation

$$\frac{\partial c}{\partial t} + v \frac{\partial c}{\partial x_1} + v_i' \frac{\partial c}{\partial x_i} - v \alpha_{ij} \frac{\partial^2 c}{\partial x_i \partial x_j} = 0 \quad (2.1)$$

The local dispersivities α_{ij} typically have different longitudinal and transverse values;

$$\alpha_{11} = \alpha_L, \quad \alpha_{22} = \alpha_{33} = \alpha_T, \quad \alpha_{ij} = 0 \quad i \neq j$$

These local dispersivities may be measured in a laboratory column, and are typically less than a centimeter for the longitudinal direction and even smaller for the transverse direction. The local dispersion process in (2.1) has been simplified to depend on the mean velocity field rather than the local velocity, which would make it spatially variable. The effect of spatial variation of diffusion coefficients is not explored here.

Defining the velocity covariance function for the statistically stationary velocity perturbation field

$$R_{v_i' v_m'}(\mathbf{x} - \dot{\mathbf{x}}) = R_{v_i' v_m'}(\dot{\mathbf{x}} - \mathbf{x}) \equiv E[v_i'(\dot{\mathbf{x}}) v_m'(\mathbf{x})]$$

its spectrum is given by

$$S_{v_i' v_m'}(\mathbf{k}) \equiv \frac{1}{(2\pi)^3} \int_{-\infty}^{+\infty} \exp[-i k_j \xi_j] R_{v_i' v_m'}(\xi) d \xi$$

See Appendix IV for a specification of the velocity field.

Decomposing concentration c into its mean and perturbation

$$c = \bar{c} + c'$$

and substituting into Equation (2.1), using the divergence free condition of the velocity

fields

$$\frac{\partial v_i}{\partial x_i} = 0$$

on taking expectations of (2.1) we get for the mean concentration

$$\frac{\partial \bar{c}}{\partial t} + v \frac{\partial \bar{c}}{\partial x_1} - v \alpha_{ij} \frac{\partial^2 \bar{c}}{\partial x_i \partial x_j} + \frac{\partial}{\partial x_i} \overline{c' v_i'} = 0 \quad (2.2)$$

Subtracting the mean concentration equation (2.2) from (2.1) gives for concentration perturbations

$$\frac{\partial c'}{\partial t} + v \frac{\partial c'}{\partial x_1} - v \alpha_{ij} \frac{\partial^2 c'}{\partial x_i \partial x_j} + \frac{\partial}{\partial x_i} (c' v_i' - \overline{c' v_i'}) = -v_i' \frac{\partial \bar{c}}{\partial x_i} \quad (2.3)$$

There have been numerous studies to analyze the macrodispersive flux term

$$\overline{c' v_i'}$$

which creates additional (and indeed dominant) flux for the mean concentration field (2.2). This term may be analyzed by multiplying the perturbation equation (2.3) by a velocity perturbation at a different location and taking expectations to get

$$\begin{aligned} \frac{\partial}{\partial t} \overline{v_m'(\dot{\mathbf{x}}) c'(\mathbf{x}, t)} + v \frac{\partial}{\partial x_1} \overline{v_m'(\dot{\mathbf{x}}) c'(\mathbf{x}, t)} - v \alpha_{ij} \frac{\partial^2}{\partial x_i \partial x_j} \overline{v_m'(\dot{\mathbf{x}}) c'(\mathbf{x}, t)} + \\ \frac{\partial}{\partial x_i} \overline{v_i'(\mathbf{x}) v_m'(\dot{\mathbf{x}}) c'(\mathbf{x}, t)} = -R_{v_i' v_m'}(\dot{\mathbf{x}} - \mathbf{x}) \frac{\partial \bar{c}(\mathbf{x}, t)}{\partial x_i} \end{aligned} \quad (2.4)$$

A new term

$$\frac{\partial}{\partial x_i} \overline{v'_i(\mathbf{x}) v'_m(\dot{\mathbf{x}}) c'(\mathbf{x}, t)}$$

has been generated and is dropped using the plausible argument that it is higher order in velocity perturbations compared to the macrodispersive flux term in (2.4), and therefore will be small for small input $\ln K$ variance. Dropping this new term in (2.4), the Green's function for the advection dispersion operator governing the macrodispersive flux term is

$$G(\mathbf{x}-\boldsymbol{\eta}, t-\tau) = \prod_{i=1}^3 \frac{\exp\left\{-\frac{[(x_i - \eta_i) - v\delta_{i1}(t-\tau)]^2}{4\alpha_{ii}v(t-\tau)}\right\}}{\sqrt{4\pi\alpha_{ii}v(t-\tau)}}$$

Therefore the solution for the macrodispersive flux is given by

$$\overline{v'_m(\dot{\mathbf{x}}) c'(\mathbf{x}, t)} = -\int_{\tau=0}^t \int_{-\infty}^{+\infty} G(\mathbf{x}-\boldsymbol{\eta}, t-\tau) R_{v'_i v'_m}(\dot{\mathbf{x}}-\boldsymbol{\eta}) \frac{\partial \bar{c}(\boldsymbol{\eta}, \tau)}{\partial \eta_i} d\boldsymbol{\eta} d\tau \quad (2.5)$$

The correlation between concentration perturbations and velocity perturbations at the same spatial point may be evaluated from (2.5). Under the condition that the mean concentration gradient in the integral solution vary in space and time much slower than the Green's function and also much slower in space than the velocity covariance function, it may be taken outside of the space time integration to approximate the integral by a local relationship

$$\overline{v'_m(\dot{\mathbf{x}}) c'(\mathbf{x}, t)} = -v A_{mi}(t) \frac{\partial \bar{c}(\mathbf{x}, t)}{\partial x_i} \quad (2.6)$$

Where A_{mi} , the 'macrodispersivities', are given by

$$A_{mi}(t) = \frac{1}{v} \int_{\tau=0}^t \int_{-\infty}^{\infty} G(\mathbf{x}-\boldsymbol{\eta}, t-\tau) R_{v_i, v_m}(\mathbf{x}-\boldsymbol{\eta}) d\boldsymbol{\eta} d\tau \quad (2.7)$$

This expression is equivalent to the expression for macrodispersivities given in Gelhar [1987], equation 4.6. As shown in Gelhar [1987],

$$t \rightarrow \infty \quad A_{mi} = \int_{-\infty}^{+\infty} \frac{S_{v_i, v_m}(\mathbf{k}) d\mathbf{k}}{[ik_1 + \alpha_L k_1^2 + \alpha_T(k_2^2 + k_3^2)]v^2} \quad (2.8)$$

In this study it is assumed that the mean concentration field is smooth enough to permit these localization approximations and the interest is on the process after large travel distances, therefore the use of a constant effective dispersivity is justified. Gelhar and Axness [1983] have computed the integral (2.8) for a variety of cases. For statistically isotropic porous medium with small local dispersivities, they present the large time result

$$A_{11} = \sigma_f^2 \lambda \gamma^2, \quad \gamma = 1 + \sigma_f^2 / 6$$

where λ and σ_f are the correlation scale and standard deviation of the $\ln K$ field.

To analyze the concentration variance, *i.e.*, $\sigma_c^2 = E[c^2]$, the exact concentration perturbation equation (2.3) is multiplied by another concentration perturbation. After taking the mean we get the exact concentration variance equation

$$\frac{1}{2} \left[\frac{\partial \sigma_c^2}{\partial t} + v \frac{\partial \sigma_c^2}{\partial x_1} - v \alpha_{ij} \frac{\partial^2 \sigma_c^2}{\partial x_i \partial x_j} + \frac{\partial}{\partial x_i} (\overline{v_i c'^2}) \right] = - \overline{v_i c'} \frac{\partial \bar{c}}{\partial x_i} - v \alpha_{ij} \frac{\partial \bar{c}'}{\partial x_i} \frac{\partial \bar{c}'}{\partial x_j} \quad (2.9a)$$

Equation (2.9a) is the mass conservation statement at the second statistical moment level. Some inferences about the concentration variance are already possible. Firstly, under the

condition of a finite mean concentration gradient and correlation between concentration perturbation and velocity perturbation in (2.9a) (in the first term on the right hand side), the inference of finite concentration variances for any value of local dispersion (including zero) is trivially afforded, recognizing that transport terms (on the right hand side of (2.9a)) cannot ever create any variance, and the dissipation term on the right hand side can only destroy concentration variance. Secondly, the concentration mean and standard deviation for a solute undergoing a first order decay with a constant decay rate coefficient κ are simply equal to those of a solute not undergoing a first order decay, multiplied by $e^{-\kappa t}$. This follows from recognizing that a first order decay can simply be scaled out of the transport equation (2.1). Therefore, a solute undergoing a first order decay will have the same coefficient of variation (*i.e.*, the concentration standard deviation divided by the mean concentration) as a nonreactive solute. These two inferences do not involve any approximations or closures, or dropping of terms, like those made in inferring the correlation between concentration perturbations and velocity perturbations. The results of Vomvoris [1986] do not agree with these inferences. In his analysis of a solute undergoing a constant first order decay, the decay rate strongly influences the implied concentration coefficient of variation, also, the variance can be made arbitrarily large by making the local dispersivity arbitrarily small. The approximations developed hereafter do not violate these two features. The results developed by Gelhar and Gutjahr [1982] also have the feature that the solute undergoing a first order decay has an implied coefficient of variation that is different from the nonreactive case.

Equation (2.9a) is the foundation for inferences of concentration variance to be made in this and the next chapter. There are two new terms in (2.9a). The divergence of the correlation between squared concentration perturbations and velocity perturbations, the last term on the left hand side. The variance dissipation term, the last term on the right hand side. These two terms will be analyzed in Section 2.3 and 2.4 respectively. Substituting the Fickian relationship (2.6) in the first term on the right hand side of (2.9a)

gives

$$\frac{\partial \sigma_c^2}{\partial t} + v \frac{\partial \sigma_c^2}{\partial x_1} - v \alpha_{ij} \frac{\partial^2 \sigma_c^2}{\partial x_i \partial x_j} + \frac{\partial}{\partial x_i} (\overline{v_i' c'^2}) = 2v A_{ij} \frac{\partial \bar{c}}{\partial x_i} \frac{\partial \bar{c}}{\partial x_j} - 2v \alpha_{ij} \frac{\partial \bar{c}'}{\partial x_i} \frac{\partial \bar{c}'}{\partial x_j} \quad (2.9b)$$

Analogous to the macrodispersive flux term for the mean concentration equation (2.2) (the divergence of the correlation between concentration perturbations and velocity perturbations) there is a macrodispersive flux term for the variance

$$\frac{\partial}{\partial x_i} (\overline{v_i' c'^2})$$

(the divergence of the correlation between squared concentration perturbations and velocity perturbations). The variance also undergoes mean advection and a local dispersive flux, and is produced and dissipated by the forcings on the right hand side (2.9b). Defining

$$\|f\| = \int_{-\infty}^{+\infty} f d\mathbf{x}$$

for homogeneous zero far field conditions and divergence free velocity perturbation fields,

$$\left\| \frac{\partial \sigma_c^2}{\partial x_1} \right\| = \left\| \frac{\partial^2 \sigma_c^2}{\partial x_i \partial x_j} \right\| = \left\| \frac{\partial}{\partial x_i} (\overline{v_i' c'^2}) \right\| = 0$$

The macrodispersive term for the variance, is a transport term and does not cause any dissipation or production of the global fluctuation measure, which on integrating (2.9b)

follows

$$\frac{d}{dt} \|\sigma_c^2\| = 2\nu A_{ij} \left\| \frac{\partial \bar{c}}{\partial x_i} \frac{\partial \bar{c}}{\partial x_j} \right\| - 2\nu \alpha_{ij} \left\| \overline{\frac{\partial c'}{\partial x_i} \frac{\partial c'}{\partial x_j}} \right\| \quad (2.10)$$

The macrodispersivities and local dispersivities have opposing roles in creating and destroying concentration fluctuations in (2.10) and (2.9b). In the absence of local dispersion there is no mechanism to destroy the variance (2.9b), and the global measure in (2.10) is nondecreasing. Consideration of fluctuation budgets of the form (2.9a) and (2.10) can be traced back to the deliberations of O. Reynolds [1895] on turbulent kinetic energy.

The variance equation (2.9b) shows that a mean concentration profile in a porous medium with a larger correlation scale is accompanied by greater fluctuations as the longitudinal macrodispersivity increases with the correlation length thereby increasing the strength of the source term in the variance equation (2.9). The source term in the variance equation (2.9b) is proportional to the square of the spatial derivatives of the mean concentration field, thereby showing that a plume scale is naturally involved in determining the rate of production of concentration variance.

2.3 MACRODISPERSIVE FLUX OF CONCENTRATION VARIANCE

2.3.1 ZERO LOCAL DISPERSION CASE

Neglecting local dispersion in (2.1), the transport of a passive scalar in the heterogeneous velocity field is governed by the hyperbolic advection operator

$$\frac{\partial c}{\partial t} + v \frac{\partial c}{\partial x_1} + v_i \frac{\partial c}{\partial x_i} = 0 \quad (2.11)$$

On taking expectations of (2.11), the mean concentration is governed by

$$\frac{\partial \bar{c}}{\partial t} + v \frac{\partial \bar{c}}{\partial x_1} + \frac{\partial}{\partial x_i} \overline{c' v_i'} = 0 \quad (2.12)$$

In order to evaluate the macrodispersive flux, the concentration perturbation equation, obtained by subtracting (2.12) from (2.11), may be multiplied by a velocity perturbation at another location. After taking expectations and dropping the new 'higher order term' (as dropped in Section 2.2 from equation (2.4))

$$\frac{\partial}{\partial t} \overline{v_m'(\dot{x}) c'(\mathbf{x}, t)} + v \frac{\partial}{\partial x_1} \overline{v_m'(\dot{x}) c'(\mathbf{x}, t)} = - R_{v_i' v_m'}(\dot{x} - \mathbf{x}) \frac{\partial \bar{c}(\mathbf{x}, t)}{\partial x_i} \quad (2.13)$$

The Green's function for the hyperbolic advection operator in (2.13) is

$$G(\mathbf{x} - \boldsymbol{\eta}, t - \tau) = \prod_{i=1}^3 \delta(x_i - \eta_i - v \delta_{i1}(t - \tau))$$

The solution for the macrodispersive flux term is

$$\overline{v_m'(\dot{x}) c'(\mathbf{x}, t)} = - \int_{\tau=0}^t R_{v_i' v_m'}(\dot{x}_i - (x_i - v \delta_{i1}(t - \tau))) \left[\frac{\partial \bar{c}(\boldsymbol{\eta}, \tau)}{\partial \eta_i} \right]_{x_i - v \delta_{i1}(t - \tau)} d\tau \quad (2.14)$$

For the correlation between velocity and concentration perturbations at the same location in (2.14), assuming that the mean gradient is slowly varying in time so that it may be taken outside the integration to get

$$\overline{v_m'(\mathbf{x}) c'(\mathbf{x}, t)} = - v A_{mi}(t) \frac{\partial \bar{c}(\mathbf{x}, t)}{\partial x_i} \quad (2.15)$$

where A_{mi} , the macrodispersivities, are given by

$$A_{mi}(t) = \frac{1}{v} \int_{\tau=0}^t R_{v'_i v'_m}(v(t-\tau), 0, 0) d\tau \quad (2.16)$$

This expression is equivalent to the expression 4.17 in Gelhar [1987]. It may be shown

$$t \rightarrow \infty \quad A_{mi} = \frac{\pi}{2} \int_{-\infty}^{+\infty} \int_{-\infty}^{+\infty} S_{v'_i v'_m}(0, k_2, k_3) dk_2 dk_3 \quad (2.17)$$

(Equation 4.19 in Gelhar [1987]). For large displacements, under conditions of sufficient smoothness of the mean concentration field, a constant macrodispersivity may be used. The longitudinal macrodispersivity found from (2.17) is indistinguishable from the one found after including local dispersion (2.8), for small local dispersivities compared to the $\ln K$ correlation scale [Gelhar and Axness, 1983]. By (2.12) and (2.15), the ensemble average of the transport quantity c is thus governed by the advection-dispersion operator

$$\frac{\partial \bar{c}}{\partial t} + v \frac{\partial \bar{c}}{\partial x_1} - v A_{ij} \frac{\partial^2 \bar{c}}{\partial x_i \partial x_j} = 0 \quad (2.18)$$

For the idealized zero local dispersion case, all powers of c are governed by the same operator (a fundamental property of the hyperbolic operator (2.11)). Define

$$s = c^2$$

It follows simply from (2.11)

$$\frac{\partial s}{\partial t} + v \frac{\partial s}{\partial x_1} + v'_i \frac{\partial s}{\partial x_i} \quad (2.19)$$

Now

$$s = c^2 = (\bar{c} + c')^2 = \bar{c}^2 + c'^2 + 2\bar{c}c' \quad (2.20)$$

and

$$\bar{s} = \bar{c}^2 + \sigma_c^2, \quad s' = s - \bar{s} = c'^2 + 2\bar{c}c' - \sigma_c^2 \quad (2.21)$$

Therefore without any new assumption on s it follows from (2.11), (2.15) and (2.19)

$$\overline{v'_m(\mathbf{x})s'(\mathbf{x},t)} = -vA_{mi} \frac{\partial \bar{s}(\mathbf{x},t)}{\partial x_i} \quad (2.22)$$

On substituting (2.21) in the Fickian relationship (2.22) and using the Fickian relationship for the mean concentration (2.15),

$$\overline{c'^2 v'_m} = -vA_{mi} \frac{\partial \sigma_c^2}{\partial x_i} \quad (2.23)$$

thereby deducing that the role played by the correlation between squared concentration perturbations and velocity perturbations (2.23) in the transport of the concentration variance field in (2.9b), is similar to that of the correlation between concentration perturbations and velocity perturbations (2.15) in the transport of mean concentration (2.12). Of course the relative orders of these macrodispersive transport terms are precisely the same in the equations for the mean concentration and concentration variance. The heterogeneous velocity field transports concentration fluctuations from regions of greater fluctuations to regions of lesser fluctuations due to this correlation between squared concentration perturbations and velocity perturbations (2.23). The

derived Fickian relationship (2.23) was hypothesized by Csanady [1973].

On taking expectations of equation (2.19) and substituting (2.22)

$$\frac{\partial \bar{c}^2}{\partial t} + v \frac{\partial \bar{c}^2}{\partial x_1} - v A_{ij} \frac{\partial^2 \bar{c}^2}{\partial x_i \partial x_j} = 0 \quad (2.24)$$

Substituting for the mean of the squared concentration given in equation (2.21), into (2.24), gives the variance conservation equation for the idealized zero local dispersion case

$$\frac{\partial \sigma_c^2}{\partial t} + v \frac{\partial \sigma_c^2}{\partial x_1} - v A_{ij} \frac{\partial^2 \sigma_c^2}{\partial x_i \partial x_j} = 2v A_{ij} \frac{\partial \bar{c}}{\partial x_i} \frac{\partial \bar{c}}{\partial x_j} \quad (2.25)$$

The derivation of equation (2.25) needed no additional assumptions on s , other than those already made on c , in deriving the mean concentration equation for the zero local dispersion case.

Dagan [1982] and [1990], analyzed the concentration variance, neglecting local dispersion, for the case of a solute injected with a concentration c_o in a finite region. Dagan's result for the variance is

$$\sigma_c^2(x,t) = \bar{c} (c_o - \bar{c}) \quad (2.26)$$

Differentiating this expression in time and space gives

$$\frac{\partial \sigma_c^2}{\partial t} = c_o \frac{\partial \bar{c}}{\partial t} - 2 \bar{c} \frac{\partial \bar{c}}{\partial t}$$

$$\frac{\partial \sigma_c^2}{\partial x_i} = c_o \frac{\partial \bar{c}}{\partial x_i} - 2\bar{c} \frac{\partial \bar{c}}{\partial x_i}$$

$$\frac{\partial^2 \sigma_c^2}{\partial x_i \partial x_j} = c_o \frac{\partial^2 \bar{c}}{\partial x_i \partial x_j} - 2 \frac{\partial \bar{c}}{\partial x_i} \frac{\partial \bar{c}}{\partial x_j} - 2\bar{c} \frac{\partial^2 \bar{c}}{\partial x_i \partial x_j}$$

These expressions yield

$$\begin{aligned} & \frac{\partial \sigma_c^2}{\partial t} + v \frac{\partial \sigma_c^2}{\partial x_1} - v A_{ij} \frac{\partial^2 \sigma_c^2}{\partial x_i \partial x_j} = \\ & (c_o - 2\bar{c}) \left(\frac{\partial \bar{c}}{\partial t} + v \frac{\partial \bar{c}}{\partial x_1} - v A_{ij} \frac{\partial^2 \bar{c}}{\partial x_i \partial x_j} \right) + 2v A_{ij} \frac{\partial \bar{c}}{\partial x_i} \frac{\partial \bar{c}}{\partial x_j} \end{aligned} \quad (2.27)$$

Recognizing that the mean concentration is governed by the advection-dispersion operator (2.18), we get from (2.27) the same equation for the concentration variance as (2.25). Therefore the mechanisms in the derived variance equation (2.25), for the creation and movement of concentration fluctuations for the nondissipative zero local dispersion case, are in complete agreement with Dagan's compact result (2.26). The important macrodispersive transport mechanism for concentration variance derived in (2.23), hypothesized by Csanady [1973], is implicitly contained in Dagan's result. Graham and McLaughlin [1989], Vomvoris and Gelhar [1990] and Li and McLaughlin [1991] have dropped this macrodispersive transport term for the concentration variance field, on account of dropping the perturbations in the macrodispersive flux in the concentration perturbation equation (2.3). It is being argued here that dropping this term in the variance equation is akin to dropping the macrodispersive flux term in the mean equation.

Since small local dispersivities (relative to the $\ln K$ correlation scales) play an insignificant role in determining the macrodispersive flux of the mean concentration field,

it is unlikely that they will play a major role in determining the macrodispersive flux of the concentration variance field. Therefore, the Fickian relationship for the concentration variance (2.23) will be substituted into the variance conservation equation including local dispersion, *i.e.*, equation (2.9b). This will result in there being a macrodispersive flux mechanism for the transport of the concentration variance field, in addition to the local dispersive flux mechanism.

2.4. DESTRUCTION OF CONCENTRATION VARIANCE BY LOCAL DISPERSION

2.4.1 VARIANCE SINK TERM

The variance sink term $d(\mathbf{x}, t)$ in the concentration variance equation (2.9) is given by

$$d(\mathbf{x}, t) = 2\nu\alpha_{ij} \overline{\frac{\partial c'}{\partial x_i} \frac{\partial c'}{\partial x_j}} \quad (2.28)$$

This term is nonnegative, and therefore acts as a sink for concentration variance. The dissipation/destruction of variance is singularly brought about by the action local dispersion. The interaction of local dispersion and the rapidly fluctuating part of the concentration perturbation field (which strongly determines the variance of the spatial partial derivatives of the concentration perturbation field in (2.28)), controls the rate of concentration variance dissipation. Such an inverse dependence of the rate of dissipation of mean squared fluctuations, on squared dimensions characterizing spatial derivatives of transport quantities, is ubiquitous in transport of heat, kinetic energy, and mass in complex velocity fields. The reason being that a fundamental characteristic of an

unsteady diffusion phenomenon is that the component of the transported quantity that varies rapidly in space, decays faster in time, and the decay rate is inversely proportional to the square of the scale that characterizes the derivatives of the variation in space. A trivial one dimensional homogeneous boundary condition example, is sufficient to demonstrate this 'wave number squared' sensitivity (See Appendix-I). Lumley [1972] discusses this feature in his exposition of the dynamics of temperature fluctuations (neglecting buoyancy, therefore treating it like a passive scalar) in complex turbulent velocity fields. Taylor [1935a] discusses the dissipation of turbulent kinetic energy and measures the scale characterizing the derivatives of the velocity field to successfully deduce the rate of dissipation of energy in turbulent flow in a pipe [1935b]. Analytical bounds on norms of the squared gradients of transport quantities have been computed by variational methods, under various constraints, in search for extremal hypothesis that might 'govern' complex flow systems [*e.g.*, Howard, 1972; Malkus and Smith, 1989]. Analysis of dissipation functions like (28) facilitate finding absolute stability criteria for fluid flows [*e.g.*, Serrin, 1959; Sorokin, 1961; Joseph, 1976]. The critical role of the dissipation function in controlling the level of fluctuation energy, is well established in a variety of continuous dissipative systems.

Due to small local dispersivities, transport in porous media is advection dominated at extremely small scales (less than a centimeter). It is expected that the fine scale features (high wave number component) of the velocity field, and therefore the $\ln K$ field, will play an important role in determining the strength of the spatial partial derivatives of the concentration perturbation field. It is also expected that the energy in the spatial partial derivatives decreases with an increase of local dispersivities due to a smoothing influence. Thus, to some extent, local dispersion may have a self inhibitory role in variance dissipation. Of course, in neglecting local dispersion, the hyperbolicity of the transport operator (2.11) precludes any fluctuation dissipation (2.28), and there is no particularly interesting role for the gradients of the concentration fluctuation field. It is

precisely the parabolic nature of the advection-local dispersion operator (1), that creates the interesting phenomenon of fluctuation dissipation (2.28). Appendix-II presents *rigorous* lower bounds on the dissipation function, sufficiently demonstrating its singular importance in controlling the level of the concentration fluctuation energy in a bounded two dimensional aquifer.

Defining the concentration spatial covariance function

$$R_{c'c'}(\hat{\mathbf{x}}, \hat{\mathbf{x}}', t) = E[c'(\hat{\mathbf{x}}, t)c'(\hat{\mathbf{x}}', t)] \quad (2.29)$$

$$\overline{\frac{\partial c'}{\partial x_i} \frac{\partial c'}{\partial x_j}} = \frac{\partial^2}{\partial \hat{x}_i \partial \hat{x}_j} R_{c'c'}(\hat{\mathbf{x}}, \hat{\mathbf{x}}', t) \Big|_{\hat{\mathbf{x}} = \hat{\mathbf{x}}' = \mathbf{x}, t} \quad (2.30)$$

The concentration covariance equation may be formulated (by multiplying the concentration perturbation equation (2.3) by a concentration perturbation at another point in space and taking expectations) to get

$$\begin{aligned} & \frac{\partial}{\partial t} \overline{c'(\mathbf{x}, t)c'(\hat{\mathbf{x}}, t)} + v \frac{\partial}{\partial x_1} \overline{c'(\mathbf{x}, t)c'(\hat{\mathbf{x}}, t)} + v \frac{\partial}{\partial \hat{x}_1} \overline{c'(\mathbf{x}, t)c'(\hat{\mathbf{x}}, t)} - \\ & v \alpha_{ij} \frac{\partial^2}{\partial x_i \partial x_j} \overline{c'(\mathbf{x}, t)c'(\hat{\mathbf{x}}, t)} - v \alpha_{ij} \frac{\partial^2}{\partial \hat{x}_i \partial \hat{x}_j} \overline{c'(\mathbf{x}, t)c'(\hat{\mathbf{x}}, t)} + \\ & \frac{\partial}{\partial x_i} \overline{c'(\mathbf{x}, t)c'(\hat{\mathbf{x}}, t)v_i'(\mathbf{x})} + \frac{\partial}{\partial \hat{x}_i} \overline{c'(\mathbf{x}, t)c'(\hat{\mathbf{x}}, t)v_i'(\hat{\mathbf{x}})} = \\ & - \overline{c'(\hat{\mathbf{x}}, t)v_i'(\mathbf{x})} \frac{\partial \bar{c}(\mathbf{x}, t)}{\partial x_i} - \overline{c'(\mathbf{x}, t)v_i'(\hat{\mathbf{x}})} \frac{\partial \bar{c}(\hat{\mathbf{x}}, t)}{\partial \hat{x}_i} \end{aligned} \quad (2.31)$$

To deduce the strength in the derivatives of the concentration perturbation field (30), an investigation of the small separation behavior of the concentration covariance function is required. The covariance equation (2.31) has a new term

$$\overline{c'(\mathbf{x},t)c'(\mathbf{x}',t)v'(\mathbf{x})}$$

The corresponding term in the variance equation creates a macrodispersive transport mechanism for the variance field (as derived in Section 2.3, shown to be implicit in Dagan's [1990] model, and, hypothesized by Csanady [1973]). There is little merit in dropping it and still retain the variance transport terms due to local dispersion. Solving the covariance equation (2.31) in a *small perturbation* analysis will involve at least formulating another equation for the correlation between squared concentration perturbations and velocity perturbations. In numerical studies of the concentration covariance, the discretization would be dictated among other factors, also by the fact that the second derivative of the concentration covariance equation (2.30) needs to be evaluated to determine the variance sink term (2.28). In numerical computations done by Graham and McLaughlin [1989] for a two-dimensional heterogeneous medium and Li and McLaughlin [1991] for a one-dimensional problem, this triple product transport term has been dropped.

If the dissipating action of local dispersion on concentration fluctuations has to be computed in a sample realization of the $\ln K$, the numerical approximations have to be able to model the gradient of the concentration perturbation field with fidelity, as it controls the local-dispersive flux, which is the only smoothing mechanism. This feature unambiguously manifests itself in the sink term (2.28) in the exact concentration variance equation (2.9a). Typically, numerical approximations are not capable of reproducing local concentration gradients, for advection dominated transport in heterogeneous velocity fields. For 'particle-tracking' methods (popularly claimed to be a panacea against intensive spatial discretization requirements) to be able to model this local-dispersive flux, it seems that a *lot* of particles will be required. There is little precedence of suggesting convergence of numerical solutions in a derivative norm (e.g., H^1 norm), or

any other norm. Ironically, almost without exception, numerical studies employ a description of $\ln K$ that is incredibly rich at the high wave number end (*i.e.*, the exponential correlation model of $\ln K$), and yields *infinite* strain rates for the velocity field that cannot possibly be reproduced on a numerical grid. The singular objective of numerically modeling the spatial second moment of plumes and the theoretically found insensitivity of it to the local dispersion process, is probably why this issue is not addressed.

Following is a simplified analytical study of the interaction of the fine scale feature of the concentration perturbation field with the velocity field in the presence of local dispersion, to assess the variance sink term (2.28), and enumerate the controlling mechanisms and parameters.

2.4.2 VARIANCE DECAY COEFFICIENT

Assuming the small separation behavior of the covariance function is that of a statistically stationary field, *i.e.*,

$$\lim_{\hat{\mathbf{x}} \rightarrow \dot{\mathbf{x}}} R_{c'c'}(\hat{\mathbf{x}}, \dot{\mathbf{x}}, t) \rightarrow R_{c'c'}(\xi, t) \quad (2.32)$$

$$\xi = \hat{\mathbf{x}} - \dot{\mathbf{x}}$$

It follows from (2.30) that

$$E \left[\left(\frac{\partial c'}{\partial x_i} \right)^2 \right] = - \frac{\partial^2 R_{c'c'}(\xi, t)}{\partial \xi_i^2} \Big|_{\xi=0} \equiv \frac{\sigma_c^2}{(\Delta_i^c)^2} \quad (2.33)$$

By definition, Δ_i^c , the microscale of the concentration perturbation field, is the scale that characterizes the derivatives of the concentration perturbation field [Tennekes and

Lumley, 1972]. Substituting (2.33) in the variance sink expression (2.28) gives

$$d(\mathbf{x}, t) = \chi \sigma_c^2 \quad (2.34a)$$

$$\chi = \frac{2\nu\alpha_{ij}}{\Delta_i^c \Delta_j^c} \quad (2.34b)$$

χ is the 'variance decay coefficient'. A sum over repeated indices is implied in (2.34b). The variance sink term, thus approximated, is a first order decay term, in the variance conservation equation (2.9). The decay coefficient χ , is the sum in the three principal directions of twice the ratio of the local dispersion coefficient and the squared concentration microscale. The larger the concentration microscale Δ_i^c is relative to the local dispersivities, the slower is the action of local dispersion in destroying the concentration variance. The 'residence time' of concentration variance, $1/\chi$, is proportional to the squared concentration microscale. The smaller the concentration microscale, the smaller the fluctuation 'residence time', as local dispersion destroys it faster. Of course, concentration variance is always being produced at a rate proportional to the squared gradient of the mean concentration field, as dictated by the source term in (2.9b). For the hypothetical zero local dispersion case, the residence time of concentration variance is infinitely large, as the concentration variance is not being destroyed at all.

2.4.3 CONCENTRATION MICROSCALE

The interaction of the strain rate of the velocity field and local dispersion in determining the concentration microscale is analyzed here. Consider a 'small spot' of solute introduced at the origin in the \mathbf{x} coordinate system. Equation (1) governs the space time evolution of the small spot. The conservation equation in a coordinate system

ξ oriented with the x coordinate but also moving with the particle originally at the origin in the x coordinate is

$$\frac{\partial c}{\partial t} + (v_i(\xi) - v_i(0)) \frac{\partial c}{\partial \xi_i} = \nu \alpha_{ij} \frac{\partial^2 c}{\partial \xi_i \partial \xi_j} \quad (2.35)$$

A Taylor expansion of the velocity field may be made *i.e.*,

$$v_i(\xi) = v_i(0) + \xi_j \frac{\partial v_i(0)}{\partial \xi_j} + O(\xi^2) \quad (2.36)$$

This first order Taylor expansion is substituted in (2.35) as the focus is on the small scale features and therefore a linear representation of the velocity is made [Batchelor, 1959; Lumley, 1972; Tennekes and Lumley, 1972]. This gives

$$\frac{\partial c}{\partial t} + \xi_j \frac{\partial v_i(0)}{\partial \xi_j} \frac{\partial c}{\partial \xi_i} = \nu \alpha_{ij} \frac{\partial^2 c}{\partial \xi_i \partial \xi_j} \quad (2.37)$$

Defining the normalized spatial moments of this small spot as

$$I_{pq}(t) = \frac{\int_{-\infty}^{+\infty} \xi_p \xi_q c(\xi, t) d\xi}{\int_{-\infty}^{+\infty} c(\xi, t) d\xi} \quad (2.38)$$

On integrating equation (2.37) in space and using the divergence free condition on the velocity perturbation field, the evolution of the normalized spatial moments of this small spot is governed by

$$\frac{d I_{pq}}{dt} - I_{pj} \frac{\partial v_q}{\partial \xi_j} - I_{qj} \frac{\partial v_p}{\partial \xi_j} = 2\nu\alpha_{pq} \quad (2.39)$$

To study the interaction between the principal strain rates of the velocity field, local dispersion, and the small spot, the off-diagonal components of the gradient of the velocity perturbation field in equation (2.39) are dropped to get

$$\frac{d I_{ii}}{dt} - 2 \frac{\partial v_i}{\partial x_i} I_{ii} = 2\alpha_{ii}\nu \quad (2.40)$$

with no sum on i . The evolution of the spatial second moment of this spot is strongly influenced by the spatial partial derivatives of the velocity field in (2.40). Dropping of the off-diagonal terms of the velocity gradient affords a local decoupling of the transport in the different dimensions. Inclusion of the flow vorticity [which is computed in Appendix-V] can be expected to have a local isotropizing influence. Lumley [1972], performs a similar analysis including the vorticity and did not find a significant change the computed concentration microscales. Equation (2.40), derived by Batchelor [1959], is the basis for inferences about the high wave number behavior of transport quantities undergoing advection-diffusion.

Decomposing $\ln K$ into its mean and perturbation,

$$\ln[K] = E[\ln[K]] + f$$

For a stationary $\ln K$ field the variance of the spatial partial derivatives is given by

$$E\left[\left(\frac{\partial f}{\partial x_i}\right)^2\right] \equiv \frac{\sigma_f^2}{(\Delta_i)^2} \quad (2.41)$$

where Δ_i^f is the microscale of the $\ln K$ field in the i th direction. The standard deviation of the velocity field may be related to the $\ln K$ description by

$$\sigma_{v_i} = \frac{\mu_i}{\gamma} \nu \sigma_f \quad (2.42)$$

Defining the variance of the derivatives of the velocity field

$$\mathbb{E} \left[\left(\frac{\partial v_i}{\partial x_i} \right)^2 \right] \equiv \frac{\sigma_{v_i}^2}{(\Delta_i^{v_i})^2} \quad (2.43)$$

The characteristic strain rates of the velocity field may be related to the $\ln K$ field to get

$$\frac{\sigma_{v_i}}{\Delta_i^{v_i}} = \frac{\beta_i}{\gamma} \nu \frac{\sigma_f}{\Delta_i^f} \quad (2.44)$$

where the constant γ is defined, and β_i, μ_i are computed, in the Appendix-IV. Results for three dimensional heterogeneous $\ln K$ fields, for both the isotropic and layered anisotropic case are presented in the Appendix-IV. The velocity field microscale is related to the $\ln K$ field microscale by

$$\Delta_i^{v_i} = \frac{\mu_i}{\beta_i} \Delta_i^f \quad (2.45)$$

The solution to (2.40) is easily found to get

$$I_{ii}(t) = I_{ii}(0) \exp \left[2 \frac{\partial v_i}{\partial x_i} t \right] + \alpha_{ii} v \left[\frac{\exp \left[2 \frac{\partial v_i}{\partial x_i} t \right] - 1}{\frac{\partial v_i}{\partial x_i}} \right] \quad (2.46)$$

with again no sum on i . It follows from the solution (2.46) that in the case that the small spot is being compressed in the i th direction with the 'characteristic' strain rate, *i.e.*,

$$\frac{\partial v_i}{\partial x_i} = - \left(\frac{\sigma_{v_i}}{\Delta_i^{v_i}} \right)$$

the local dispersion and convective compression counteract each others influence and the normalized spatial second moment in the i th direction of the small spot saturates to a value

$$\frac{\alpha_{ii} v}{\left(\frac{\sigma_{v_i}}{\Delta_i^{v_i}} \right)} \quad (2.47)$$

This reveals that features with dimension less than the square root of (2.47) cannot be sustained in the advection-local dispersion transport process. The velocity strain rate field was assumed to persist over dimensions larger than the small spot in using a one term Taylor expansion of the velocity field in the transport equation in (2.36). Therefore it is being assumed that the transport at the velocity microscale is advection dominated,

$$\Delta_i^{v_i} > \alpha_{ii} \quad (2.48)$$

In addition, it is also being assumed that the contribution from the initial dimensions of the 'spot' can be ignored in (2.46). Arguing that in an advection dominated transport system, the initial dimensions of the 'spot' are that of the velocity microscale, it is being assumed

$$\frac{\alpha_{ii} \nu}{\left(\frac{\sigma_{v_i}}{\Delta_i^{v_i}} \right)} > (\Delta_i^{v_i})^2 \quad (2.49)$$

Using (2.42), the range of velocity microscales being entertained are

$$\frac{\alpha_{ii}}{\left(\frac{\mu_i}{\gamma} \right) \sigma_f} > \Delta_i^{v_i} > \alpha_{ii} \quad (2.50)$$

In this range, the concentration microscale is of the order

$$(\Delta_i^c)^2 \approx \frac{\alpha_{ii} \nu}{\left(\frac{\sigma_{v_i}}{\Delta_i^{v_i}} \right)} \quad (2.51)$$

This estimate is therefore made for 'moderate advection domination' (2.50). At conditions of extreme advection domination of the velocity microscale, it is expected that the scales governing the spatial derivatives of the velocity field are superimposed on the concentration field. The estimate of the squared concentration microscale may be extended to larger velocity microscale by adding the squared velocity microscale, to account for the initial dimension of the spot in (2.46)

$$(\Delta_i^c)^2 = \frac{\alpha_{ii} \nu}{\left(\frac{\sigma_{v_i}}{\Delta_i^{v_i}} \right)} + (\Delta_i^{v_i})^2 \quad (2.52)$$

This may be written as

$$(\Delta_i^c)^2 \equiv \frac{\alpha_{ii} \Delta_i^f}{\frac{\beta_i}{\gamma} \sigma_f} + \left(\frac{\mu_i}{\beta_i} \right)^2 (\Delta_i^f)^2 \quad (2.53)$$

using (2.42),(2.44),(2.45). The concentration microscale estimate in (2.52) is argued under the condition that the velocity microscale is greater than the local dispersivity, which using (2.45) is expressed as

$$\Delta_i^f > \frac{\beta_i}{\mu_i} \alpha_{ii} \quad (2.54)$$

The estimate of the concentration microscale in (2.53), has a linear dependence on the $\ln K$ microscale, at very large microscales. As the $\ln K$ microscale approaches the local dispersivity, the feedback from the smoothing effects of local dispersion, weakens the dependence of the concentration microscale on the $\ln K$ microscale.

The variance decay coefficient, on substituting (2.53) in (2.34b), is

$$\chi \approx \sum_{i=1}^3 \frac{2\alpha_{ii}\nu}{\left(\frac{\alpha_{ii} \Delta_i^f}{\frac{\beta_i}{\gamma} \sigma_f} + \left(\frac{\mu_i}{\beta_i} \right)^2 (\Delta_i^f)^2 \right)} \quad (2.55)$$

The decay coefficient thus represented, approximately incorporates the features of an

increase in the strength of the spatial partial derivatives of the concentration perturbation field with an increase in the relative proportion of the high wave number component of the $\ln K$ spectrum (*i.e.*, a decrease in the $\ln K$ microscale), and therefore an increased rate of destruction of concentration fluctuations. Also, as the $\ln K$ microscale increases (due to a greater proportion of low wave number energy in the $\ln K$ spectrum), the concentration microscale increases (2.53), which creates a smaller decay coefficient for concentration variance (2.55), *i.e.*, a larger 'residence-time' for the concentration variance.

2.5 CONCLUSIONS

Substituting the correlation between squared concentration perturbations and velocity perturbations estimated in Section 2.3 Equation (2.23), and the variance dissipation term (Equations (2.28) and (2.34)) estimated in Section 2.4, into the conservation equation for the concentration variance (2.9b) yields

$$\frac{\partial \sigma_c^2}{\partial t} + v \frac{\partial \sigma_c^2}{\partial x_1} - v(A_{ij} + \alpha_{ij}) \frac{\partial^2 \sigma_c^2}{\partial x_i \partial x_j} = 2vA_{ij} \frac{\partial \bar{c}}{\partial x_i} \frac{\partial \bar{c}}{\partial x_j} - \chi \sigma_c^2 \quad (2.56)$$

$$\chi \equiv \frac{2v\alpha_{ij}}{\Delta_i^c \Delta_j^c}$$

The variance decay coefficient χ may be computed using (2.55) (and the constants evaluated in the Appendix-IV). The variance conservation equation (2.56) is coupled to the mean concentration governed by

$$\frac{\partial \bar{c}}{\partial t} + v \frac{\partial \bar{c}}{\partial x_1} - v(A_{ij} + \alpha_{ij}) \frac{\partial^2 \bar{c}}{\partial x_i \partial x_j} = 0 \quad (2.57)$$

The constant macrodispersivities A_{ij} used in (2.56), (2.57) hold under the condition of

sufficient smoothness of the mean concentration field, as compared to the correlation scales of the $\ln K$ field, and after sufficient travel time to enable sampling of the heterogeneity of the velocity field. The mean and variance of the concentration field undergo a translation with the mean velocity field. The macrodispersive flux for the mean and variance embodies the mechanism of transport due to the correlation of concentration and squared concentration perturbations, with the velocity perturbations, respectively.

The source term in the variance equation shows that the rate of creation of fluctuations increases quadratically with the mean concentration gradients. Therefore the rate of production of fluctuations decreases with an increase in the plume scale. The increase in the rate of production of concentration variance with an increase in the macrodispersivities points to an increased capacity of a mean concentration profile to produce concentration fluctuations in porous material with larger correlation scales and therefore greater longitudinal macrodispersivities.

If local dispersion is excluded, there is absolutely no mechanism to destroy the concentration variance created by the gradients in the mean concentration field (2.56). Therefore, the spatial integral of the concentration variance, a global measure of fluctuations, is nondecreasing (putting $\alpha_{ij} = 0$ in (2.10)). As argued in Section 2.2, in the absence of infinite gradients of the mean concentration field, there is absolutely no possibility of infinite variance; no matter what the value of local dispersion, positive or zero. Of course, the zero local dispersion case never occurs in real porous material. On assuming the small separation behavior of the concentration covariance function to be statistically stationary, the destruction of variance due to the action of local dispersion may be represented as a first order decay term with a decay coefficient equal to a sum in the three principal directions of twice the local dispersion coefficient divided by the squared concentration microscale (Equations (2.34a,b)). Therefore the smaller the ratio of the local dispersivity to the concentration microscale is, the slower is the action of local dispersivities in destroying concentration variance. A simplified analysis was made to

estimate the square of the concentration microscale (2.53). This estimate is made under the assumption that the $\ln K$ microscale is larger than the local dispersivities. The resulting variance decay coefficient χ increases with a decrease in the $\ln K$ microscale (2.55). This embodies the increased ability of local dispersion to destroy concentration fluctuations when the solute undergoes small scale chopping up due to the high wave number part of the velocity spectrum. Also, an increase in the low wave number energy of the $\ln K$ spectrum, will decrease the variance decay coefficient, due to the larger time taken by local dispersion, in dissipating concentration fluctuations with a larger microscale.

Since the growth of the spatial second moments of plumes is sensitive to the low wave number part of the $\ln K$ spectrum and most of the current studies of transport seek to refine the description of the spatial second moment of plumes, it may be (mistakenly) argued that a $\ln K$ statistical characterization strategy should focus primarily on the low wave number behavior. The mistake being the overlooking of the extreme insensitivity of spatial second moments to any measure of attenuation of point concentrations, and the strong role played by the small scale (high wave number) features of the $\ln K$ fields, along with the low wave number portion, in controlling the rate of destruction of concentration fluctuations and therefore attenuation of solute concentrations. If one eliminates the fine scale structure of $\ln K$ to a point that the plume consists of a few big 'blobs', they would be less amenable to the action of local dispersion and are likely to contain high concentration levels. Once the overall dimension of the plume is larger than the correlation scale, 'meandering' of the center of mass cannot be significant (by the law of large numbers). The spatial second moment of the plume would still be growing at an enhanced rate, yet the peak concentration would decrease at a much slower rate than the peak mean concentration, which is inversely proportional to the plume volume. The synergetic interaction of the high wave number $\ln K$ variations and the dissipating action of local dispersion, modeled approximately in (2.56), quantifies this phenomenon as it determines the concentration variance.

Dagan's [1982] and [1990], zero local dispersion analysis of concentration variance is shown (in Section 2.3, (2.26) and (2.27)) to be equivalent to (2.56) on putting local dispersivities equal to zero in it, *i.e.*, after dropping the local dispersive flux of the variance field, and more importantly, the variance dissipation term (the negative term on the right hand side of (2.56)) which is singularly created by the action local dispersion.

The variance equation (2.56) may be routinely solved along with the mean concentration, in numerical models using effective parameters. The spatial discretization requirements will be exactly the same as that for the mean concentration field. The time discretization for the variance field will also be dictated by the decay coefficient χ . Expressions for the decay coefficient for both isotropic and anisotropic, three dimensionally heterogeneous porous medium have been presented. Analytical solutions to the coupled concentration mean-variance system (2.56) and (2.57), for a multi-dimensional finite size impulse input, excluding and including local dispersion, are presented in Chapter 3.

CHAPTER 3

ADVECTION-DIFFUSION IN THREE-DIMENSIONALLY HETEROGENEOUS AQUIFERS: CONCENTRATION VARIANCE FOR A FINITE IMPULSE INPUT

For a multi-dimensional finite size impulse input, analytical solutions to the conservation equation for concentration variance σ_c^2 , derived in Chapter 2, are presented. Due to the dissipating action of local dispersion, at large times, σ_c is a decreasing fraction of the mean concentration. The Cape Cod bromide tracer exhibits this decrease. The larger the log-conductivity microscale is, the slower is the action of local dispersion, and the slower is the predicted rate of decrease of the ratio of σ_c and the mean concentration (*i.e.*, the coefficient of variation), with time, at large times, and vice-versa. The coefficient of variation increases with distance from the center. A balance between the rates of production and dissipation of σ_c^2 relates it linearly to the squared gradients of the mean concentration field, away from the center of mass. For the zero local dispersion case, σ_c is an unboundedly growing multiple of the mean concentration, with time. The longitudinal spatial second moment and macrodispersivities are insensitive to the inclusion/exclusion of local dispersion, therefore do not differentiate between the concentration fields for the two different cases. In contrast, the spatial-temporal evolution of σ_c^2 is singularly determined by the dissipating action of local dispersion. σ_c^2 quantifies the risk of exposure to large concentration levels as the probability that the concentration exceeds the mean by δ_c is bounded above by $(\sigma_c / \delta_c)^2$.

3.1 INTRODUCTION

The modeling of contaminant transport using an effective advection-dispersion equation, with effective (macro)dispersivities is common practice. The effective dispersion coefficient embodies the effect of (unresolved) advective-heterogeneity on the spatial second moment, *i.e.*, the squared radius (of gyration) of plumes. The 'mean concentration' plume that results from such an exercise is smooth, due to the lack of resolution of the detailed advective heterogeneity. While the spatial extent of the plume may be reproduced in the 'mean concentration' plume, actual concentrations will vary around the 'mean concentration'. How large are these variations? Are these variations a large multiple of the mean concentration? Do concentration levels show a decrease commensurate with the rate of increase of the spatial extent of the plume? Do the concentration variations become smaller fractions of the mean concentration in time, or do they become progressively larger multiples of the mean concentration with time? Is the peak of the mean concentration a good predictor of peak concentration levels at large times? How unlikely is it that a point will be hit by a concentration 10, 50, 100..... times the mean concentration? These questions arise in assessing exposure levels to toxic substances in aquifers. The mean squared concentration fluctuations, *i.e.*, concentration variance, was shown to be governed by a conservation equation in Chapter 2. In this chapter is presented the solution to the concentration variance equation and answers to aforementioned questions.

The scale of fluctuations of the hydraulic conductivity being entertained in this study are small compared to the plume scale, as it is under this scale disparity that an effective advection-dispersion equation is applicable to determine the mean concentration. In the absence of this scale disparity, any spatially-temporally local approximations for the macrodispersive flux are indefensible, as argued in Chapter 2. The importance of explicitly incorporating large-scale identifiable trends in assessing bulk

transport features can be appreciated from the recent work of Adams and Gelhar [1992]. The implications of the lack of knowledge of such large scale trends is not explored here. The fluctuations associated with the enhanced dispersion caused by the smaller scale fluctuations are the concern in this work. Another fundamental property, that the $\ln K$ field is assumed to have, is a finite microscale. The $\ln K$ microscale being the scale that characterizes the derivatives of the $\ln K$ field. The fluctuation dissipation mechanism is shown to be sensitive to this scale in Chapter 2, under the assumption that it is larger than the local dispersivities.

The coefficient of variation of the concentration is defined as the standard deviation of concentration divided by its mean. A decrease in the concentration standard deviation with time alone is no indication of the proximity of a sample plume with the ensemble mean, as the mean concentration itself decreases with time. The point at which the concentration standard deviation is the largest is not necessarily the point where our ability to predict concentrations is the poorest, because the mean concentration itself may be large at that point. The regions in which the coefficient of variation is small are the regions for which the mean concentration is a good predictor of the actual concentration levels in a sample realization of a hydraulic conductivity field.

The concentration variance equation which is coupled to the mean concentration equation (derived in Chapter 2) is solved for the case of a finite size impulse input in Section 3.2. Simple analytical expressions for the variance and coefficient of variation for a macroscopically multi-dimensional plume, being transported in three dimensionally heterogeneous medium, are presented. A sharp qualitative and quantitative contrast is found between the hypothetical hyperbolic-nondissipative-zero local dispersion case in Section 3.3, and the more realistic parabolic-dissipative case including local dispersion. Section 3.4 presents an analyses of the Cape-Cod bromide tracer for concentration fluctuations and compares observations with the developed theory. In Section 3.5 is presented a discussion of the implications of the results developed in this work.

**3.2 CONCENTRATION VARIANCE FOR A MULTIDIMENSIONAL
FINITE-SIZE IMPULSE INPUT IN THREE DIMENSIONALLY
HETEROGENEOUS AQUIFERS
(INCORPORATING FLUCTUATION DISSIPATING ACTION OF
LOCAL DISPERSION)**

The pair of partial differential equations needed to study concentration variance from Chapter 2 are for the mean concentration

$$\frac{\partial \bar{c}}{\partial t} + v \frac{\partial \bar{c}}{\partial x_1} - v(A_{ij} + \alpha_{ij}) \frac{\partial^2 \bar{c}}{\partial x_i \partial x_j} = 0 \quad (3.1a)$$

with an initial condition

$$\bar{c}(\mathbf{x}, t) = f(\mathbf{x}) \quad (3.1b)$$

and for the concentration variance

$$\frac{\partial \sigma_c^2}{\partial t} + v \frac{\partial \sigma_c^2}{\partial x_1} - v(A_{ij} + \alpha_{ij}) \frac{\partial^2 \sigma_c^2}{\partial x_i \partial x_j} = 2vA_{ij} \frac{\partial \bar{c}}{\partial x_i} \frac{\partial \bar{c}}{\partial x_j} - \chi \sigma_c^2 \quad (3.2a)$$

with the initial condition

$$\sigma_c^2(\mathbf{x}, 0) = 0 \quad (3.2b)$$

Recall the definition of the variance dissipation coefficient;

$$\chi \equiv \frac{2v\alpha_{ij}}{\Delta_i^c \Delta_j^c} \quad (3.2c)$$

The variance equation (3.2a) is coupled to the mean equation (3.1a) on account of the source term, which is the mechanism of producing concentration variance. In (3.1a) and (3.2a), A_{ij} and α_{ij} are the macrodispersivities and local dispersivities respectively. The mean velocity in the x_1 direction is v . Δc_i are the microscales of the concentration field in the i th direction. It needs to be kept in mind that the description of the mean concentration using constant macrodispersivities A_{ij} holds well for impulse inputs after the plume has sampled the heterogeneous velocity fluctuations and the mean concentration field is sufficiently smooth. The fluctuations in point concentrations that are embodied in the ensemble of realizations (for which the mean is computed by solving (3.1)) may be assessed by solving (3.2) for the point concentration variance. The parameter A_{ij} may be computed from the various results, in previously developed theories, and the variance decay coefficient χ may be computed from the results developed for the concentration microscales Δc_i in Chapter 2. The variance decay coefficient χ embodies the effect of increased ability of local dispersion to destroy fluctuations for smaller concentration microscales and vice-versa, a feature ubiquitous in advection-dispersion phenomenon (due to the parabolic transport operator), as discussed in Chapter 2, and Appendix-I and II.

3.2.1 SOLUTION

The mean concentration, governed by Equation (3.1a), for a point impulse input, is a Gaussian. The squared spatial partial derivatives of that Gaussian will be the source term in the variance equation (3.2a). To account for a finite initial size and avoid the unreal problem of an infinite source term in the variance equation due to a *point* impulse input, it is replaced by a finite size Gaussian. Thus, consistent with the mean concentration equation (3.1a), and the chosen initial conditions, the mean concentration is taken to be

$$\bar{c}(\mathbf{x}, t) = \frac{M}{n} \prod_{i=1}^N \frac{\exp\left[-\frac{(x_i - v\delta_{i1}t)^2}{4(A_{ii} + \alpha_{ii})v(t + t_{0i})}\right]}{\sqrt{4\pi(A_{ii} + \alpha_{ii})v(t + t_{0i})}} \quad (3.3)$$

where t_{0i} , the 'initial dilation time', provide an initial dimension to the concentration field. N is the macroscopic dimensionality of the plume being transported in the three dimensionally heterogeneous medium of porosity n . M is the total mass of solute. Defining the radius (of gyration) of the mean concentration plume in the i th direction to be

$$R_i(t) = \left[\frac{\int_{-\infty}^{+\infty} \bar{c}(\mathbf{x}, t) (x_i - v\delta_{i1}t)^2 dx}{\int_{-\infty}^{+\infty} \bar{c}(\mathbf{x}, t) dx} \right]^{\frac{1}{2}} \quad (3.4)$$

For the Gaussian mean concentration in equation (3.3) it may be shown that

$$R_i(t) = \sqrt{2(A_{ii} + \alpha_{ii})v(t + t_{0i})} \quad (3.5)$$

therefore the relationship of the initial dilation time t_{0i} to the initial radius of the plume is

$$t_{0i} = \frac{R_i(0)^2}{2(A_{ii} + \alpha_{ii})v} \quad (3.6)$$

Defining L_{AD} as the advection-dispersion operator

$$L_{AD} \equiv \frac{\partial}{\partial t} + v \frac{\partial}{\partial x_1} - v(A_{ij} + \alpha_{ij}) \frac{\partial^2}{\partial x_i \partial x_j} \quad (3.7)$$

the solution for ψ governed by

$$L_{AD} \psi = F(x, t) \quad (3.8a)$$

is

$$\psi(x, t) = \int_{-\infty}^{+\infty} G(x - \eta, t) \psi(\eta, 0) d\eta + \int_{\tau=0}^t \left\{ \int_{-\infty}^{+\infty} G(x - \eta, t - \tau) F(\eta, \tau) d\eta \right\} d\tau \quad (3.8b)$$

where G , the impulse response function (Green's function) for the advection-dispersion operator (3.7) is

$$G(x - \eta, t - \tau) = \prod_{i=1}^N \frac{\exp\left\{ -\frac{[(x_i - \eta_i) - v\delta_{i1}(t - \tau)]^2}{4(A_{ii} + \alpha_{ii})v(t - \tau)} \right\}}{\sqrt{4\pi(A_{ii} + \alpha_{ii})v(t - \tau)}} \quad (3.9)$$

Scaling the variance in time as

$$s(x, t) \equiv \sigma_c^2(x, t) \exp(\chi t) \quad (3.10)$$

and substituting into the variance equation (3.2a) gives

$$L_{AD} s(x, t) = 2vA_{ij} \frac{\partial^2}{\partial x_i \partial x_j} \exp(\chi t) \quad (3.11)$$

The solution for the scaled variable may be computed by (3.8b). Transforming the solution back into the concentration variance gives

$$\sigma_c^2(\mathbf{x}, t) = \int_{\tau=0}^t e^{-\lambda(t-\tau)} \left\{ \int_{-\infty}^{+\infty} G(\mathbf{x}-\boldsymbol{\eta}, t-\tau) \left[2\nu A_{ij} \frac{\partial \bar{c}}{\partial x_i} \frac{\partial \bar{c}}{\partial x_j} \right]_{\boldsymbol{\eta}, \tau} d\boldsymbol{\eta} \right\} d\tau \quad (3.12)$$

The concentration variance (3.12) may be split into different parts, created due to mean gradients in the different principal directions

$$\sigma_c^2(\mathbf{x}, t) = \sum_{i=1}^N \sigma_{c[i]}^2(\mathbf{x}, t) \quad (3.13)$$

where

$$\sigma_{c[i]}^2(\mathbf{x}, t) = \int_{\tau=0}^t e^{-\lambda(t-\tau)} \left\{ \int_{-\infty}^{+\infty} G(\mathbf{x}-\boldsymbol{\eta}, t-\tau) \left[2\nu A_{ii} \left(\frac{\partial \bar{c}}{\partial x_i} \right)^2 \right]_{\boldsymbol{\eta}, \tau} d\boldsymbol{\eta} \right\} d\tau \quad (3.14)$$

From the expression for the mean concentration (3.3) we have for its spatial partial derivatives

$$\frac{\partial \bar{c}}{\partial x_i} = - \frac{(x_i - \nu \delta_{i1} t)}{2(A_{ii} + \alpha_{ii})\nu(t + t_{0i})} \bar{c} \quad (3.15)$$

This is substituted into the integrand in (3.14). The integrand, becomes a product of exponentials, each having an argument quadratic in a spatial dummy variable, and is multiplied by the square of the i th dummy spatial variable. Therefore using the two simple integrals

$$\int_{-\infty}^{+\infty} e^{-\frac{(ay^2 + by + c)}{d}} dy = \sqrt{\frac{\pi d}{a}} \exp\left[-\left(\frac{c}{d} - \frac{b^2}{4ad}\right)\right] \quad (3.16a)$$

and

$$\int_{-\infty}^{+\infty} y^2 e^{-\frac{(ay^2 + by + c)}{d}} dy = \frac{\sqrt{\pi}}{2} \left(\frac{d}{a}\right)^{\frac{3}{2}} \left(1 + \frac{b^2}{2ad}\right) \exp\left[-\left(\frac{c}{d} - \frac{b^2}{4ad}\right)\right] \quad (3.16b)$$

the spatial integration in (3.14) may be exactly carried out to get

$$\sigma_{c[i]}^2(\mathbf{x}, t) = \quad (3.17)$$

$$2vA_{ii} \int_{\tau=0}^t \left[\left(\frac{M}{n}\right)^2 \prod_{j=1}^N \frac{\exp\left[-\frac{(x_j - v\delta_{j1}\tau)^2}{2(A_{jj} + \alpha_{jj})v(2t + t_{0j} - \tau)}\right]}{4\pi(A_{jj} + \alpha_{jj})v\sqrt{(2t + t_{0j} - \tau)(\tau + t_{0j})}} \right] \times$$

$$\left[\frac{(t - \tau)}{2(A_{ii} + \alpha_{ii})v(2t + t_{0i} - \tau)(\tau + t_{0i})} + \frac{(x_i - v\delta_{i1}\tau)^2}{4[(A_{ii} + \alpha_{ii})v(2t + t_{0i} - \tau)]^2} \right] e^{-\chi(t-\tau)} d\tau$$

At large times, the primary contribution for this one-dimensional time integral (3.17) comes from a region around t , due to the exponential weighting in time and the non zero t_{0i} . Therefore, approximately

$$\sigma_{c[i]}^2(\mathbf{x}, t) = 2vA_{ii} c^{-2} \left[\frac{1}{2(A_{ii} + \alpha_{ii})v(t + t_{0i})^2} \int_{\tau=0}^t (t - \tau) e^{-\chi(t-\tau)} d\tau + \frac{(x_i - v\delta_{i1}t)^2}{4[(A_{ii} + \alpha_{ii})v(t + t_{0i})]^2} \int_{\tau=0}^t e^{-\chi(t-\tau)} d\tau \right] \quad (3.18)$$

In making this approximation it is being assumed that the primary contribution for the first part of integral (3.17) comes from the point of maximum of

$$(t - \tau) e^{-\chi(t - \tau)}$$

i.e., from

$$\tau = t - \frac{1}{\chi}$$

To be able to take terms (evaluated at time t) out of the integrand in (3.17) it is being assumed that

$$t \gg \frac{1}{\chi} \quad (3.19)$$

Moreover for the maximum contribution in the integral (3.17) to come from around time t it is assumed that the function

$$\phi_i(\tau) = \frac{(t - \tau) e^{-\chi(t - \tau)}}{(\tau + t_{0i}) \left(\prod_{j=1}^N \sqrt{\tau + t_{0j}} \right)} \quad (3.20)$$

evaluated at $\tau = t - 1/\chi$, is much larger than what it is at its other potential maximum point, at $\tau = 0$. Thus, the finite initial size and finite χ enables a localization of the time integral (3.17). The exponential (3.20) in this approximation condition, will help it to be met, for finite size impulse inputs. For the integrals in (3.18) we have at large time that

$$t \gg \frac{1}{\chi} \quad \Rightarrow \quad \int_{\tau=0}^t e^{-\chi(t - \tau)} d\tau \cong \frac{1}{\chi} \quad (3.21a)$$

and

$$\ln[t] + \chi t \gg \ln[\chi] \Rightarrow \int_{\tau=0}^t (t - \tau) e^{-\chi(t-\tau)} d\tau \cong \frac{1}{\chi^2} \quad (3.21b)$$

Substituting these integrals into (3.18) and substituting for the partial derivative of the concentration field (3.15) appropriately in (3.18) gives for the variance *created* due to spatial partial derivatives of the mean concentration field in the i th direction

$$\sigma_{c[i]}^2(\mathbf{x}, t) = \frac{A_{ii}}{(A_{ii} + \alpha_{ii})(t + t_{0i})^2 \chi^2} \bar{c}^2 + \frac{2\nu A_{ii}}{\chi} \left(\frac{\partial \bar{c}}{\partial x_i} \right)^2 \quad (3.22)$$

Therefore for the total concentration variance (3.13) we have

$$\sigma_c^2(\mathbf{x}, t) = \sum_{i=1}^N \left[\frac{A_{ii}}{(A_{ii} + \alpha_{ii})(t + t_{0i})^2 \chi^2} \bar{c}^2 + \frac{2\nu A_{ii}}{\chi} \left(\frac{\partial \bar{c}}{\partial x_i} \right)^2 \right] \quad (3.23)$$

Dividing the variance (3.23) by the square of the mean concentration (3.3) and taking the square root gives for the concentration coefficient of variation

$$\frac{\sigma_c(\mathbf{x}, t)}{\bar{c}(\mathbf{x}, t)} = \left[\sum_{i=1}^N \left\{ \frac{A_{ii}}{(A_{ii} + \alpha_{ii})(t + t_{0i})^2 \chi^2} + \frac{2\nu A_{ii}}{\chi} \left(\frac{\partial \ln \bar{c}}{\partial x_i} \right)^2 \right\} \right]^{\frac{1}{2}} \quad (3.24)$$

Substituting the expressions for the mean concentration (3.3) and its spatial partial derivatives (3.15) into (3.23) and (3.24), we have for the space-time description of the concentration variance and the coefficient of variation,

$$\sigma_c^2(x, t) = \frac{M^2}{n^2} \left\{ \prod_{i=1}^N \frac{\exp\left[-\frac{(x_i - v\delta_{i1}t)^2}{2(A_{ii} + \alpha_{ii})v(t + t_{0i})}\right]}{4\pi v (A_{ii} + \alpha_{ii})(t + t_{0i})} \right\} \times \left[\sum_{i=1}^N \frac{A_{ii}}{(A_{ii} + \alpha_{ii})(t + t_{0i})^2} \left(\frac{1}{\chi^2} + \frac{(x_i - v\delta_{i1}t)^2}{2(A_{ii} + \alpha_{ii})v\chi} \right) \right] \quad (3.25)$$

and

$$\frac{\sigma_c(x, t)}{\bar{c}(x, t)} = \left[\sum_{i=1}^N \frac{A_{ii}}{(A_{ii} + \alpha_{ii})(t + t_{0i})^2} \left(\frac{1}{\chi^2} + \frac{(x_i - v\delta_{i1}t)^2}{2(A_{ii} + \alpha_{ii})v\chi} \right) \right]^{1/2} \quad (3.26)$$

The large time asymptotic nature of the time localization approximations of the one-dimensional time integral (3.17) to derive the expressions (3.23)-(3.26) has been corroborated by machine (shown in Section 3.4). Equations (3.23)-(3.26) present the correct 'large time' (quantified by conditions (3.19)-(3.21)) solution to the variance equation (3.2a) for finite size impulse inputs (3.3). The implications and interpretations of the simple analytical solution (3.23)-(3.26) are presented in the following subsection.

3.2.2 SPATIAL-TEMPORAL CHARACTERISTICS OF CONCENTRATION FLUCTUATIONS

From the expressions (3.25) and (3.26) it is evident that away from the center of the plume, *i.e.*, for

$$|x_i - v\delta_{i1}t| \gg \sqrt{\frac{(A_{ii} + \alpha_{ii})v}{\chi}} \quad (3.27)$$

we may write approximately for the variance (3.25)

$$\sigma_c^2(\mathbf{x},t) \equiv \frac{2\nu A_{ij}}{\chi} \frac{\bar{c}}{\partial x_i} \frac{\bar{c}}{\partial x_j} \quad (3.28)$$

and for the coefficient of variation (3.26)

$$\frac{\sigma_c(\mathbf{x},t)}{\bar{c}(\mathbf{x},t)} \equiv \left[\frac{2\nu A_{ij}}{\chi} \frac{\partial \ln \bar{c}}{\partial x_i} \frac{\partial \ln \bar{c}}{\partial x_j} \right]^{\frac{1}{2}} \quad (3.29)$$

Note that a sum over repeated indices is implied in (3.28), and (3.29). These local relationships in space and time (3.28)-(3.29), hold under the condition that the point under consideration be away from the center of mass as given by (3.27), in addition to the condition of large time, imposed in evaluating (3.17). The local relationships may be directly argued from the variance equation (3.2a); when the concentration variance spatial derivatives and temporal rate of change are relatively small, then the source and sink terms on the right hand side of equation (3.2a) must balance each other. Under these conditions, the rate at which the concentration variance is being produced, is matched, by the rate at which local dispersivities is destroying it. This balance is expressed by the linear relationship between the variance and the squared gradients in (3.28). The fluctuations created by the mean gradients are being destroyed by the action of local dispersion, before they can be significantly transported. The smaller the variance decay coefficient in (3.27), the further away from the center of the plume is such a balance going to take place. The balance (3.28), deduced here under explicit conditions, is often presumed in studying mean squared fluctuations of transport quantities [*e.g.*, Tennekes and Lumley, 1972, Equation 3.4.2]. The variance decay coefficient χ and the

macrodispersion coefficient directly determine the fluctuations a mean concentration gradient will be accompanied with as expressed in (3.28) and (3.29).

Vomvoris and Gelhar [1991] have also presented a linear relationship between concentration variance and the squared spatial derivatives of the mean concentration field. They do not present their linear relationship as a balance between the rates of production and destruction of concentration variance, as is the case in this work under explicit conditions of large time and distance from the center of mass of the plume. The conditions under which the linear relationship (3.28) holds, the advective, local dispersive and macrodispersive transport, and local rate of change terms in the variance equation are unimportant, as the rate of production and dissipation of concentration variance are balancing each other. Vomvoris and Gelhar [1991] have dropped the macrodispersive term for the variance field (as pointed out in Chapter 2), yet retain the local dispersive and advective transport terms. Therefore the linear relationship (3.28) between concentration variance and the squared gradients of the mean concentration field (a limiting case of the general result (3.23) for a finite impulse input), reflecting a balance in the rates of production and dissipation of concentration variance, is different from Vomvoris and Gelhar's [1991] result.

Some of the results of Vomvoris and Gelhar [1991] contradict inferences from the variance conservation equation (3.2a). For example, for finite gradients of the mean concentration field, in the variance formulation (3.2a), the concentration variance can never be infinite, for any value of local dispersivity, even if it is set to zero, unlike Vomvoris and Gelhar [1991]. Also, concentration variance is never zero, even at points of zero gradients of the mean concentration field, due to the local and macrodispersive flux of the variance field. Whereas in Vomvoris and Gelhar [1991], the concentration variance at points of zero gradients of the mean concentration field is identically zero. In Vomvoris and Gelhar [1991], it is the transverse local dispersion that plays a singularly important role. In the formulation over here, a priori, there is no such preferential

importance of the transverse local dispersion, as the variance decay coefficient reflects the ratio of local dispersion and the concentration microscale in different directions. As pointed out in Section 2.2, in Vomvoris's [1986] and Gelhar and Gutjahr's [1982] results, the coefficient of variation for the case of a solute undergoing a first order decay with a constant decay coefficient is different from that for a nonreactive solute. In this work, the coefficient of variation is the same for both the cases.

As the local dispersion decreases, the variance decay coefficient decreases, and the concentration variance and coefficient of variation increases in (3.28) and (3.29). However, the large time condition (3.19)-(3.21) on the analytical solution, explicitly dictates that as the variance decay coefficient becomes smaller, the simple analytical expressions derived here, hold at increasingly larger times. In that sense, the large time solution to the variance equation is found to be singularly dependent on the action of local dispersion. The solution for concentration variance for the hypothetical zero-local dispersion case (presented in the next section) bears no resemblance to the large time solution for the concentration variance developed here (3.23)-(3.26).

The increase in the mean models ability to predict actual concentrations with time may be seen from the expression for coefficient of variation (3.26) from which it follows for points

$$\mathbf{x} \text{ such that } x_i \leq \eta R_i(t), \quad \frac{\sigma_c(\mathbf{x}, t)}{\bar{c}(\mathbf{x}, t)} < \left[N \left(\frac{1}{(\chi t)^2} + \frac{\eta^2}{\chi t} \right) \right]^{1/2} \quad (3.30)$$

Recall that N is the macroscopic dimensionality of the plume.

The global fluctuation measure (defined as a spatial integral of the concentration variance) may be studied by integrating (3.2a) in space to get

$$\frac{d}{dt} \|\sigma_c^2\| = 2\nu A_{ij} \left\| \frac{\partial \bar{c}}{\partial x_i} \frac{\partial \bar{c}}{\partial x_j} \right\| - \chi \|\sigma_c^2\| \quad (3.31)$$

For the macroscopically one dimensional mean concentration ($N = 1$ in (3.3)), the global fluctuation measure may be solved for, to get at large time

$$\| \sigma_c^2(x_1, t) \| = \frac{1}{8} \sqrt{\frac{2}{\pi}} \left(\frac{M}{n} \right)^2 \frac{A_{11}}{\sqrt{v}(A_{11} + \alpha_L)^{3/2} \chi(t + t_{01})^{3/2}} \quad (3.32)$$

therefore

$$\lim_{t \rightarrow \infty} \| \sigma_c^2(x_1, t) \| \rightarrow 0 \quad (3.33)$$

Also, for the macroscopically three dimensional case ($N = 3$ in (3.3)), it may be shown that

$$\lim_{t \rightarrow \infty} \| \sigma_c^2(\mathbf{x}, t) \| \propto \frac{1}{t^{5/2}} \rightarrow 0 \quad (3.34)$$

The generic properties of concentration standard deviation in space, and the coefficient of variation in space and in time (at a fixed point) for the macroscopically one dimensional case at large times, are given in Figures 3.1, 3.2 and 3.3. The double peaked behavior in Figure 3.1 simply reflects the nature of the spatial derivative of the mean concentration field, the square of which is a source term in the variance equation (3.2a). Gelhar *et al.* [1981], Vomvoris [1986] and Vomvoris and Gelhar [1990] report such a dependence of the concentration variance. Graham and McLaughlin [1989] and Li and McLaughlin [1991] observed such bi-modal structures in their numerical results. The non zero value of the concentration standard deviation at the center in Figure 3.1 reflects the effects of transport of fluctuations (variance) by local and macrodispersive mechanisms as embedded in the variance conservation equation (3.2a). In their numerical results, Graham and McLaughlin [1989], and Li and McLaughlin [1991] observe nonzero

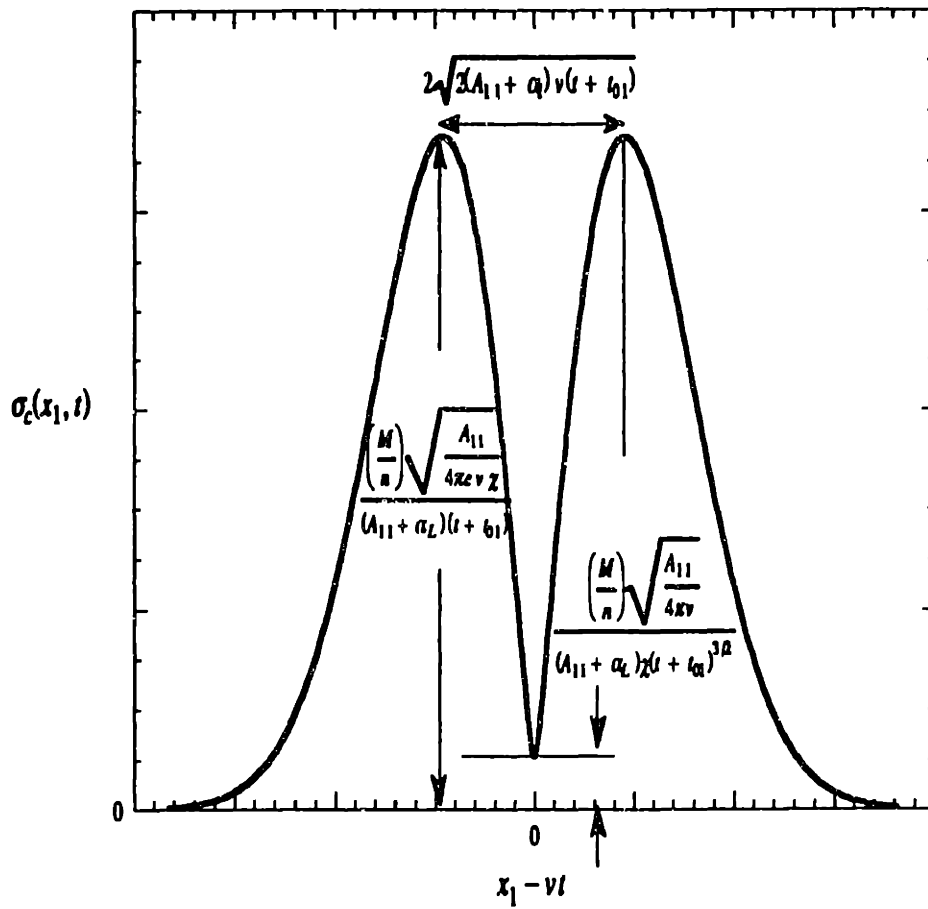


Figure 3.1
Standard deviation of concentration.

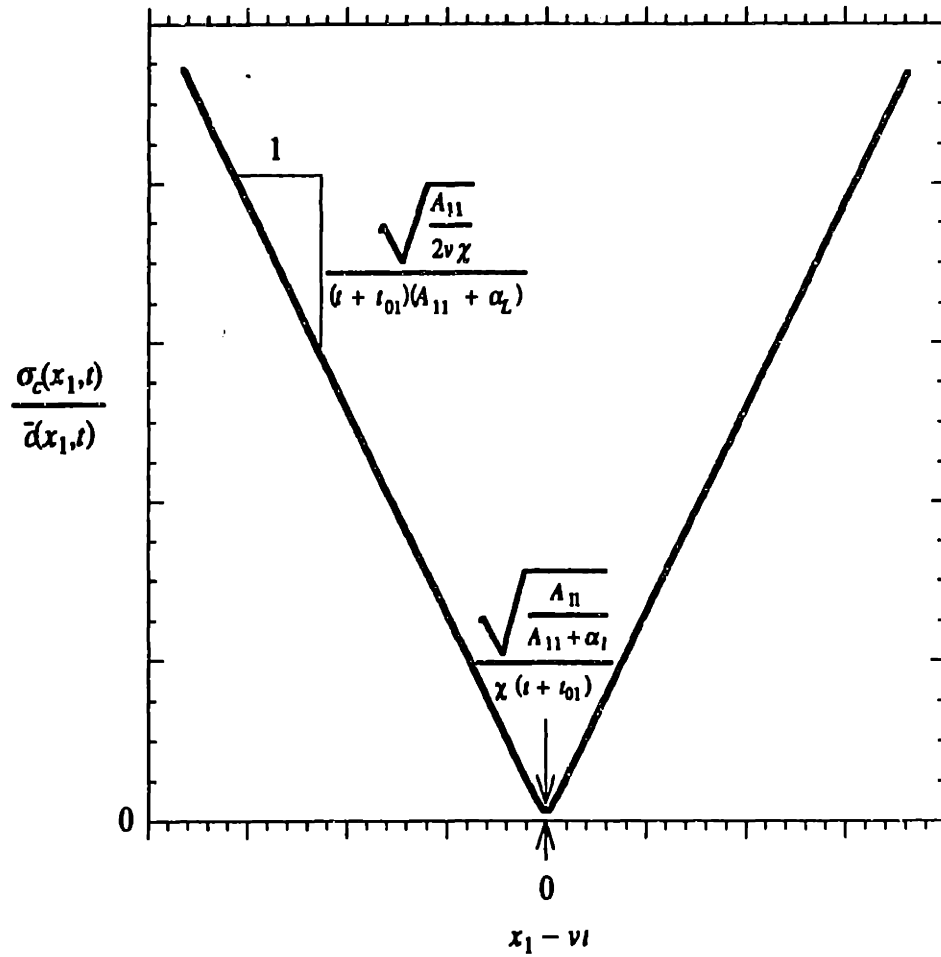


Figure 3.2

Coefficient of variation of concentration.

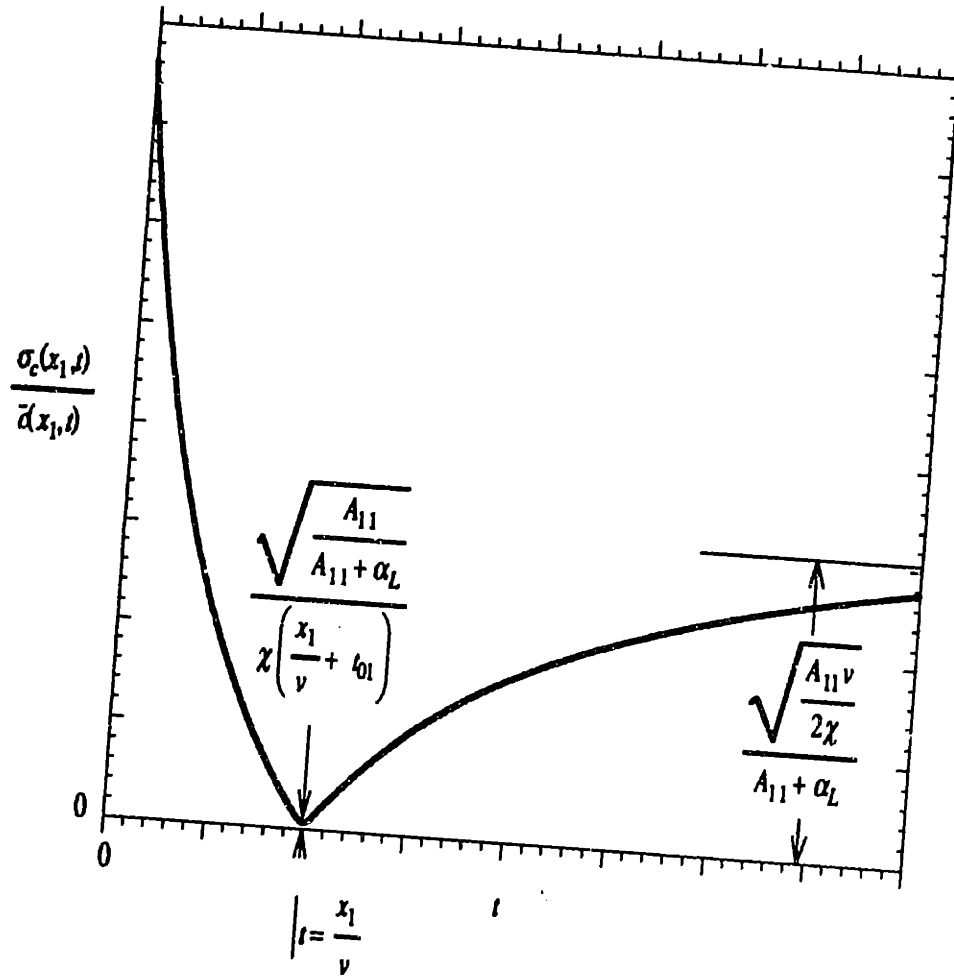


Figure 3.3
Breakthrough coefficient of variation of concentration.

concentration variances at points of zero gradients of the mean concentration field. In contrast, the results of Gelhar *et al.* [1981], Vomvoris [1986] and Vomvoris and Gelhar [1990] predict zero concentration variance at points of zero gradients for the mean concentration field. In this work, the reflection of the squared gradient of the mean concentration field in the shape of the concentration variance is sustained at large times, as the dissipating action of local dispersion destroys fluctuations created at previous times. In the absence of the destruction of concentration variance, the dispersive (local and macrodispersive) fluxes of variance would get rid of the bi-modality as time progresses. The bi-modality of the concentration standard deviation is interesting, insofar it is related to the dynamics of creation and destruction of concentration variance, as is explicitly described in this work. However, as the mean concentration varies in space, a plot of the standard deviation on its own is not very useful in assessing the capacity of the mean concentration to predict concentrations. In fact the occurrence of the peak of the standard deviations near the center of the plume is quite misleading, as the coefficient of variation is actually small at the center of the plume, in Figure 3.2. The decrease in the coefficient of variation in time at the center of mass and throughout the plumes is evident in Figure 3.2. Equally important to note in this figure is the linear increase in the coefficient of variation with distance away from the center of mass (Equation(3.26)) thereby showing the inevitable difficulty in predicting concentrations at the fringes of plumes using the mean concentration equation. An associated feature is that the coefficient of variation at a point asymptotes to a non zero constant value at a given point in space at large times as shown in Figure 3.3 (after the plume has passed that point).

Most importantly it is shown in Figure 3.2 that the coefficient of variation at the center goes down inversely with time. The variance decay coefficient determines how fast this decrease takes place. Therefore, for the case of a finite impulse input, the rate of decrease in peak mean concentration of the solute with time (determined by the value of the macrodispersivity) will indeed be matched by the peak concentration in a sample

realization at large times. Thus if peak concentrations are to define a measure of "dilution", the enhanced rate of increase of the spatial second moment of the plume due to velocity heterogeneities do translate into enhanced dilution at *large time* for impulse inputs. The variance decay coefficient, which increases as the concentration microscales decrease, strongly determines how long a time it takes for this to happen. The greater the low-wave number component of the $\ln K$ spectrum (subject to assumption that the mean concentration field is smoother than the $\ln K$ field) the slower is the action of local dispersion in dissipating fluctuations, the smaller is the variance decay coefficient χ , the slower the rate of decrease of the coefficient of variation (3.26). The greater the high wave number component of the $\ln K$ spectrum (subject to $\ln K$ microscales being greater than local dispersivities), the faster the action of local dispersion in destroying concentration fluctuations, the larger the variance decay coefficient χ , the faster the rate of decrease of the coefficient of variation (3.26). For impulse inputs it needs to be recognized that the gradients in the mean concentration field which are responsible for creating fluctuations are themselves dying out with time. The feature of the standard deviation of concentration dying out faster in time than the mean concentration in (3.30) is strongly influenced by the rate of decrease of the gradients of the mean concentration as evident from (3.28).

The results for the variance and coefficient of variation (3.25) and (3.26), show a weak dependence on the t_{0i} , and therefore initial dimensions of the plume. The initial dilution time always appears as a sum with time, and therefore plays a role of decreasing importance at large times. At large times, the initial dimensions of the plume, are only weakly reflected in the concentration fluctuations. It needs to be kept in mind though, the results (3.25), and (3.26) were computed on assuming a finite initial plume dimension, and the large time, after which they hold is inversely dependent on the initial plume dimension, in (3.20).

3.3 HYPOTHETICAL, HYPERBOLIC, NON-DISSIPATIVE, ZERO LOCAL DISPERSION CASE

The mean concentration for a macroscopically multidimensional plume for the zero local dispersion case is governed by

$$\frac{\partial \bar{c}}{\partial t} + v \frac{\partial \bar{c}}{\partial x_1} - v A_{ij} \frac{\partial^2 \bar{c}}{\partial x_i \partial x_j} = 0 \quad (3.35)$$

For the zero local dispersion case there is no sink term in the concentration variance equation (3.2a), therefore the variance is governed by

$$\frac{\partial \sigma_c^2}{\partial t} + v \frac{\partial \sigma_c^2}{\partial x_1} - v A_{ij} \frac{\partial^2 \sigma_c^2}{\partial x_i \partial x_j} = 2v A_{ij} \frac{\partial \bar{c}}{\partial x_i} \frac{\partial \bar{c}}{\partial x_j} \quad (3.36)$$

which is equivalent to

$$\frac{\partial \bar{c}^2}{\partial t} + v \frac{\partial \bar{c}^2}{\partial x_1} - v A_{ij} \frac{\partial^2 \bar{c}^2}{\partial x_i \partial x_j} = 0 \quad (3.37)$$

Equation (3.37) reflects the trivial fact that all powers of concentration field are governed by the same hyperbolic transport operator, for the non-dissipative zero local dispersion case. Consequently the expectations of the two powers are governed by the same operator (see Chapter 2). The mechanisms of creation and dispersal of concentration variance embodied in (3.36) and (3.37) are precisely the same as in Dagan's [1982], [1990] zero local dispersion concentration variance model, as shown in Chapter 2.

3.3.1 SOLUTION

Consider the mean concentration solution to (3.35) to be a Gaussian

$$\bar{c}(\mathbf{x}, t) = \frac{M}{n} \prod_{i=1}^N \frac{\exp\left[-\frac{(x_i - v\delta_{i1}t)^2}{4A_{ii}v(t + t_{0i})}\right]}{\sqrt{4\pi A_{ii}v(t + t_{0i})}} \quad (3.38)$$

which has finite dimensions at initial time. The initial conditions on the mean of the squared concentration for zero initial variance is

$$\overline{c^2(\mathbf{x}, 0)} = [\bar{c}(\mathbf{x}, 0)]^2 = \left(\frac{M}{n}\right)^2 \prod_{i=1}^N \frac{\exp\left[-\frac{x_i^2}{2A_{ii}v t_{0i}}\right]}{4\pi A_{ii}v t_{0i}} \quad (3.39)$$

The solution for the mean value of the squared concentration may be easily found by the integral

$$\overline{c^2(\mathbf{x}, t)} = \int_{-\infty}^{+\infty} G(\mathbf{x}-\boldsymbol{\eta}, t) \overline{c^2(\boldsymbol{\eta}, 0)} d\boldsymbol{\eta} \quad (3.40)$$

with

$$G(\mathbf{x}-\boldsymbol{\eta}, t-\tau) = \prod_{i=1}^N \frac{\exp\left\{-\frac{[(x_i - v\delta_{i1}(t-\tau)) - \eta_i]^2}{4A_{ii}v(t-\tau)}\right\}}{\sqrt{4\pi A_{ii}v(t-\tau)}} \quad (3.41)$$

the Green's (or impulse response) function. The integral (3.40) may be computed exactly as the integrand is an exponential with a quadratic argument (a feature exploited in the evaluations in Section 3.2). This gives for the coefficient of variation

$$\left[\frac{\sigma_c(x,t)}{\bar{c}(x,t)} \right]^2 = \left\{ \prod_{i=1}^N \frac{(t+t_{0i})}{\sqrt{t_{0i}(2t+t_{0i})}} \exp \left[\frac{2t}{2t^2+3t t_{0i}+t_{0i}^2} \cdot \frac{(x_i - v\delta_{i1}t)^2}{4A_{ii}v} \right] \right\} - 1 \quad (3.42)$$

3.3.2 EXPLODING HYPERBOLIC PLUMES

From the solution (3.42), at the center of the plume

$$\left[\frac{\sigma_c}{\bar{c}} \right]_{x_i = \delta_{i1}vt} = \left[\left(\prod_{i=1}^N \frac{(t+t_{0i})}{\sqrt{t_{0i}(2t+t_{0i})}} \right) - 1 \right]^{1/2} \quad (3.43)$$

which under the condition $t \gg t_{01}$ becomes

$$\left[\frac{\sigma_c}{\bar{c}} \right]_{x_i = \delta_{i1}vt} = \left[\left(\prod_{i=1}^N \sqrt{\frac{t}{2t_{0i}}} \right) - 1 \right]^{1/2} \quad (3.44)$$

Therefore at the center of mass of a macroscopically three dimensional plume ($N = 3$) which is also the point of minimum coefficient of variation,

$$\lim_{t \rightarrow \infty} \left[\frac{\sigma_c}{\bar{c}} \right]_{x_i = \delta_{i1}vt} \approx \frac{t^{3/4}}{2^{3/4}(t_{01}t_{02}t_{03})^{1/4}} \rightarrow \infty \quad (3.45)$$

The plume is 'exploding'. This unbounded increase in the coefficient of variation is in sharp contrast to the case including local dispersion (Figure 3.2 and Equation 3.30), in

which the coefficient of variation decreases with time. This unbounded growth of the coefficient of variation with time is implied by Dagan's [1982], [1990] model of concentration variance and was observed in non diffusive particle simulations by Rubin [1991]. The difference between the hypothetical zero local dispersion case and the more realistic case including the dissipating action of local dispersion is a stark one; it is a difference in the sign of the rate of change of the coefficient of variation at large times.

For the idealized zero local dispersion case, at any time, the fluctuations are a cumulative addition of fluctuations created since the initial time. The rate at which fluctuations were created is the greatest, at the initial time, and strongly determined by the initial radius of the plume. Therefore the coefficient of variation is strongly determined by the initial plume dimensions, even at large times (3.45). On including local dispersion, the initial dimensions of the plume play a role of decreasing importance, as the time increases. This is because fluctuations are destroyed by the dissipating action of local dispersion. The fluctuations at any given time reflect the initial plume dimensions to the extent, that the initial plume dimensions are reflected in the current plume dimensions, and therefore in the gradients of the mean concentration field. At large times the current fluctuations *forget* the past. This feature of time localization comes out mathematically by the exponential weighting in (3.17). The absence of any dissipating mechanism causes *infinite memory* of initial conditions in the zero local dispersion transport.

The global fluctuation measure for the macroscopically one dimensional case, which is the spatial integral of the concentration variance, is governed by

$$\frac{d}{dt} \|\sigma_c^2\| = 2\nu A_{11} \left\| \left(\frac{\partial \bar{c}}{\partial x_1} \right)^2 \right\| \quad (3.46)$$

It is easily shown that

$$\| \sigma_c^2(x_1, t) \| = \left(\frac{M}{n} \right)^2 \frac{\left(\frac{1}{\sqrt{t_{01}}} - \frac{1}{\sqrt{t_{01} + t}} \right)}{\sqrt{8\pi A_{11} \nu}} \quad (3.47)$$

It follows from (3.47) that

$$\lim_{t \rightarrow \infty} \| \sigma_c^2(x_1, t) \| \rightarrow \left(\frac{M}{n} \right)^2 \frac{1}{\sqrt{8\pi A_{11} \nu t_{01}}} > 0 \quad (3.48)$$

which is again in sharp contrast to the case in which local dispersion is included (3.32)-(3.34).

For the idealized zero local dispersion case, the ability to predict concentrations continually deteriorates with time as the coefficient of variation grows unboundedly (3.42). For any non-infinite concentration microscale in (3.2c), the coefficient of variation for the case including local dispersion decreases with time at large times. In neglecting local dispersion, the only mechanism to destroy mean squared concentration fluctuations is being neglected (3.2a). The importance of local dispersion in destroying concentration variance increases with a decrease in the concentration microscales, which is caused by a decrease in $\ln K$ microscale (which are assumed to be larger than the local dispersivities). As the $\ln K$ microscale increases, the dissipating action of local dispersion decreases (the variance decay coefficient χ decreases).

3.4 CONCENTRATION FLUCTUATIONS IN THE BROMIDE TRACER AT CAPE COD, MA

The Cape Cod bromide tracer is analyzed here for concentration fluctuations. In particular, theoretical predictions are made for the coefficient of variation, at the center of

the plume, for the idealized non-dissipative zero local dispersion case, and the more realistic case including local dispersion. The coefficient of variation, estimated from the bromide concentration data, is compared with the theoretical predictions. Let it be made clear at the outset, that a characteristic of the $\ln K$ field, the $\ln K$ microscale, argued here to be importantly controlling the dissipation of concentration fluctuations, has not been measured, notwithstanding the value of zero, implied by the popular exponential covariance function with absolutely no empirical basis (Plot any estimated $\ln K$ spectrum. Is there infinite area under the graph of wave number squared multiplied by the spectrum? The ratio of the area under the spectrum to that under the wave number squared multiplied spectrum is the squared $\ln K$ microscale. Discussed in Chapter 4). In this study it has been assumed that the $\ln K$ microscale is larger than the local dispersivity. In light of the sensitivity of fluctuation dissipation phenomenon to the scale characterizing the spatial partial derivatives of the concentration field, an accurate prediction of concentration variance needs realistic information about the low and high wave number variations of $\ln K$. In the absence of this information, sensitivity of the results will be shown to different ratios of the $\ln K$ microscale and correlation scales. Information from Leblanc *et al.* [1991], and Garabedian *et al.* [1991], is used in the analysis. Dennis Leblanc, provided the bromide sampling data, and data on the plume orientation.

The mean velocity v of the groundwater is 0.42 meters/day. The $\ln K$ variance and correlation scales are

$$\sigma_f^2 = 0.24$$

$$\lambda_1 = \lambda_2 = 2.6 \text{ m}, \lambda_3 = 0.19 \text{ m}$$

Taking the local dispersivities as

$$\alpha_{11} = .005 \text{ m}, \alpha_{22} = \alpha_{33} = .0005 \text{ m}$$

The empirically fitted macrodispersivities from the tracer experiment are (after subtracting local dispersivities)

$$A_{11} = .96 \text{ m}, A_{22} = .018 \text{ m}, A_{33} = .001 \text{ m}$$

The initial plume dimensions yield the radii of gyrations of an equivalent Gaussian

$$R_1(0) = R_2(0) = 1.1 \text{ m}, R_3(0) = 0.3 \text{ m}$$

therefore from equation (3.6) the 'initial dilation times' are computed to be

$$t_{01} = 1.4 \text{ days}, t_{02} = 77 \text{ days}, t_{03} = 71 \text{ days}$$

3.4.1 THEORETICAL PREDICTIONS OF COEFFICIENT OF VARIATION

For the idealized zero local dispersion case, this information is sufficient to make a theoretical prediction of the coefficient of variation, using the simple expression (3.43). For the case including local dispersion, different ratios of the $\ln K$ microscale to correlation scale are considered in estimating the variance decay coefficient, listed in Table 3.1 (using Equation (2.55), and the Appendix-IV). The coefficient of variation at large times may be computed using the simple expression (3.24). A numerical evaluation of the one dimensional time integral (3.17) at the center of mass is done to confirm the validity of the large time analytical solution (3.23)-(3.26), and explore the behavior at small times (Figure 3.4). At injection the coefficient of variation is of course zero. It

$\frac{\Delta_i^f}{\lambda_i}$	χ (days ⁻¹)	$\frac{1}{\chi}$ (days)
0.2	0.068	14.0
0.4	0.017	58.8
0.6	0.008	125.0
0.8	0.004	250.0
1.0	0.003	333.3

$$\lambda_1 = \lambda_2 = 2.6 \text{ m}, \lambda_3 = 0.19 \text{ m}$$

Table 3.1
Variance decay coefficient and variance 'residence time'.

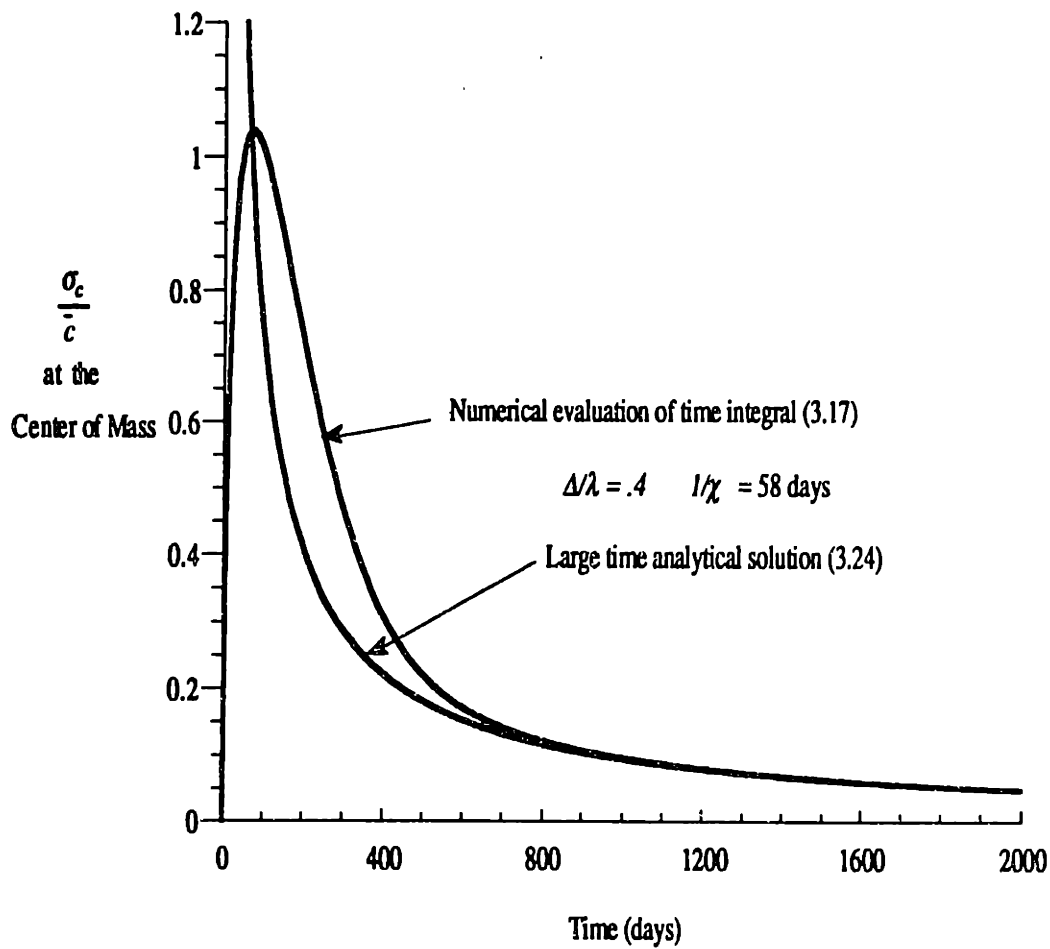


Figure 3.4

Coefficient of variation at the center of mass:

Comparison of large time analytical solution with numerical integration of time integral (3.17) for a ratio of $\ln K$ microscale to correlation scale of 0.4.

jumps rapidly to its maximum value, as it is at the injection time that the gradients of the mean concentration field are the greatest, and the square of the gradient of the mean concentration field is the source term in the variance equation (3.2a), thereby producing fluctuations at the largest rate at injection. However the dissipating action of local dispersion dampens the growth of the coefficient of variation. The coefficient of variation decreases with time at large times. The conditions in evaluating the large time analytical solution were verified against a numerical evaluation of the time integral (3.17). For three different ratios of $\ln K$ microscale and correlation scale, Figure 3.5 shows the sharp qualitative-quantitative contrast between the zero local dispersion case and the more realistic case, including local dispersion (which of course is expressed equally vividly in (3.30) and (3.45)).

3.4.2 ESTIMATION OF COEFFICIENT OF VARIATION FROM BROMIDE SAMPLING DATA

The coefficient of variation is estimated from the bromide concentration sampling data. A box is placed at the center of the plume, aligned with the principal axis. The dimensions of the box are varied as 3, 3.5, and 4 times the correlation scales in the different directions. The box therefore reflects the anisotropy of the $\ln K$ field. The arithmetic averages of the concentration and squared concentrations of samples in the box are computed to estimate the mean concentration and mean squared concentration. The concentration variance is found by subtracting the squared mean concentration from the mean squared concentration. The estimated concentration standard deviation divided by the estimated mean concentration is the estimated concentration coefficient of variation, shown in Figure 3.6, as a function of time. The sampling volume of about 10 ml at the Cape is certainly much smaller than the $\ln K$ correlation volume (the product of the three correlation lengths) of 1000000 ml, *i.e.*, about a meter cube, hence the sampled data

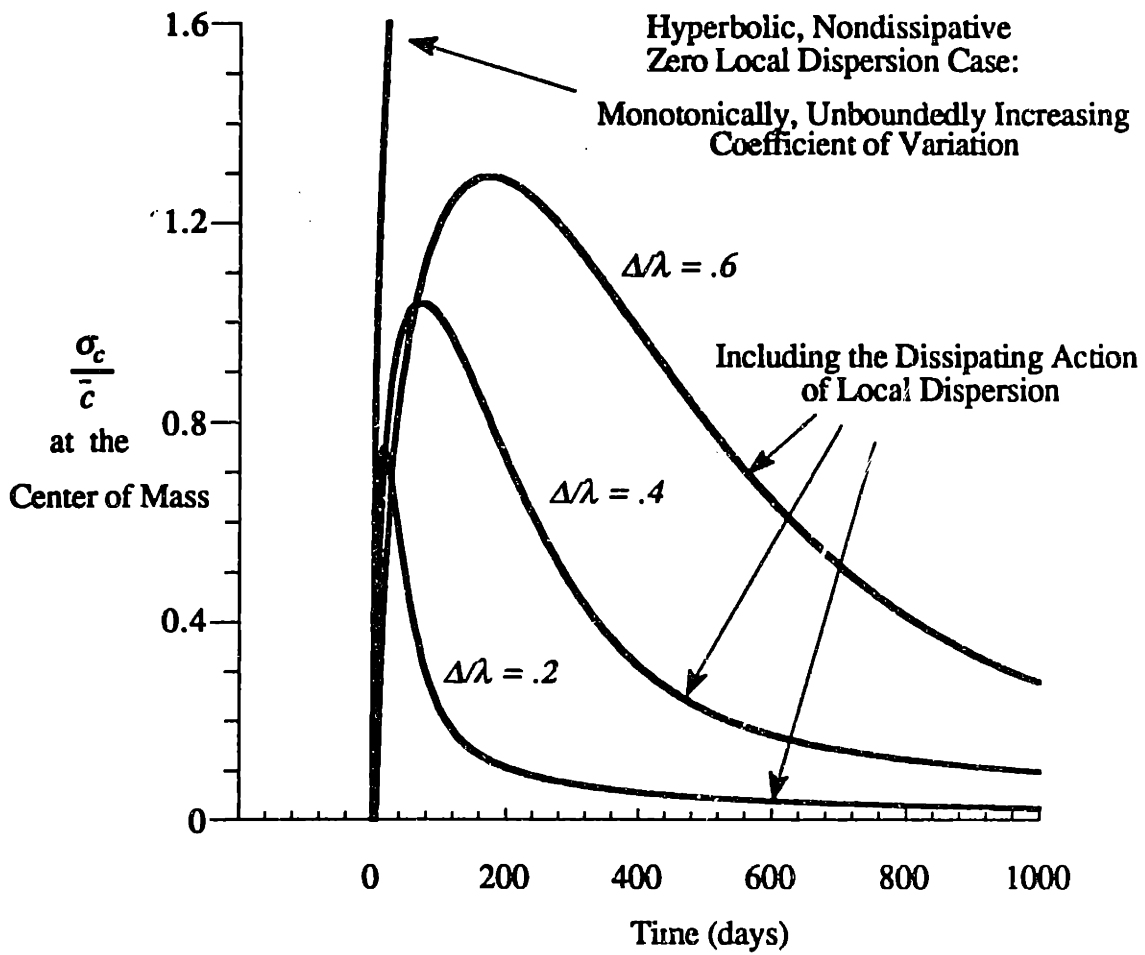


Figure 3.5

Sensitivity of the coefficient of variation to $\Delta\lambda$,
the ratio of the $\ln K$ microscale to correlation scale.

reflects the fluctuations of 'point' concentration samples. The coefficient of variation of the point concentration samples for the bromide tracer at Cape Cod, MA, decreases with time between 200 and 500 days (Figure 3.6). The coefficient of variation was estimated at large times only because a scale disparity between the plume volume (the product of twice the radii of gyration in the three directions) and $\ln K$ correlation volume (product of the three correlation scales) is necessary for any estimation of mean and variance of concentration to be possible. At 200 days the plume volume is more than two hundred times the $\ln K$ correlation volume. After 200 days, the estimating box volume is less than the plume volume, yet greater than the $\ln K$ correlation volume.

3.4.3 COMPARISON OF THEORY AND OBSERVATIONS

Figure 3.7 shows how the estimated coefficient of variation compares with the theoretical predictions for the idealized zero local dispersion case, and on including local dispersion, with different ratios of the $\ln K$ microscale to correlation scale. The idealized zero local dispersion case predicts an ever increasing coefficient of variation, and therefore fares quite miserably. The observed decrease in the coefficient of variation is in sharp qualitative contrast with this implication of the zero local dispersion case. The plume is not headed for a 'mean square explosion', as it would be, if the zero local dispersion case were reality. The feature of ever increasing coefficient of variations is contradicted by observations.

The predicted and observed decrease in the coefficient of variation with time (Figure 3.7) provides a qualitative support of the theory developed here. The quantitative performance of the theory can be judged if independent estimates of the ratio of the $\ln K$ microscale to the correlation scale are made. A ratio of one, or more, implies that the $\ln K$ field, has rather well defined 'blobs' of dimensions of the order of the correlation scale, that dominate the fluctuation energy. If the ratio is much less than one, it means that the

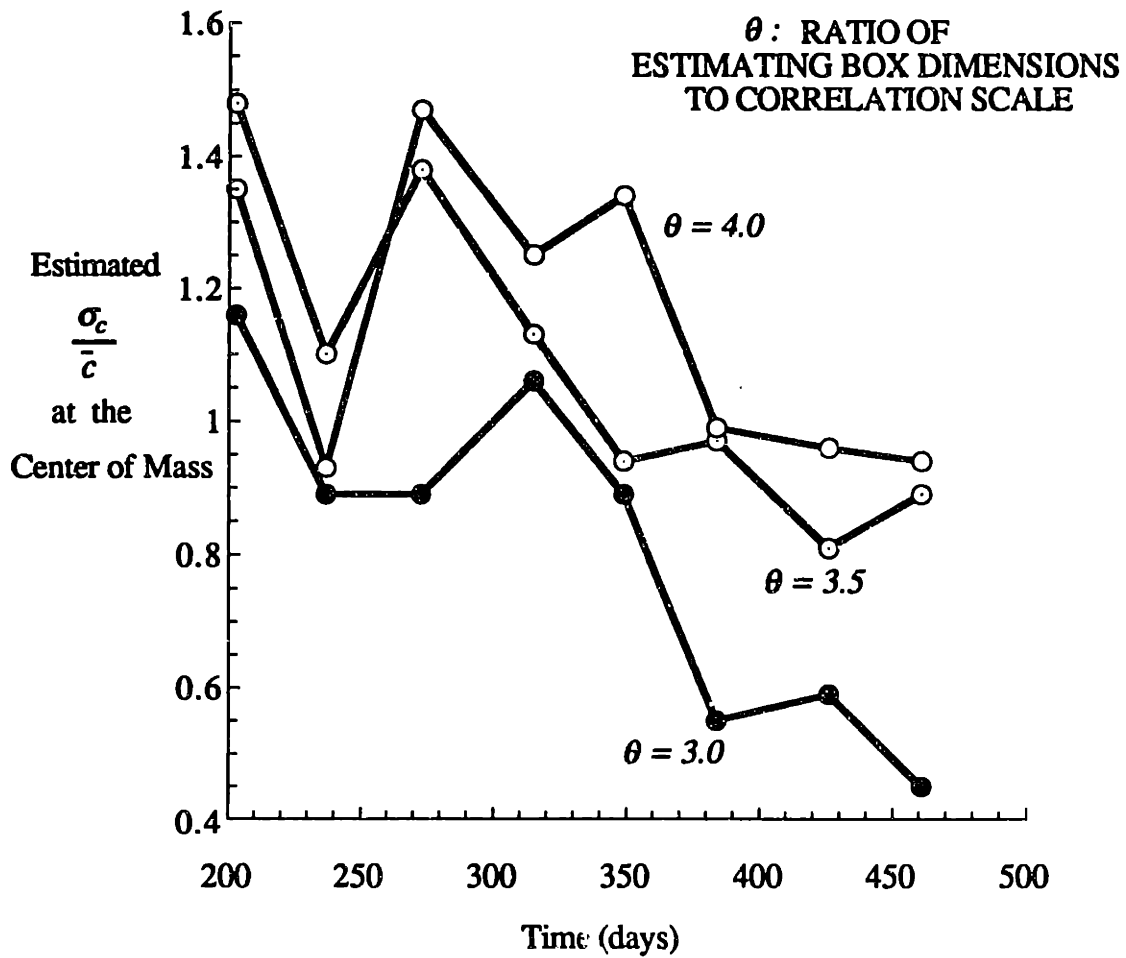


Figure 3.6
Estimated coefficient of variation for the bromide tracer
at Cape-Cod, MA.

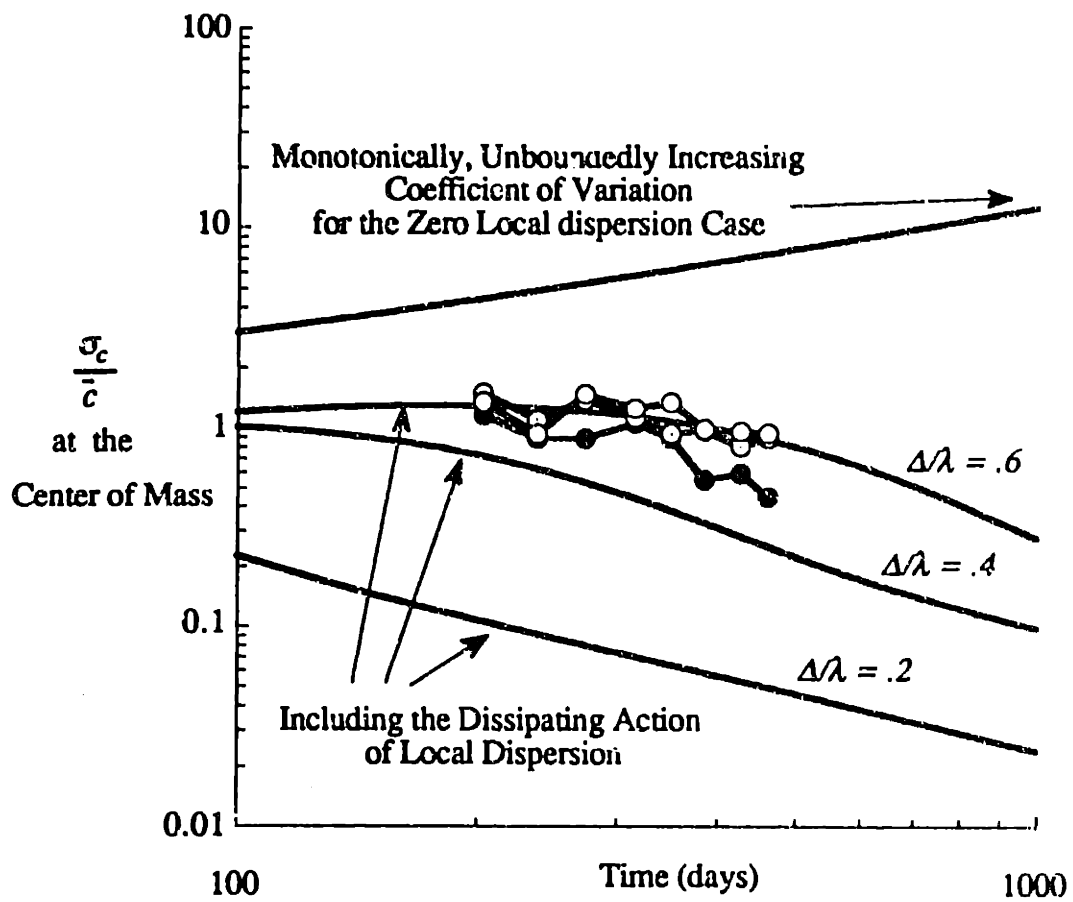


Figure 3.7
Comparison of estimated coefficient of variation with
theoretical predictions.

finer (than the correlation scale) scale variations, are a significant portion of the total energy of fluctuations. The fundamental feature of the fluctuation dissipation mechanism is that, the smaller the scale characterizing the derivatives of fluctuations, the faster local dispersion can destroy fluctuations.

Figure 3.8 shows a plot of peak sampled concentrations as a function of the product of the three observed radii of the plume, (a surrogate for the 'plume volume'). At early times the peak concentration does not decrease rapidly. The decrease is much weaker than an inverse relationship with the plume volume. Enhanced rates of growth of the spatial second moments, at early times, are not accompanied by a commensurate reduction of the peak concentration. However, at later times, the peak behaves almost inversely as the plume volume. This feature is consistent with the prediction of decreasing coefficient of variation with time, due to the dissipating influence of local dispersion. The mean concentration plus two standard deviations, plotted in Figure 3.8, as a crude theoretical prediction of the peak concentration, shows a weak decrease at early times, and a more rapid decrease, later. The discrepancy at early times in Figure 3.8 raises an important limitation of the comparisons made here. A constant macrodispersivity is being used in this analysis. While this may be a reasonable assumption at large times, its violation at early times, coupled with the strong dependence of the fluctuations at early times on the plume scale may cause additional effects, not explored here. However, the observed fall in the peak concentration by an order of magnitude, directly indicates that the idealization of the zero local dispersion is not even a crude approximation of the behavior of the Cape Cod tracer test. In fact, the observed behavior of the peak concentration implies that local dispersion has a dramatic role in the variable advection-diffusion phenomenon. Aided by advective heterogeneities that create more *surface area* for the local dispersion to act, the local dispersion is able to create a rate of attenuation of point concentrations, that can be orders of magnitude faster than what would happen with local dispersion alone, in the absence of advective

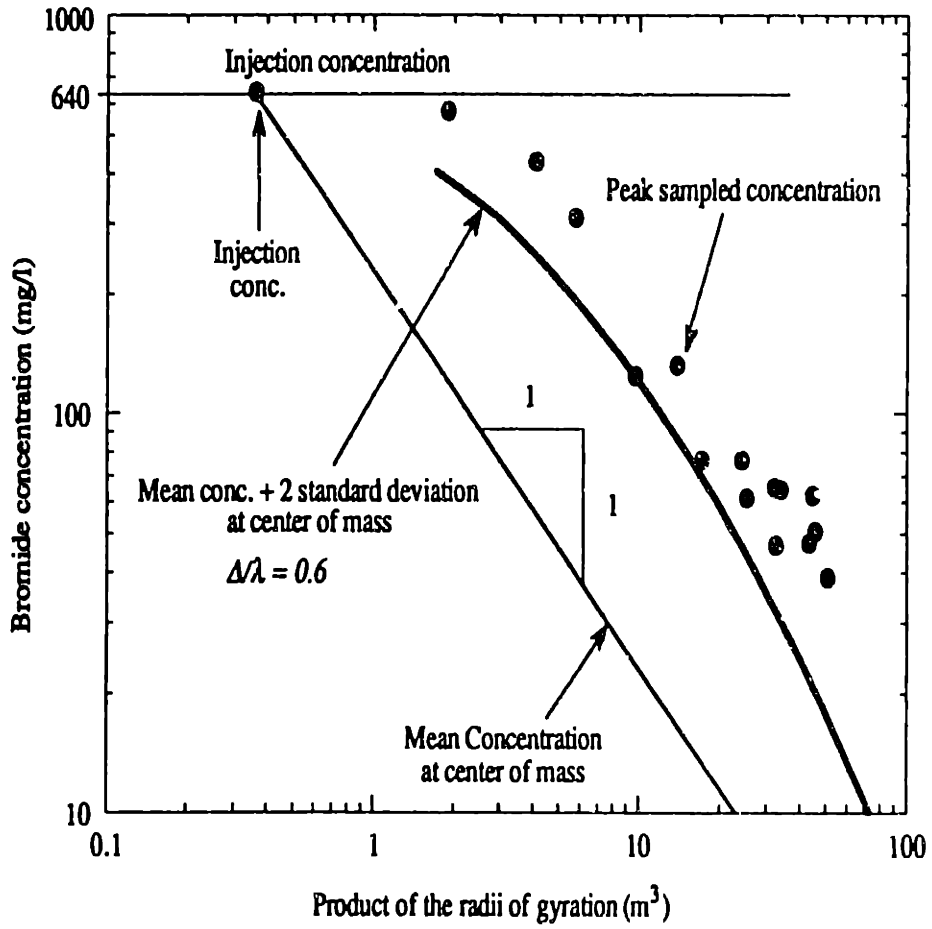


Figure 3.8

Peak sampled bromide concentrations at Cape Cod, MA.

heterogeneities. The synergetic role of local dispersion and the high wave number $\ln K$ fluctuations in facilitating this *dilution* process is the single most important finding of the analysis presented here.

In light of the theoretical and numerical agreement on the ever increasing coefficient of variations for idealized zero local dispersion case, and the field observations to the contrary, it may be concluded that, in order to realistically predict mean squared concentration fluctuations, *i.e.*, concentration variance, at large travel distances, it is critically important to include the dissipating action of local dispersivities, notwithstanding the smallness of local dispersivities.

In comparing the peak concentrations for the bromide tracer (Figure 3.8), two standard deviations of the peak mean concentration were added to the peak mean concentration. How many standard deviations should one add to the mean concentration in anticipating contamination exposure levels? Ideally one would like to have the space-time description of the concentration probability density function (pdf) f_c from which probabilistic inferences could be made. A priori, there is no basis for assuming the concentration fluctuations to have a normal pdf, or a log-normal pdf, or any other. We may never have a complete probabilistic description of concentration fluctuations. The concentration variance, however, does provide an upper bound on exceedance probabilities, *i.e.*,

$$\sigma_c^2 = \int_0^{\infty} (c - \bar{c})^2 f_c(c) dc \geq \int_{\bar{c} + \delta_c}^{\infty} (c - \bar{c})^2 f_c(c) dc \geq \delta_c^2 \int_{\bar{c} + \delta_c}^{\infty} f_c(c) dc \quad (3.49)$$

which is simply Chebyshev's inequality. Therefore the probability that the concentration is going to exceed the mean by an amount δ_c is less than or equal to $(\sigma_c/\delta_c)^2$. A conservative assessment of risk is afforded through this bound. For example, in delineating the 'unsafe zone' due to a contaminant plume, it may be postulated that if at a point, the mean concentration is below some safe concentration, and the probability of

exceeding that safe concentration can be shown to be sufficiently small, it is safe, otherwise, it is unsafe. Recall that the coefficient of variation keeps growing with distance from the center of mass, Figure 3.2. However that does not imply that if a point is far enough, it will be unsafe, according to this rule. That is because the mean concentration also keeps decreasing with distance from the center of mass. The method to compute concentration variance developed here and the upper bound on exceedance probabilities (3.49) may be used in such an exercise.

3.5 SUMMARY AND DISCUSSION

Due to the action of local dispersion, the concentration variance dissipation term is a first order decay term on assuming the small separation behavior of the concentration field to be statistically stationary. The variance decay coefficient χ multiplying the concentration variance in the first order decay term, is the sum of twice the local dispersion coefficients divided by the square of the concentration microscale in the three principal directions. The estimate of the concentration microscales made in Chapter 2 render the decay coefficient a decreasing function of the $\ln K$ microscale, when the microscales are larger than the local dispersivities in each of the three principal directions. The derived analytical expressions (3.23)-(3.26) show that the mere assumption of a non zero variance decay coefficient (a non-infinite concentration microscale) results in a dramatic influence of local dispersion on concentration fluctuations, at large times. The global measure of fluctuations goes to zero at large times, as shown in equations (3.33) and (3.34), and the coefficient of variation (the concentration standard deviation divided by the mean concentration) also decreases with time as expressed compactly in equation (3.30). The rate of decrease of the coefficient of variation is determined by the variance decay coefficient. The smaller the microscale of $\ln K$ (assumed larger than the local dispersivities), the smaller the concentration

microscales, the greater the rate at which local dispersivities can destroy mean squared concentration fluctuations, and therefore result in a smaller coefficient of variation of concentration fluctuations. The mechanism of dissipation of concentration fluctuations embedded in the decay coefficient is that of a synergetic interaction of local dispersion and the high wave number component of the velocity field. If the hydraulic conductivity field is progressively stripped of its fine scale features, then the concentration microscale will increase, resulting in a slower action of local dispersion. The $\ln K$ microscale will generally be proportional to the $\ln K$ correlation scale. As the low-wave number energy of the $\ln K$ spectrum increases the $\ln K$ microscale also increases. This nature of the fluctuation dissipation mechanism creates the need for extensive and intensive characterization of hydraulic conductivity.

The concentration coefficient of variation increases with distance from the center of mass. Therefore at any given time, at points far enough in the plume, the coefficient of variation will be large. This jaggedness of plume fringes will make the predictions of concentration levels by the mean concentration poor ones. The center of mass of the plume is the point of minimum coefficient of variation, which is decreasing in time, at large times. If the coefficient of variation is small enough, the peak mean concentration may become an adequate predictor of the peak concentration in a plume. However, the time taken for this to happen depends on the scale of heterogeneities and the local dispersion coefficients, as they determine the variance decay coefficient. The analytical solution to the coupled variance equation revealed that away from regions of large gradients in the variance field, at large times, the source term and the dissipation term balance each other, thereby creating a linear relationship between concentration variance and the square of the partial derivatives of the mean concentration field (3.28). Such a linear relationship is of course singularly created by the dissipating action of local dispersion, which creates a time localization effect in (3.17). This linear relationship may be used to assess the concentration variance for a more general mean concentration profile

than the one analyzed in this work, in regions of weak gradients for the mean concentration field.

If local dispersion is not included, there is no dissipation of concentration variance, which is produced due to the gradients in the mean concentration field in its conservation equation (3.2a). The analysis of this case is trivial because concentration and squared concentration are governed by the same hyperbolic equation (in Chapter 2), therefore the results for the mean concentration can be extrapolated to the mean of the squared concentration, at similar levels of approximation. The analytical expressions, developed in section (3.3) for the mean squared concentration fluctuations resulting from a finite size macroscopically multidimensional impulse input, show that the coefficient of variation (the concentration standard deviation divided by the mean concentration) at the center of mass, (the point where it is the minimum at a given time) increases unboundedly with time and also increases by decreasing the initial plume dimensions (Equation (3.43)). This unbounded increase was observed in numerical simulations by Rubin [1991], and is also implied by Dagan's [1982], [1990] theory for concentration variance, neglecting local dispersion. The coefficient of variation also increases with distance from the center of mass as an exponential with the square of the distance as its argument. Another measure of fluctuations, the spatial integral of concentration variance, at large times, approaches a constant value inversely proportional to the initial plume radius. Recall, on including local dispersion this measure decreases and approaches zero at large times. The expression for the coefficient of variation for the zero local dispersion case (3.42) bears no resemblance to the expression that includes the effect of local dispersion (3.26). The large time solution of the concentration fluctuations is singularly influenced by the action of local dispersion. If the zero local dispersion case were a good model for the concentration statistics at large times, the information in the mean concentration would be absolutely useless as a predictor of point concentration exposure

levels, as the deviations around the predicted mean would be an ever increasing multiple of the mean.

The estimated coefficient of variation at the center of the Cape Cod tracer plume, albeit large (a value of 1.4 at 203 days and .6 at 461 days) even after traveling dozens of horizontal correlation distances, decreases with time. This decrease is predicted by the theory as a consequence of including the dissipating action of local dispersion, and is in sharp qualitative contrast with the predicted ever increasing coefficient of variation with time, for the zero local dispersion case. Consistent with the decreasing coefficient of variation with time, the peak sampled concentration is found to be inversely proportional to the plume volume at large times, and falls by an order of magnitude in 500 days. The observations at the Cape along with the theoretical results show that it is critically important to include the dissipating action of local dispersion in any realistic assessment of concentration fluctuations. The zero local dispersion model of solute transport is not even a crude approximation of observations.

The critical role of the fluctuation dissipation function in determining concentration variance has important implications for the construction of numerical approximations of advection-diffusion in heterogeneous medium. To incorporate the fluctuation dissipating action of local dispersion, numerical approximations have to be able to adequately model the spatial partial derivatives of the concentration field, which control the local dispersive flux. It would be desirable to at least show some empirical evidence of convergence (with respect to grid size) of solutions in a concentration derivative norm. The usual methods of introduction of numerical dispersion to produce a 'wiggle-resistant' solution of the concentration field are unacceptable because the real solution probably has lots of wiggles. The creation of wiggles by the advective heterogeneity and their interaction with the local dispersion (and not numerical dispersion) is what needs to be simulated. For 'Particle-Tracking' methods to be able to reproduce the local dispersive flux, a lot of particles will be required. It is recommended

in numerical modeling exercises, modest spectral descriptions be employed, the microscales of which can be resolved by the numerical grids. We recommend not to use the popular exponential spectrum for three reasons: 1) There is no dataset of $\ln K$ measurements that supports the feature of infinite area under the plot of the squared wave number multiplied by the estimated $\ln K$ spectrum, versus wave number. 2) It is impossible to resolve even a fraction of the strain rate of the velocity field implied by this spectrum (infinite shear, vorticity, principal strain rates!) 3) At the small scales contained in this spectrum that make the variance of the $\ln K$ derivatives infinite, it is not even sensible to talk about a porous continuum and its constitutive parameters like hydraulic conductivity and local dispersion coefficients.

The nature of the variance dissipation implies an increase in the concentration standard deviation with an increase in the low wave number energy of the $\ln K$ spectrum. While the computation of dispersivities in scale-less, multiple-scale media is being undertaken, the theory developed here shows that the use of these dispersivities in making predictions of contamination levels needs to be looked at with great skepticism, until researchers finding effective dispersivities in such media also come up with estimates of the concentration coefficient of variation. In this connection, it needs to be kept in mind that there are three scales operative in determining concentration fluctuations and therefore contamination exposure levels; the plume-scale, the heterogeneity scale and the local dispersivity scale. The plume scale and the heterogeneity scale determine the rate of production of concentration variance. The local dispersivity and the heterogeneity scale determines the rate at which local dispersion destroys concentration fluctuations. As the heterogeneity scale increases, the capacity of local dispersion to destroy concentration variance diminishes, and decreases the information contained in the 'mean concentration', or plume volume, about actual concentration levels. The act of adding increasingly large scale heterogeneity into the 'random' description and coming up with a larger effective dispersivity and therefore

diminished mean concentrations is potentially dangerous, until it is recognized that the concentration standard deviation will also be large. At issue is not only meandering of the center of mass of the plume (which cannot be significant after the plume is larger than the correlation volume, by the law of large numbers) but meandering and distortions of different parts of the plume. The theory developed here explicitly assumes that the mean concentration is smoother than the $\ln K$ correlation scale. Yet, there is a range of correlation scales for which this assumption is valid, given a plume scale. If the correlation scale is at the higher end, then the concentration fluctuations will be greater, compared to a smaller correlation scale. A pragmatic modeling approach may be to limit the low wave number features that are labeled random, *i.e.*, identify these features and incorporate them into a numerical model. With the rest of the spectrum compute macrodispersivities and employ them in the model. An estimate of the coefficient of variation may serve as a guideline in deciding the scale below which the hydraulic conductivity features are labeled random.

While 'variance reduction' via conditioning has the allure of giving optimum estimates of concentration levels, the information of the $\ln K$ spectrum required to model the second order concentration statistics of the concentration field needs to be appreciated. Due to the singular importance of the fluctuation dissipation function in determining the concentration variance, an estimate of the $\ln K$ microscale is necessary in any prediction of the concentration statistics. Of course any conditioning scheme presumes the existence of reliable model of the covariance structure of the concentration field. The uncertainties in estimating the $\ln K$ microscale, along with the correlation scales and variance may be significant. In this light, 'variance acknowledgment' with a range of the estimated values of the statistical parameters is probably of greater practical importance. To that end, an upper bound on exceedance probabilities (3.49) may be a useful risk assessment tool.

The two most important findings of this Chapter are 1) In terms of concentration exposure levels and deviations around the ensemble mean, a solute undergoing transport even with even a very small local dispersion coefficient will behave dramatically different from a solute undergoing pure advection. In the hypothetical zero local dispersion case the ratio of the concentration standard deviation and mean concentration (*i.e.*, coefficient of variation or 'noise to signal ratio') increases unboundedly with time. On including local dispersion, the growth of the coefficient of variation is dampened and it decreases with time at large times, as was observed for the Cape Cod, bromide tracer. In contrast, the longitudinal spatial second moment does not differentiate between these two cases. 2) The high wave number $\ln K$ variations facilitate the action of local dispersion in destroying concentration fluctuations, and therefore importantly determine the level of concentration deviations from the ensemble mean. Finally, intensively and extensively characterized sites and large scale tracer experiments with intense monitoring need to be undertaken in order to compare contrasting theories and test their abilities to predict concentration variance, and concentration exposure levels, in addition to spatial second moments of plumes.

CHAPTER 4

THE HYDRAULIC CONDUCTIVITY MICROSCALE

The log-hydraulic conductivity correlation function is found to be distinctly upward convex at the origin, yielding a nonzero log-conductivity microscale, the scale characteristic to the variations of the spatial derivatives of the log-hydraulic conductivity field. A disparity between the log-conductivity microscale and the square root of the mean permeability is consistent with the observed upward convexity of the log-conductivity correlation function at the origin. In the absence of this disparity, it is argued that the effects of viscous transfer of momentum in the fluid, as represented in the Darcy-Brinkman 'law', will dampen velocity strain rates in heterogeneous porous medium.

4.1 INTRODUCTION

The hydraulic conductivity (or permeability) is a *Darcy scale* constitutive property of a porous medium continuum that provides a simplified dynamic model of the viscous creeping flow through the soil interstices, integrated over a large number of particle diameters (*i.e.*, Darcy Scale or REV) via Darcy's 'law'. While aggregation over a large number of pores is required for Darcy's law to be found, the constitutive property of the porous medium, the hydraulic conductivity, may vary from one location to the other in a heterogeneous porous medium continuum. The statistical description of the variation of Darcy constitutive properties is sought to analyze its consequences on flow and transport.

The spatial partial derivatives of the $\ln K$ (K being the hydraulic conductivity) are coefficients in the flow equation. The velocity being a linear function of the hydraulic conductivity is linearly proportional to the exponential of the $\ln K$. Therefore the spatial

partial derivatives of the $\ln K$ field determine the shear, vorticity, convective compression and tension of the velocity field. The intensity of strain rates of the velocity field are expected to strongly influence the small scale distribution of solute undergoing the advection-dispersion process [e.g., Lumley, 1972; Batchelor, 1959]. Transport being advection dominated at very small scales (local dispersivities are typically less than a centimeter), the fluctuations in the velocity field at such small scales are reflected in the solute concentration field. Indeed, in the concentration variance equation the variance sink term (that models the destruction of fluctuations by the local dispersion process), is equal to the local dispersion coefficient multiplied by the variance of the derivatives of the concentration perturbation field, which are expected to reflect the intensity of fluctuations of the velocity field at small scales (Chapter 2).

In light of aforementioned sensitivities, a realistic model of the high wave number fluctuations of $\ln K$ is needed. In a continuum analysis of porous medium the high wave number behavior of the $\ln K$ is constrained by the requirement of a scale disparity between the continuum scale (Darcy scale/REV) and the first scale at which continuum properties vary. Constitutive parameters like hydraulic conductivity and local dispersivities can be meaningful only on a finite local support. Moreover, it may be expected that there exists an upper bound on the spatial partial derivative of the hydraulic conductivity field, above which, the process of fluid momentum transfer associated with gradients in the velocity field will alter the velocity field inferred by using Darcy's 'law'.

The small separation behavior of the $\ln K$ correlation function is explored in Section 4.2. The scale characterizing the spatial derivatives of the hydraulic conductivity, the $\ln K$ microscale (defined in Section 4.2) is found by fitting a parabola to the correlation function at the origin. The correlation function is found to be unambiguously upward convex, at zero separation distance, thereby ensuring the feasibility of such a process. Bakr's [1976] spectral estimates were found to imply a ratio of the microscale to

correlation scale of 0.5. The popular exponential correlation function implying a zero microscale is found to be a gross extrapolation on the high wave number end.

The unbounded increase in velocity strain rates as the microscales become smaller, as implied by Darcy's law, is inconsistent with a picture of viscous creeping flow through the porous medium. A viscous transfer of momentum in the fluid is argued to limit the velocity strain rates in rapidly varying hydraulic conductivities, in Section 4.3. A three dimensional velocity spectrum incorporating this effect is also presented. Section 4.4 summarizes the findings of this chapter.

4.2 THE MICROSCALE

Decomposing the logarithm of the hydraulic conductivity into its mean and perturbation

$$\ln K = E[\ln K] + f$$

its spatial covariance function may be defined as

$$R_{ff}(x_1, x_2) = E[f(x_1)f(x_2)]$$

It follows from the linearity of differentiation and expectations that

$$E\left[\frac{\partial f}{\partial x_1} \frac{\partial f}{\partial x_2}\right] = \frac{\partial^2 R_{ff}(\xi_1, \xi_2)}{\partial \xi_1 \partial \xi_2} \Big|_{\xi_1=x_1, \xi_2=x_2}$$

Assuming stationarity of the $\ln K$ conductivity perturbations to second moments

$$R_{ff}(x_1, x_2) = R_{ff}(x_2, x_1) = R_{ff}(x_1 - x_2) = R_{ff}(x_2 - x_1)$$

defining a new variable

$$\tau = \xi_1 - \xi_2$$

and using the fact

$$\frac{\partial \xi_1}{\partial \tau} \Big|_{\xi_2} = - \frac{\partial \xi_2}{\partial \tau} \Big|_{\xi_1} = 1$$

and

$$\frac{\partial^2 R_f(\xi_1, \xi_2)}{\partial \xi_1 \partial \xi_2} = - \frac{\partial^2 R_f(\tau)}{\partial \tau^2} \Big|_{\tau = \xi_1 - \xi_2}$$

the variance of the spatial derivatives may be expressed as

$$\mathbb{E} \left[\left(\frac{\partial f}{\partial x} \right)^2 \right] = - \frac{\partial^2 R_f(\tau)}{\partial \tau^2} \Big|_{\tau=0} \quad (4.1)$$

Defining the variance as usual

$$\sigma_f^2 \equiv \mathbb{E}[f^2] = R_f(0)$$

and the variance of the derivatives

$$\left(\frac{\sigma_f}{\Delta} \right)^2 \equiv \mathbb{E} \left[\left(\frac{\partial f}{\partial x} \right)^2 \right] \quad (4.2)$$

where Δf is called the microscale of $\ln K$. The microscale may be thought of as the representative scale from which the strength of the spatial partial derivatives of the $\ln K$ field is derived. A zero microscale corresponds to a infinite variance of the derivatives of the $\ln K$.

For small separations, the $\ln K$ spatial covariance may be expanded around its value at zero separation to get

$$R_{ff}(x) = R_{ff}(0) + x \left. \frac{\partial R_{ff}(\tau)}{\partial \tau} \right|_{\tau=0} + \frac{x^2}{2!} \left. \frac{\partial^2 R_{ff}(\tau)}{\partial \tau^2} \right|_{\tau=0} + \dots$$

Recognizing that the covariance is the maximum at zero separation, using (4.1) and (4.2) we may therefore approximately write for small separations x ,

$$R_{ff}(x) \cong \sigma_f^2 - \frac{x^2}{2} \left(\frac{\sigma_f}{\Delta f} \right)^2$$

Defining the correlation function as

$$\rho(x) = \frac{1}{\sigma_f^2} R_{ff}(x)$$

it follows that

$$\rho(x) \cong 1 - \frac{x^2}{2(\Delta f)^2} \tag{4.3}$$

Therefore a parabola with a value of 1 at the origin, may be fitted to the correlation function at small separations, and the point x_0 at which the fitted parabola intercepts the separation axis ($\rho(x_0) = 0$) is related using Equation 4.3, to the $\ln K$ microscale;

$$x_0 = \sqrt{2} \Delta^f \quad (4.4)$$

From Equation (4.2), it follows that in the spectral domain the squared microscale is a ratio of the area under the spectrum and that under squared wave number multiplied by the spectrum;

$$(\Delta^f)^2 \equiv \frac{\int_{-\infty}^{+\infty} S_{ff}(k) dk}{\int_{-\infty}^{+\infty} k^2 S_{ff}(k) dk} \quad (4.5)$$

From (4.5), if the $\ln K$ spectrum has more low wave number energy, its microscale will be larger, and if we add more high wave number energy to the $\ln K$ spectrum, its microscale will be smaller. Therefore the value of the $\ln K$ microscale is influenced by both low and high wave number features in the hydraulic conductivity description. Of course a value of zero for the microscale (for a nonzero variance) implies that the denominator in (4.5) is infinite. In contrast the 'correlation scale' is a scale typically associated with the location of the center of gravity of the spectrum (see Appendix-IV).

4.2.1 ESTIMATION OF THE MICROSCALE

The empirical estimation of the $\ln K$ microscale and the verification of the usual continuum assertion of the existence of a scale disparity between the first scale at which a continuum property may vary and the 'Darcy scale' or REV, will require sampling Darcy scale properties at small separations. Typically $\ln K$ measurements are not made intensely enough for such an investigation to be done. Ringrose and Pickup [1993], have created a dataset of measurements of permeability made at the rate of 2 mm using a probe of internal radii 1mm (see Figure 4.1). The measurements are made on a crossbedded

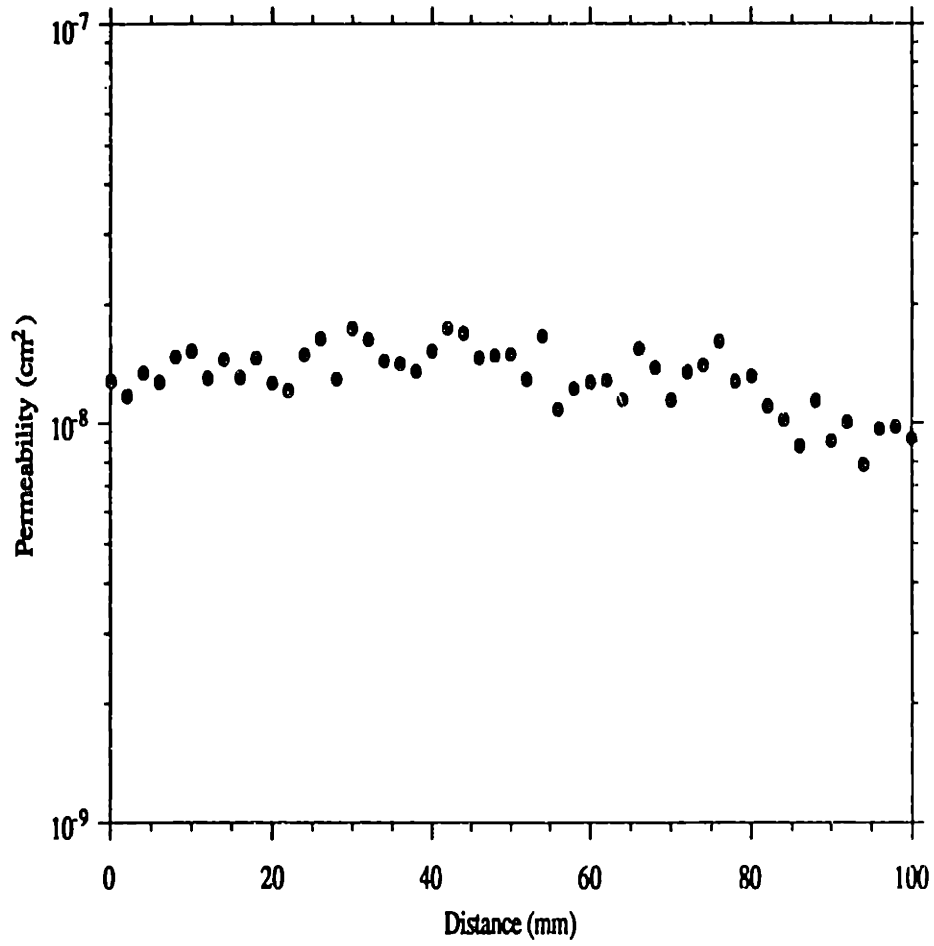


Figure 4.1

lnk measurements by Ringrose and Pickup [1993].

sandstone from a Carboniferous outcrop near St. Monaco, Fife, Scotland. The permeability of the rock is of the order 10^{-8} cm². It may therefore be assumed that the probe is sampling continuum scale permeability. Furthermore it is hypothesized that the measurements are 'point' measurements of Darcy scale permeability of the rock. This amounts to assuming that the microscale will be greater than 1 mm, thereby the measured value is a local value. Of course, this may be checked once we estimate the $\ln K$ microscale.

Given a set of observations

$$f_i, i = 1, \dots, NDP \text{ are observed values of } f \text{ @ } \delta$$

the covariance function may be estimated by

$$\hat{R}_{ff}(n\delta) = \frac{1}{(NDP - n)} \sum_{i=1}^{NDP-n} (f_{i+n}f_i) \quad , n = 1, \dots, N$$

where NDP is the number of data points. Thus the estimated correlation function is given by

$$\hat{\rho}(n\delta) = \hat{R}_{ff}(n\delta) / \hat{R}_{ff}(0) \quad , n = 1, \dots, N$$

Choosing N to be a small number so that we are dealing with the small separation part of the correlation function, the mean square error between the observations and a parabola fitted at the origin (corresponding to a microscale Δ^f) is

$$MSE(\Delta^f) = \frac{1}{N} \sum_{n=1}^N [\hat{\rho}(n\delta) - \rho(n\delta)]^2 \quad (4.6)$$

where

$$\rho(n\delta) = 1 - \frac{(n\delta)^2}{2(\Delta')^2}$$

A 'good' estimate of the microscale may be defined as the argument that minimizes the mean square error in (4.6), *i.e.*,

$$\hat{\Delta}' = \arg_{0 < \Delta' < \infty} \{ \min MSE(\Delta') \} \quad (4.7)$$

Figure 4.2 shows the computed correlation function at small separations, and also the best parabola fitted at small separations. Figure 4.3 shows the square root of the mean square error as a function of the microscale. The mean squared error has a distinct minimum that yields a microscale of about 1 cm. This being much greater than the probe diameter of 1mm is consistent with the assumption that the measurements were indeed point, local Darcy scale measurements. The upward convexity of the correlation function in Figure 4.2 is strikingly unambiguous. This feature directly rules out the widely used exponential correlation function as a realistic model, at small separations. The observed upward convexity is an empirical validation of the hypothesis that there must be a separation between the scales at which the continuum scale properties vary and the continuum scale itself, the former being greater than the latter. Note that in Figure 4.2, the e^{-1} decrease in the auto correlation function occurs over approximately a centimeter too. That is, for the range of scales in the dataset, the ratio of the microscale to correlation scale is order 1. The history of fitting exponential correlation functions with zero microscales makes this a little surprising. Of course if we were addicted to fitting a

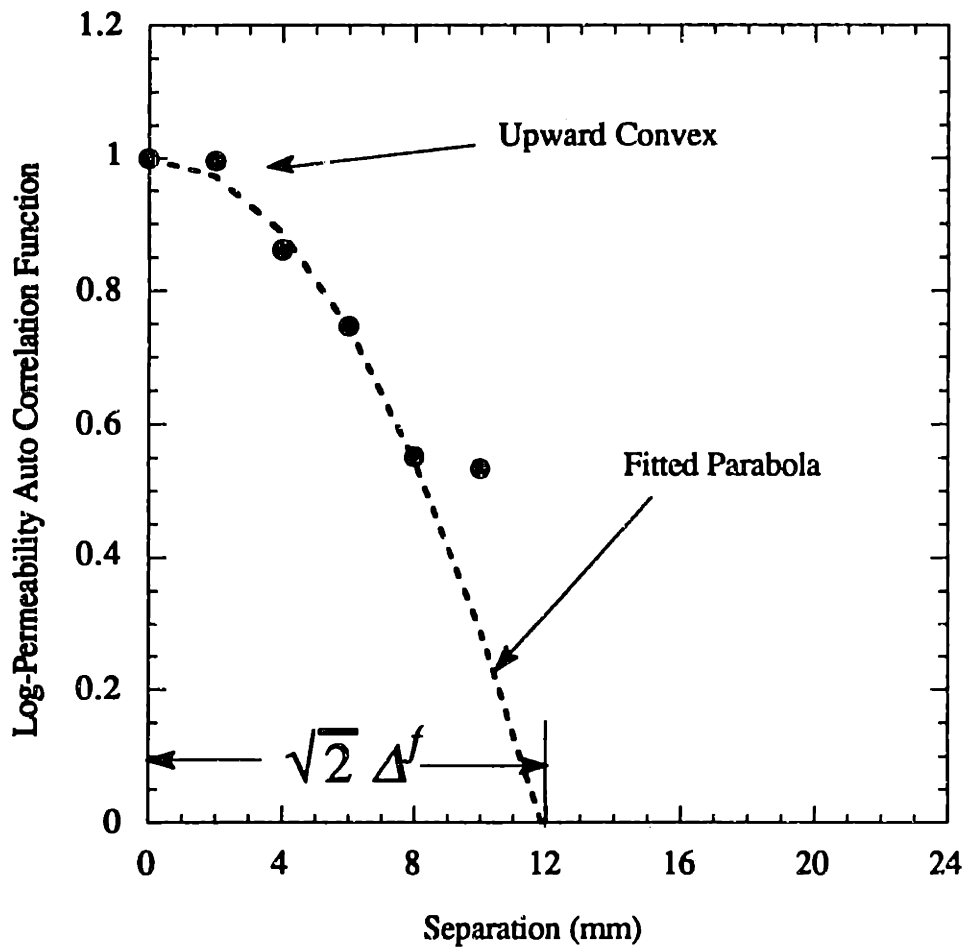


Figure 4.2

Upward convexity of $\ln k$ correlation function at the origin.

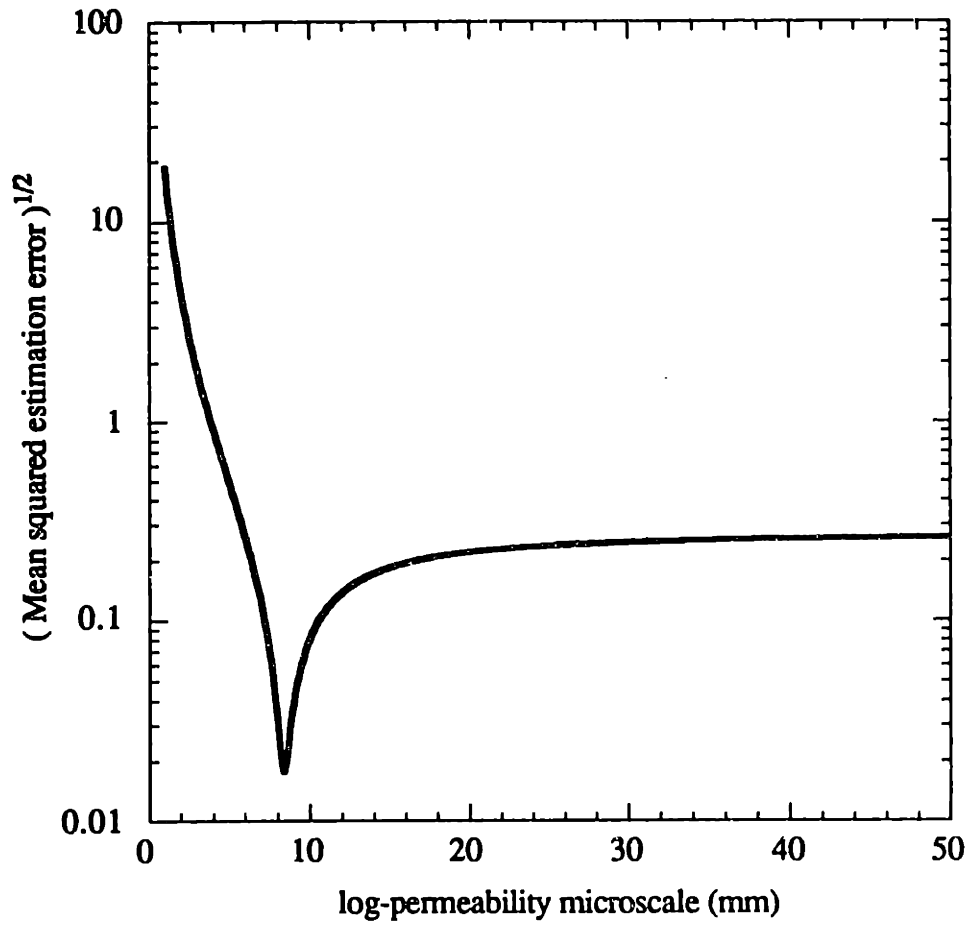


Figure 4.3
Root mean square estimation error.

Gaussian correlation function, we would not be surprised at all, because it has a ratio of microscale to correlation scale of about 1.

A reexamination of existing datasets will reveal that there was never any empirical basis for the zero microscale implied by the popular exponential correlation function. For example, one of Bakr's [1976] spectral estimates is shown in Figure 4.4. In addition, the frequency squared times spectrum is also shown. The ratio of the microscale to his inferred correlation scale is about 0.5. Of course, we would like a long series of closely sampled hydraulic conductivity covering a wide range of scales to make better inferences, considering the fact that the spectrum and the frequency square multiplied spectrum are truncated near their peaks in Figure 4.4. In the absence of such a dataset we are free to speculate on models for extrapolating both low wave number and high wave number behavior. On the low wave number end our imagination is constrained by the fact that we may run out of aquifer (and the earth is a finite sized ellipsoid, thus providing a lower bound on the low wave number cutoff). On the high wave number end, our flight of speculation hits a limit when our description of the spatial variation of hydraulic conductivity becomes incompatible with our model for flow. This incompatibility is discussed in the next section.

4.3 LIMITATION OF DARCY'S 'LAW' IN COMPUTING VELOCITY STRAIN RATES

The fluid velocity is proportional to the hydraulic conductivity, therefore, as the microscale of the $\ln K$ becomes smaller the characteristic velocity strain rate becomes larger (see Appendix-IV). Can this inverse relationship can go on for ever increasing strain rates? This inverse relationship is precisely a consequence of Darcy's 'law'. Yet in fluid flow through the soil interstices, the continuity of velocity and stress in the fluid phase and the viscous transfer of fluid momentum may be expected to have a smoothing

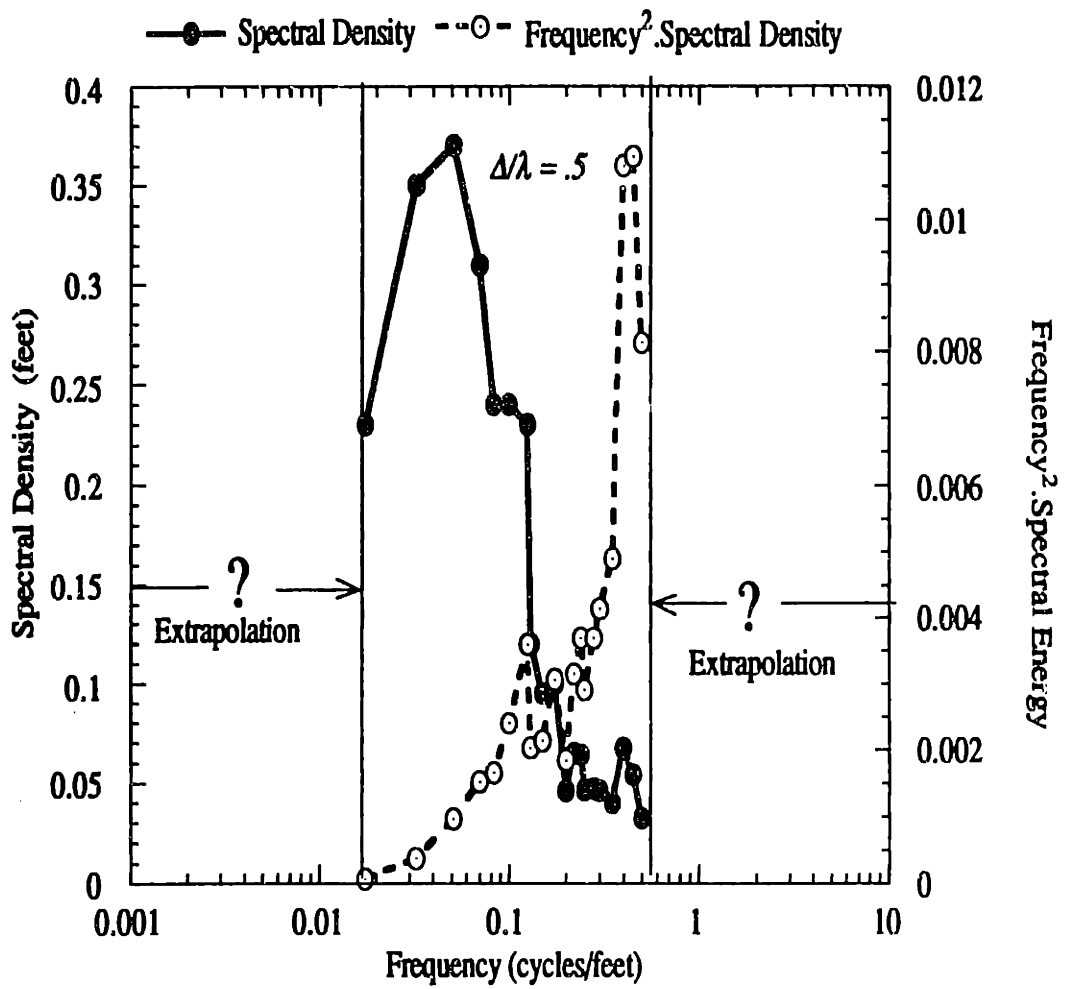


Figure 4.4
 Bakr's [1976] spectral analysis.

influence on the velocity strain rates. This feature is not embedded in Darcy's 'law'. To examine this feature, consider the Navier-Stokes equations of conservation of fluid momentum for an incompressible (Newtonian) fluid,

$$\rho \left[\frac{\partial v_i}{\partial t} + v_j \frac{\partial v_i}{\partial x_j} \right] = - \frac{\partial P}{\partial x_i} + \mu \frac{\partial^2 v_i}{\partial x_j \partial x_j} + \rho g_i$$

The acceleration term on the right hand side may be dropped in considering the creeping viscous flow through the porous media, to get

$$0 = - \frac{\partial P}{\partial x_i} + \mu \frac{\partial^2 v_i}{\partial x_j \partial x_j} + \rho g_i \quad (4.8)$$

Darcy's 'law' is heuristically derived from the preceding by modeling the volume averaged viscous forces on the fluid, as the force exerted by a solid sphere upon laminar flow by Stokes law, *i.e.*,

$$\left\| \mu \frac{\partial^2 v_i}{\partial x_j \partial x_j} \right\| \equiv - \frac{\mu}{k_d} q_i \quad (4.9)$$

where q_i is the volumetric flow rate. Substituting (4.9) in the volume averaged version of (4.8), using the same symbols for volume averaged variables, gives Darcy's 'law'. However, it may also be argued that a fraction of the viscous force exerted on a fluid element is also due to viscous transfer of momentum in the fluid phase. After all, a substantial fraction of a bulk volume of porous media is not occupied by solid particles, but by fluid. The volume averaged viscous force term may thus be argued to be a combination of a Stokes term and the original Laplacian viscous momentum transport term in the Navier-Stokes equation, suitably weighted, *i.e.*,

$$\| \mu \frac{\partial^2 v_i}{\partial x_j \partial x_j} \| \equiv - \frac{\mu}{k_d} q_i + \omega \mu \frac{\partial^2 q_i}{\partial x_j \partial x_j} \quad (4.10)$$

4.3.1 THE DARCY-BRINKMAN 'LAW'

Substituting (4.10) in the creeping flow equations (4.8) yields

$$q_i = - \frac{k_d \rho g}{\mu} \frac{\partial \phi}{\partial x_i} + k_b \frac{\partial^2 q_i}{\partial x_j \partial x_j} \quad (4.11)$$

This is the equation used by Brinkman [1947 a,b] in his attempt to relate the permeability and porosity for an assembly of spheres, using a 'self-consistent' procedure. This equation will henceforth be referred to as the Darcy-Brinkman 'law'. The weakness of both the arguments in 'deriving' Darcy's and the Darcy-Brinkman's 'law' is the introduction of new parameters k_d and k_b (both having units of length squared) that have to be experimentally determined. The fundamental difference is that Darcy-Brinkman's 'law' facilitates transfer of momentum in the fluid phase in addition to the force exerted by the solid matrix on the fluid.

4.3.2 EXAMPLES

Three examples are constructed to illustrate the impact of the Brinkman term on modeling the flow field in a porous medium.

SINUSOIDALLY VARYING HYDRAULIC CONDUCTIVITY:

Consider a porous medium with its permeability varying sinusoidally in the x_2 direction;

$$k_d(x_2) = \bar{k}_d \left\{ \left(1 + \theta \sin\left(\frac{2\pi x_2}{\Delta}\right) \right) \right\}$$

and with a unidirectional hydraulic gradient in the x_1 direction,

$$\frac{\partial \phi}{\partial x_1} = -J, \quad \frac{\partial \phi}{\partial x_2} = 0$$

A Darcy law based analysis of this system gives the flow in the x_1 direction to be

$$q_1(x_2) = \frac{\bar{k}_d \rho g}{\mu} J \left\{ 1 + \theta \sin\left(\frac{2\pi x_2}{\Delta}\right) \right\}$$

The shear rate of the flow field is

$$\frac{\partial q_1(x_2)}{\partial x_2} = \frac{2\pi\theta}{\Delta} \frac{\bar{k}_d \rho g}{\mu} J \cos\left(\frac{2\pi x_2}{\Delta}\right)$$

Defining the norm

$$|f| = \sqrt{\frac{1}{\Delta} \int_0^{\Delta} f^2(x_2) dx_2}$$

the norm of the shear rate is

$$\left| \frac{dq_1}{dx_2} \right| = \frac{\sqrt{2}}{\Delta} \pi \theta \frac{\bar{k}_d \rho g}{\mu} J \quad (4.12)$$

If the flow were governed by the Darcy-Brinkman 'law' (Equation (4.11) with a constant Brinkman parameter k_b) then it may be shown that the flow is given by

$$q_1(x_2) = \frac{k_d \rho g}{\mu} J \left\{ 1 + \frac{\theta}{1 + 4\pi^2 k_y / \Delta^2} \sin\left(\frac{2\pi x_2}{\Delta}\right) \right\}$$

and therefore the shear by

$$\frac{d q_1}{d x_2} = \frac{2\pi}{\Delta} \left(\frac{\theta}{1 + 4\pi^2 k_y / \Delta^2} \right) \frac{k_d \rho g}{\mu} J \cos\left(\frac{2\pi x_2}{\Delta}\right)$$

The norm of the shear is

$$\left| \frac{d q_1}{d x_2} \right| = \frac{\sqrt{2} \pi}{\Delta} \frac{\theta}{1 + 4\pi^2 k_y / \Delta^2} \cdot \frac{k_d \rho g}{\mu} J \quad (4.13)$$

The impact of the Brinkman term on the shear may be seen from Figure 4.5, which contrasts (4.12) and (4.13). The Brinkman term, at small scales of fluctuations, dampens out the velocity fluctuations, limiting the unbounded inverse dependence of shear on the scale of fluctuations, as implied by Darcy's 'law'.

TWO LAYERED POROUS MEDIUM:

Consider a two layered porous medium, with the upper layer having a greater permeability than the bottom one. Locating the junction at $x_2 = 0$, and the variables pertaining exclusively to the positive x_2 region are indicated by the superscript 1, and variables pertaining to the negative x_2 region by a superscript 2. A Darcy analysis leads to the simple description of flow;

$$q_1^1(x_2) = \frac{k_d^1 \rho g}{\mu} J$$

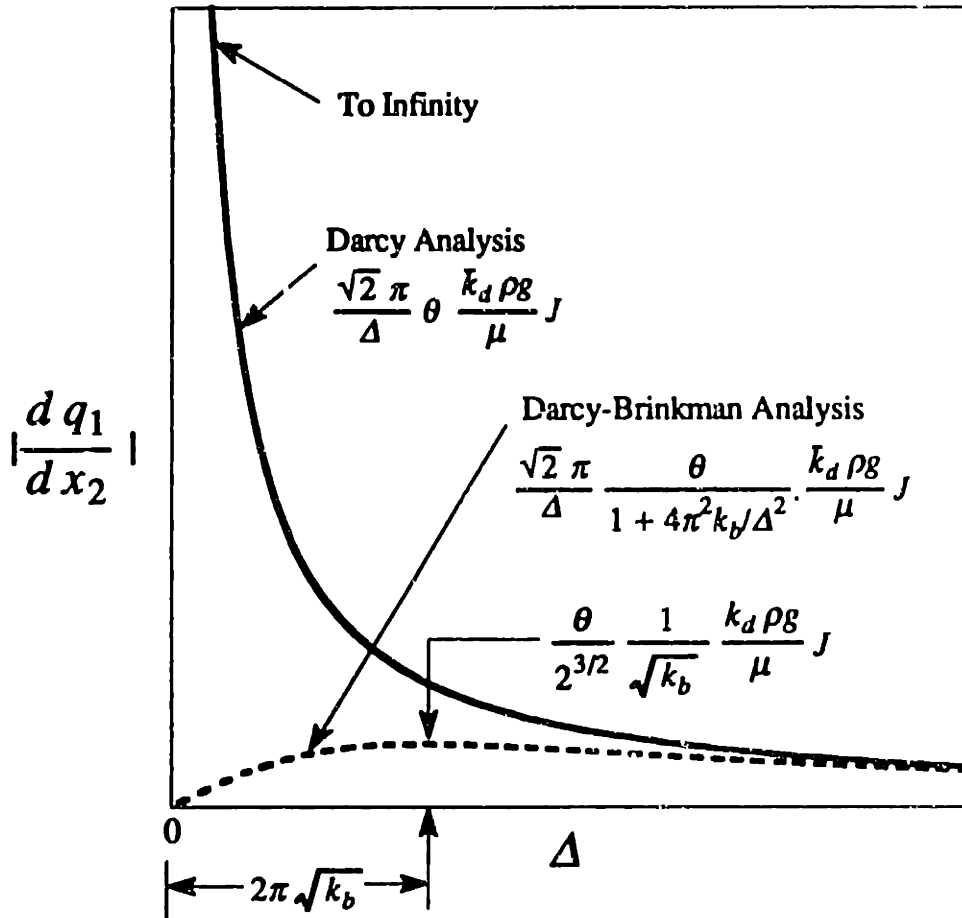


Figure 4.5

Shear in sinusoidally varying permeability:
 Importance of the Brinkman term at small wavelengths.

$$q_1^2(x_2) = \frac{k_d^2 \rho g}{\mu} J$$

To investigate the impact of including a Brinkman term with a constant k_b , we will have to impose conditions at the junction of the two media. Matching the flow rates and the shear,

$$q_1^1(x_2) = q_1^2(x_2), \quad \frac{\partial q_1^1(x_2)}{\partial x_2} = \frac{\partial q_1^2(x_2)}{\partial x_2}, \quad \text{at } x_2 = 0,$$

the flow may be shown to be given by

$$q_1^1(x_2) = \frac{\rho g}{\mu} J \left\{ k_d^1 - \frac{(k_d^1 - k_d^2)}{2} \exp\left(-\frac{x_2}{\sqrt{k_b}}\right) \right\}$$

$$q_1^2(x_2) = \frac{\rho g}{\mu} J \left\{ k_d^2 + \frac{(k_d^1 - k_d^2)}{2} \exp\left(+\frac{x_2}{\sqrt{k_b}}\right) \right\}$$

This also reveals an upper limit on the shear rate as

$$\max \left| \frac{d q_1^i}{d x_2} \right| = \frac{k_d^1 - k_d^2}{2\sqrt{k_b}} \quad (4.14)$$

FLOW IN A POROUS COLUMN WITH NO SLIP CONDITIONS AT WALLS:

Consider flow in a porous column of radius R , imposing zero slip boundary conditions at the boundaries. The flow is governed by the polar coordinate version of (4.11)

$$q(r) = \frac{k_d \rho g}{\mu} J + k_b \frac{1}{r} \frac{\partial}{\partial r} \left(r \frac{\partial q(r)}{\partial r} \right)$$

where r is the radial distance from the center of the column cross-section, and J is the hydraulic gradient along the column axis. The solution for the discharge is the series solution;

$$q(r) = \frac{k_d \rho g}{\mu} J \left[1 - \frac{\sum_{n=0}^{\infty} \frac{\left(\frac{r}{\sqrt{k_b}} \right)^{2n}}{2^{2n} (n!)^2}}{\sum_{n=0}^{\infty} \frac{\left(\frac{R}{\sqrt{k_b}} \right)^{2n}}{2^{2n} (n!)^2}} \right]$$

The cross-section average discharge, which is a function of the column radius R , is therefore

$$\bar{q}(R) = \frac{k_d \rho g}{\mu} J \left[1 - \frac{\sum_{n=0}^{\infty} \frac{\left(\frac{R}{\sqrt{k_b}} \right)^{2n}}{2^{2n} n! (n+1)!}}{\sum_{n=0}^{\infty} \frac{\left(\frac{R}{\sqrt{k_b}} \right)^{2n}}{2^{2n} (n!)^2}} \right]$$

The zero slip boundary conditions reduce the average discharge. This reduction effect decreases as the column radius becomes much larger than the square root of the Brinkman parameter k_b as shown in Figure 4.6.

The scales of fluctuations affected by the Brinkman term is of course dependent on the magnitude of the Brinkman parameter k_b in (4.11). Comprehensive tests of the

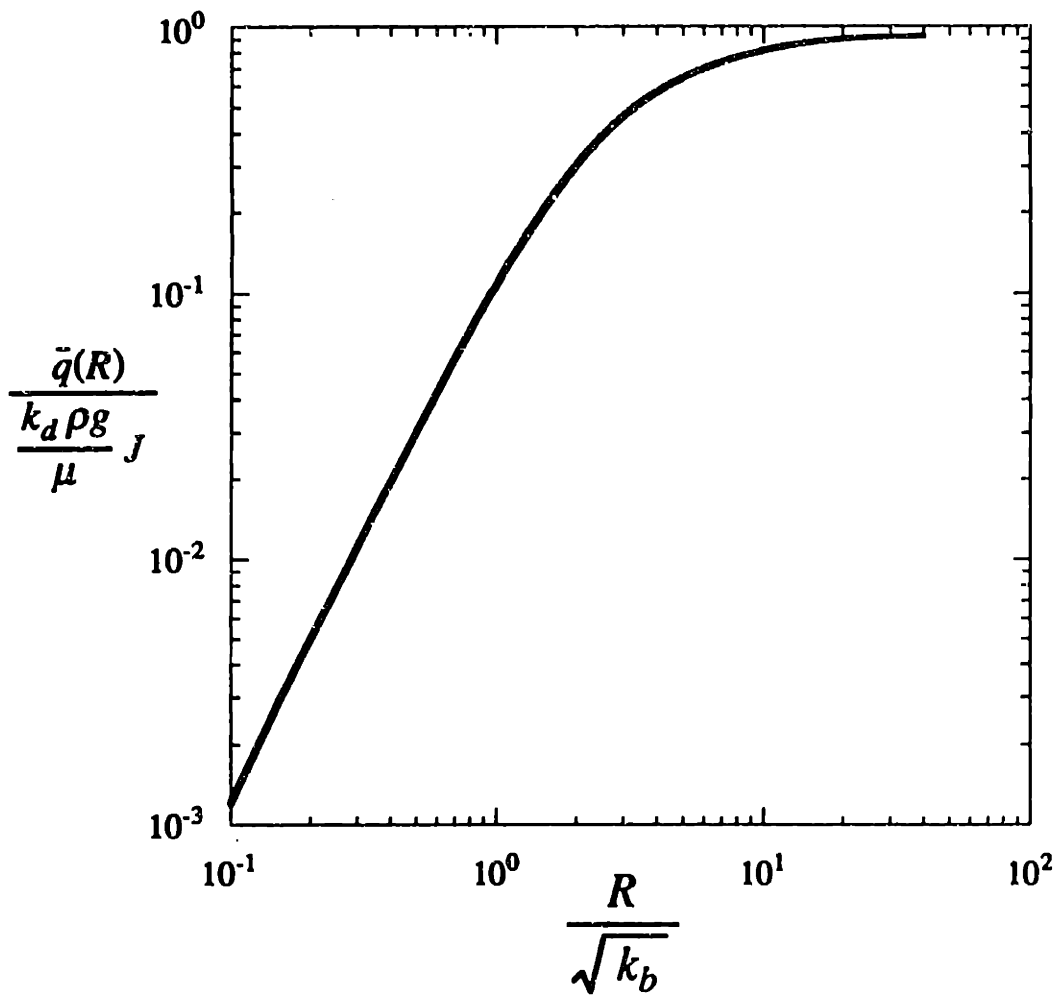


Figure 4.6

Discharge through a column of porous media.

Brinkman 'law' have not been performed. The previous example of flow in a column shows that despite the additional fluid momentum transfer mechanism, the bulk flow in a given column remains linearly proportional to the hydraulic gradient. From the point of view of computing the bulk flow, the Darcy-Brinkman 'law' may be replaced by a Darcy 'law' with a modified permeability, for that column. Perhaps this is a reason why the Brinkman parameter is not routinely measured. However it must be kept in mind, laboratory experiments are typically done on 'homogenous' porous material, and not done to explore the validity or limitations of the Darcy framework for modeling the details of flow in heterogeneous porous continuum. Is there an experiment on a heterogeneous porous medium, where the details of the flow field have been mapped and the relation between flow strain rates and permeability variations can be studied? The additional term in the Darcy-Brinkman law, modifies the unlimited inverse dependence of the velocity strain rate on the scale of heterogeneity of the spatially varying permeability. Nield and Bejan [1992] have discussed the Brinkman's equation and applications. Dagan [1979] presents an estimate of k_b . Experiments done with the aim of studying the interaction of porous and ordinary laminar flows [Beavers and Joseph, 1967; Taylor, 1971] suggest

$$k_b \approx 10k_d \text{ to } 100 k_d$$

In that case as long as the scale of heterogeneity is much larger than the square root of the permeability k_d , the effect of the Brinkman term is negligible. However, if we were to choose a nondifferentiable spectrum like the exponential, even the small Brinkman parameter would decrease the variance of the derivatives of the velocity field from infinite to a finite value.

4.3.3 VELOCITY SPECTRUM WITH BRINKMAN SMOOTHING

Coupling the Darcy-Brinkman 'law' (Equation (4.11)) with the divergence free flow condition yields the same hydraulic head equation, obtained using Darcy's law (Appendix-IV). Therefore the Brinkman fluid momentum transfer term may be routinely incorporated in the velocity spectrum for flow in a three dimensional heterogeneous medium to get

$$S_{v_i v_j}(k) = \frac{(v/\gamma)^2}{(1 + k_b k^2)^2} \left(\delta_{i1} - \frac{k_i k_1}{k^2} \right) \left(\delta_{j1} - \frac{k_j k_1}{k^2} \right) S_{ff}(k) \quad (4.15)$$

The additional term in the denominator provides a 'high wave number Brinkman filter'. Of course, if the $\ln K$ spectrum already has a high wave number cutoff corresponding to a scale much larger than the square root of the Brinkman parameter k_b , the influence of the additional terms on the velocity strain rates will be minimal. The reality of momentum transfer in the fluid phase in a heterogeneous medium will impose a high wave number cutoff, notwithstanding our choice of the $\ln K$ spectrum.

4.4 CONCLUSIONS

For the crossbedded sandstone permeability series analyzed in this paper it is shown that the $\ln K$ correlation function is upward convex at the origin, implying finite energy in the spectrum of the spatial derivatives of the $\ln K$. The $\ln K$ microscale, the scale associated with the derivatives of the $\ln K$ field, was estimated. The choice of $\ln K$ fields with unbounded spatial derivatives everywhere, is a triply poor one. Firstly, it is not compatible with the continuum requirements of a scale disparity between the REV scale and the first scale at which fluctuations occur. Secondly, it results in unbounded strain rates of the velocity field, which is only a reflection of the inability of the simple Darcy scale continuum analysis to model the strain rates of the velocity field under conditions of

extremely small scale heterogeneity. Thirdly, there is no dataset that supports unbounded variances for the spatial partial derivatives of $\ln K$. In light of the important role the velocity strain rates play in determining small scale properties of the solute distribution in the advection dispersion process [Lumley, 1972; Batchelor, 1959] it is recommended that analysis into finer details of solute distribution like the concentration variance and covariance, adapt realistic representations of the $\ln K$ correlation function at small separations. In numerical approximations of flow and transport, it will be infinitely easier to resolve the fluctuations of the $\ln K$ field and the straining action of the velocity field, if the energies in the spatial derivatives is finite. It is also argued, that the process of transfer of momentum in the fluid phase will provide a high wave number filter for the velocity field, in the absence of a scale disparity between the $\ln K$ heterogeneities, and the square root of the permeability of the porous material.

CHAPTER 5

NONLINEAR COMPUTATION OF MACRODISPERSIVITIES IN THREE DIMENSIONALLY HETEROGENEOUS AQUIFERS VIA CORRSIN'S CONJECTURE

It is proven that the correlation coefficient (*i.e.*, covariance divided by the product of the standard deviations) between a correlated stochastic process and its integral over a time period is a decreasing function of the time period. This is a rationale of Corrsin's [1962] conjecture of *asymptotic* statistical independence between a particles velocity and position in a correlated velocity field. Corrsin's conjecture is inapplicable for small displacements for which the particles position and velocity are strongly correlated. Applying Corrsin's conjecture to compute Lagrangian velocity statistics from Eulerian velocity statistics (which are generally a lot easier to compute) yields a nonlinear formulation for macrodispersivities. For the isotropic case nonlinear analytical algebraic equations are derived for the macrodispersivities. The longitudinal macrodispersivity remains practically unchanged from the linear results of Gelhar and Axness [1983]. The transverse macrodispersivity shows a correlation scale dependence not exhibited in the linear results. For the anisotropic imperfectly layered case it is shown for highly layered aquifers the vertical macrodispersivities will be greater than the transverse horizontal ones. The field scale observations to the contrary are therefore not explained by this nonlinear result. Zhang and Neuman [1990] in their two-dimensional 'depth averaged' considerations concluded otherwise on account of dropping the vertical dimension altogether. This supports the analysis of Rehfeldt and Gelhar [1992] on flow unsteadiness as a possible controlling mechanism for transverse horizontal macrodispersion.

5.1 THEOREM

Let $v(t)$ be a zero mean second order stationary stochastic process with a continuous covariance function

$$E[v(t)v(t+\tau)] = \sigma_v^2 \rho_v(\tau) = \sigma_v^2 \rho_v(-\tau)$$

and

$$x(t) = \int_0^t v(\tau) d\tau$$

with

$$E[x(t)x(t)] = \sigma_{x(t)}^2$$

Define the cross-correlation coefficient between $v(t)$ and $x(t)$ as

$$\rho_{x(t)v(t)} = \frac{E[x(t)v(t)]}{\sigma_{x(t)}\sigma_v} \quad (5.1)$$

Let there exist $c_1 \in \mathfrak{R}$ such that

$$\lim_{t \rightarrow \infty} \int_0^t \rho_v(\tau) d\tau \rightarrow c_1 \quad (5.2)$$

Then

$$\lim_{t \rightarrow \infty} \rho_{x(t)v(t)} \rightarrow 0 \quad (5.3)$$

if

1) $c_1 \neq 0$ and there exists $c_2 \in \mathfrak{R}$ such that

$$\lim_{t \rightarrow \infty} \int_0^t \tau \rho_v(\tau) d\tau \rightarrow c_2 \quad (5.4)$$

2) $c_1 = 0$ and there exist $t_0 > 0$ and $\delta > 0$ such that for every $t > t_0$

$$t \int_0^t \rho_v(\tau) d\tau - \int_0^t \tau \rho_v(\tau) d\tau \geq \delta > 0 \quad (5.5)$$

Proof:

$$E[x(t)v(t)] = \int_0^t E[v(\tau)v(t)] d\tau = \sigma_v^2 \int_0^t \rho_v(t-\tau) d\tau$$

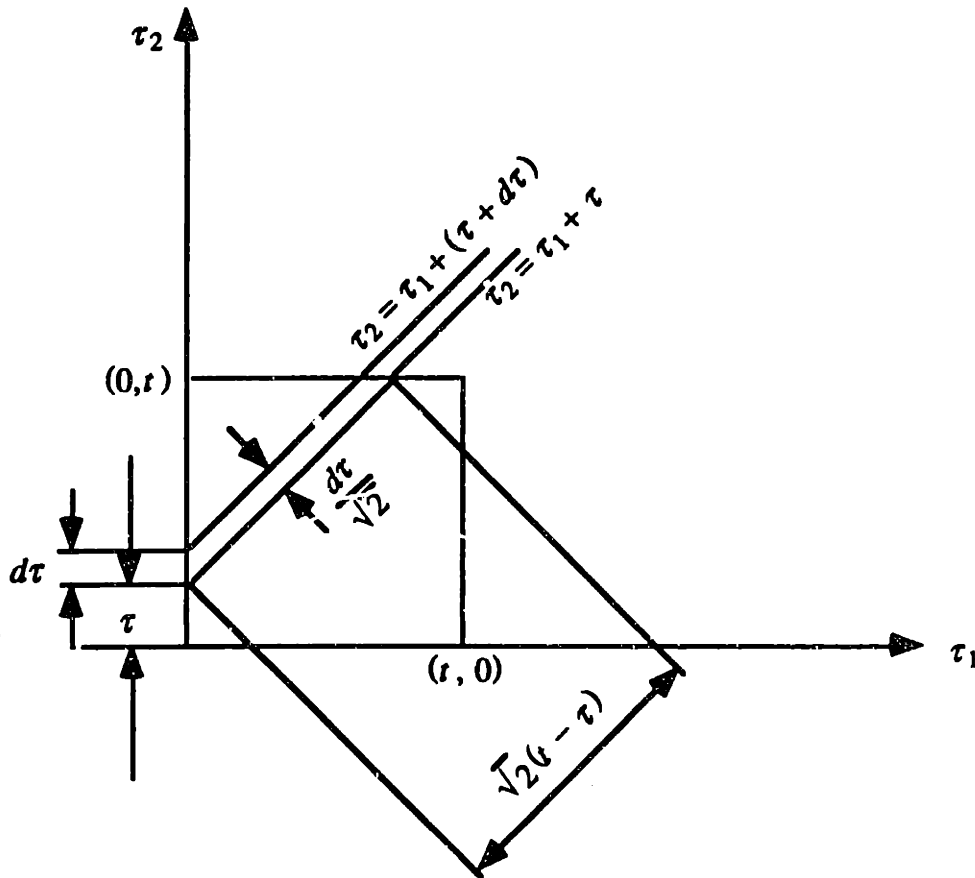
therefore

$$E[x(t)v(t)] = \sigma_v^2 \int_0^t \rho_v(\tau) d\tau \quad (5.6)$$

Now

$$E[x(t)x(t)] = \sigma_{x(t)}^2 = \int_0^t \int_0^t E[v(\tau_1)v(\tau_2)] d\tau_1 d\tau_2 \quad (5.7a)$$

Recognizing the constancy of $E[v(\tau_1)v(\tau_2)]$ over lines of constant $\tau_2 - \tau_1$ as shown in the sketch below, the double integral may be transformed into a single integral over $\tau = \tau_2 - \tau_1$.



As in Taylor [1921], it follows that

$$E[x(t)x(t)] = 2\sigma_v^2 \int_0^t (t-\tau)\rho_v(\tau)d\tau \quad (5.7b)$$

Using (5.6), (5.7b), the cross correlation coefficient (5.1) may be written as

$$\rho_{x(t)v(t)} = \frac{\int_0^t \rho_v(\tau)d\tau}{\sqrt{2} \left[t \int_0^t \rho_v(\tau)d\tau - \int_0^t \tau \rho_v(\tau)d\tau \right]^{1/2}} \quad (5.8)$$

1) As $c_1 \neq 0$, it follows from the continuity of ρ_v and (5.4) that

$$\lim_{t \rightarrow \infty} \rho_{x(t)v(t)} \rightarrow \frac{c_1}{\sqrt{2} [t c_1 - c_2]^{1/2}}$$

Now

$$\lim_{t \rightarrow \infty} \sqrt{2} [t c_1 - c_2]^{1/2} \rightarrow \sqrt{2 t c_1}$$

therefore

$$\lim_{t \rightarrow \infty} \rho_{x(t)v(t)} \rightarrow \sqrt{\frac{c_1}{2t}} \rightarrow 0 \quad (5.9)$$

2) From (5.5) and (5.8) it follows that for every $t > t_0$, $|\rho_{x(t)v(t)}| \leq \left| \frac{\int_0^t \rho_v(\tau)d\tau}{(2\delta)^{1/2}} \right|$

It follows from

$$\lim_{t \rightarrow \infty} \int_0^t \rho_v(\tau)d\tau \rightarrow c_1 = 0$$

that

$$\lim_{t \rightarrow \infty} |\rho_{x(t)v(t)}| \leq 0, \text{ i.e., } \lim_{t \rightarrow \infty} \rho_{x(t)v(t)} \rightarrow 0 \quad \square$$

5.1.1 EXAMPLES

Example 1.

For an exponential velocity correlation function

$$\rho_v(\tau) = e^{-\frac{|\tau|}{\lambda}}, \lambda > 0$$

It follows

$$\int_0^t \rho_v(\tau) d\tau = \lambda - \lambda e^{-\frac{t}{\lambda}} \quad \therefore \lim_{t \rightarrow \infty} \int_0^t \rho_v(\tau) d\tau \rightarrow \lambda = c_1 > 0$$

and

$$\int_0^t \tau \rho_v(\tau) d\tau = \lambda^2 - (\lambda^2 + \lambda t) e^{-\frac{t}{\lambda}} \quad \therefore \lim_{t \rightarrow \infty} \int_0^t \tau \rho_v(\tau) d\tau \rightarrow \lambda^2 = c_2$$

By part 1 of the theorem, these are sufficient conditions for $\lim_{t \rightarrow \infty} \rho_{x(t)v(t)} \rightarrow 0$

In fact the cross-correlation coefficient between position $x(t)$ and velocity $v(t)$ is

$$\rho_{x(t)v(t)} = \frac{\lambda - \lambda e^{-\frac{t}{\lambda}}}{\sqrt{2} [t(\lambda - \lambda e^{-\frac{t}{\lambda}}) - (\lambda^2 - (\lambda^2 + \lambda t) e^{-\frac{t}{\lambda}})]^{1/2}}$$

therefore

$$\lim_{t \rightarrow \infty} \rho_{x(t)v(t)} \equiv \sqrt{\frac{\lambda}{2t}} \rightarrow 0$$

Figure 5.1 shows the monotonically decreasing correlation between velocity and position.

Example 2.

For a 'zero integral scale' velocity correlation function

$$\rho_v(\tau) = \left(1 - \frac{|\tau|}{\lambda}\right) e^{-\frac{|\tau|}{\lambda}}, \lambda > 0$$

It follows that

$$\int_0^t \rho_v(\tau) d\tau = t e^{-\frac{t}{\lambda}} \quad \therefore \lim_{t \rightarrow \infty} \int_0^t \rho_v(\tau) d\tau \rightarrow 0 = c_1$$

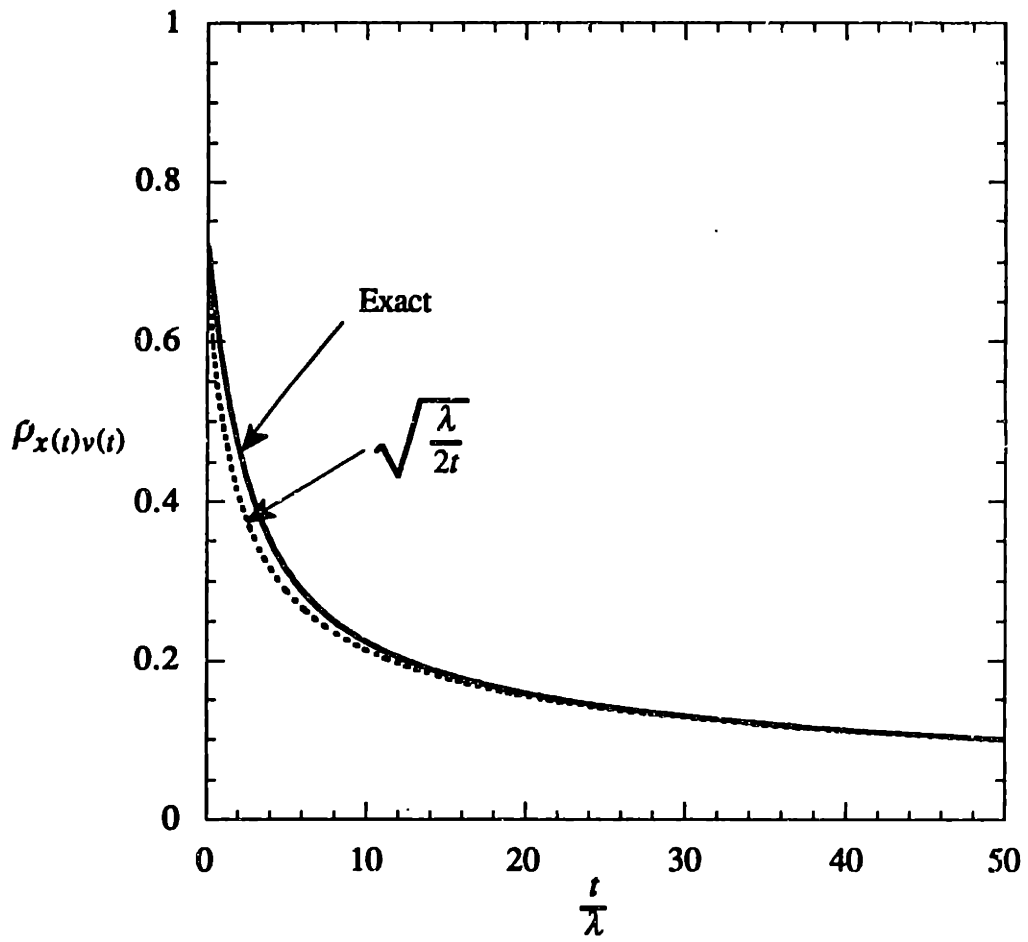


Figure 5.1

Correlation coefficient between position and velocity: Example 1.

Now

$$\int_0^t \tau \rho_v(\tau) d\tau = -\lambda^2 + (\lambda^2 + \lambda t + t^2) e^{-\frac{t}{\lambda}}$$

therefore

$$f(t) = t \int_0^t \rho_v(\tau) d\tau - \int_0^t \tau \rho_v(\tau) d\tau = \lambda^2 - (\lambda^2 + \lambda t) e^{-\frac{t}{\lambda}}$$

Since

$$\frac{df(t)}{dt} = t e^{-\frac{t}{\lambda}} > 0 \text{ for every } t > 0$$

condition 2 of the theorem is met, e.g.,

$$t_0 = \lambda, \delta = f(t_0) = \lambda^2 \left(1 - \frac{2}{e}\right)$$

and

$$\text{for every } t > \lambda, t \int_0^t \rho_v(\tau) d\tau - \int_0^t \tau \rho_v(\tau) d\tau \geq \lambda^2 \left(1 - \frac{2}{e}\right) > 0$$

therefore $\lim_{t \rightarrow \infty} \rho_{x(t)v(t)} \rightarrow 0$. In fact, the correlation coefficient between the position $x(t)$ and velocity $v(t)$ is

$$\rho_{x(t)v(t)} = \frac{t e^{-t/\lambda}}{\sqrt{2} [\lambda^2 - (\lambda^2 + \lambda t) e^{-t/\lambda}]^{1/2}}$$

therefore

$$\lim_{t \rightarrow \infty} \rho_{x(t)v(t)} \cong \frac{t e^{-t/\lambda}}{\sqrt{2} \lambda} \rightarrow 0$$

as shown in Figure 5.2.

It is worth reiteration that two sets of conditions in the Theorem were shown to be *sufficient* to result in an asymptotic decay of the cross-correlation coefficient between a correlated stochastic process and its integral. The conditions are quite unrestrictive, but

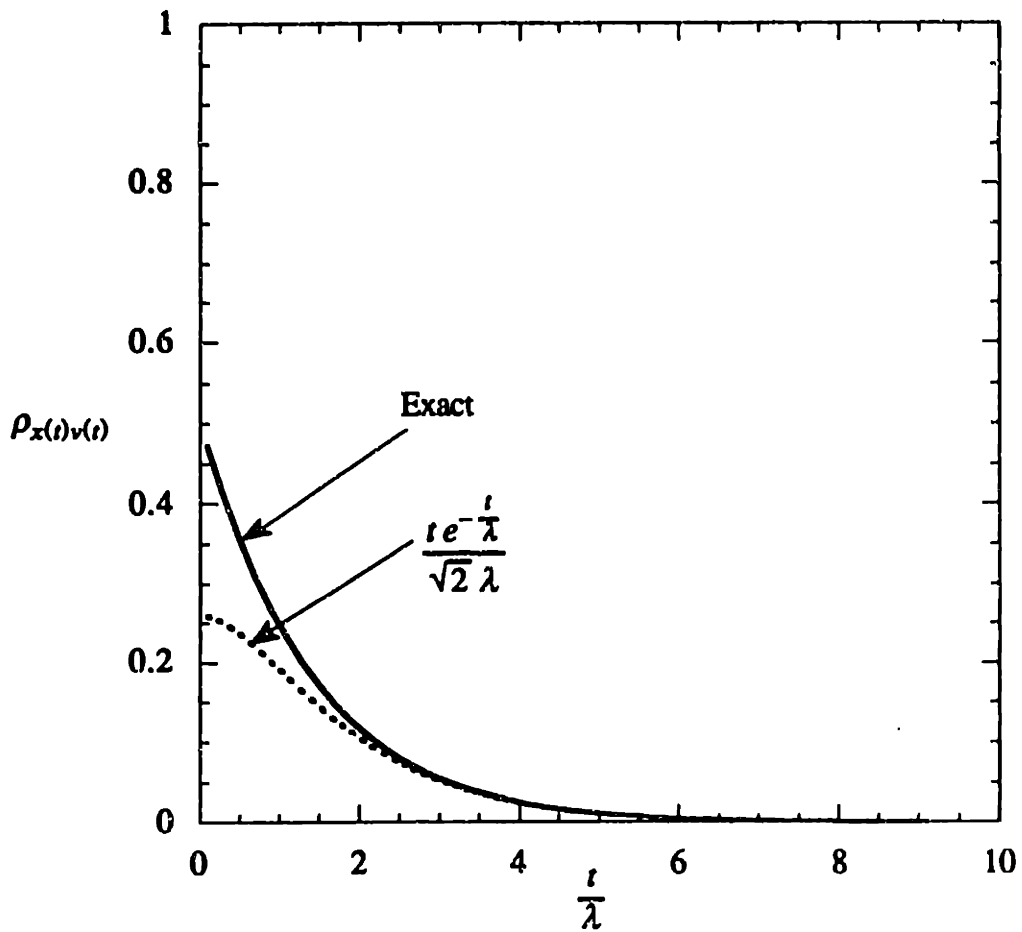


Figure 5.2

Correlation coefficient between position and velocity: Example 2.

by no means were *shown to be necessary*. The Theorem may hold true for an even bigger class of velocity correlation functions.

5.2 MEAN SQUARED DISPLACEMENT OF A PARTICLE IN A CORRELATED VELOCITY FIELD

Taylor's [1921] analysis of the mean squared deviation of a particle in a turbulent velocity field is repeated here. Consider $\mathbf{x}(t; \mathbf{0})$ to be the position of a particle that was at the origin at $t = 0$, *i.e.*, $\mathbf{x}(0; \mathbf{0}) = \mathbf{0}$. Let the particle be carried along in a velocity field with a mean v in the x_1 direction, and a three dimensional-zero mean-statistically stationary perturbation v_i' . The perturbation in the particles position around the ensemble mean position $(vt, 0, 0)$ is given by

$$x_i'(t; \mathbf{0}) = \int_0^t v_i'(\mathbf{x}(\tau; \mathbf{0})) d\tau \quad (5.10)$$

The mean squared perturbation in the particles position is therefore

$$R_i^2(t) \equiv E[x_i'^2(t; \mathbf{0})] = \int_0^t \int_0^t E[v_i'(\mathbf{x}(\tau_1; \mathbf{0}))v_i'(\mathbf{x}(\tau_2; \mathbf{0}))] d\tau_1 d\tau_2 \quad (5.11)$$

where

$$E[v_i'(\mathbf{x}(\tau_1; \mathbf{0}))v_i'(\mathbf{x}(\tau_2; \mathbf{0}))] = \mu_i(\tau) = \mu_i(-\tau); \tau = \tau_1 - \tau_2 \quad (5.12)$$

is the Lagrangian velocity covariance function (which is assumed to be stationary on account of the Eulerian velocity covariance function being assumed stationary). It follows that

$$R_i^2(t) = 2 \int_0^t (t - \tau) \mu_i(\tau) d\tau$$

therefore

$$\frac{1}{2} \frac{d R_i^2(t)}{dt} = \int_0^t \mu_i(\tau) d\tau \quad (5.13)$$

5.3 COMPUTATION OF LAGRANGIAN VELOCITY STATISTICS FROM EULERIAN VELOCITY STATISTICS

The simplest approximation to relate Lagrangian velocity statistics to the Eulerian ones involves substituting the mean particle positions instead their actual positions, in the Lagrangian velocity covariance expression (5.12). This yields

$$\mu_i(\tau) \approx E[v_i'(E[\mathbf{x}(\tau; \mathbf{0})])v_i'(E[\mathbf{x}(0; \mathbf{0})])] \equiv R_{v_i v_i}(v\tau, 0, 0) \quad (5.14)$$

This approximation may be understood as taking a Taylor expansion of the velocity of a particle about its ensemble mean position;

$$v_i'(\mathbf{x}(\tau; \mathbf{0})) = v_i'(E[\mathbf{x}(\tau; \mathbf{0})]) + x_i'(\tau; \mathbf{0}) \left. \frac{\partial v_i'}{\partial x_i} \right|_{E[\mathbf{x}]} + \dots$$

and assuming the partial derivatives of the velocity in space to be sufficiently small so that all but the leading term may be dropped.

5.3.1 CORRSIN'S [1962] CONJECTURE

Assuming that the joint probability density function (pdf) of

$$v_i'(x(\tau; 0)), v_i'(0), x(\tau; 0)$$

can be expressed as a product of the joint pdf of

$$v_i'(x(\tau; 0)), v_i'(0)$$

and

$$x(\tau; 0)$$

(*i.e.*, assuming the particles current position to be statistically independent of its current velocity and the velocity at the origin. *i.e.*, Corrsin's [1962] conjecture) the Lagrangian velocity covariance function (5.12) may be expressed as

$$\mu_i(\tau) = \int_{-\infty}^{+\infty} R_{v_i v_i}(x(\tau; 0)) \psi_x dx \quad (5.15)$$

where ψ_x is the pdf of the particle position at time τ (the particle was at the origin at initially). While this statistical independence assumption is a very strong assumption and (Corrsin's conjecture) certainly cannot be exactly correct (as the particle velocity is the rate of change of the particles position), the Theorem in Section 5.1 shows that the covariance between a particles position and its current velocity is a decreasing fraction of the product of the standard deviation of the particles position and the standard deviation of its velocity. The same applies for the covariance between a particles current position

and the velocity at the origin. The fluctuations in velocity at any point are only infinitesimally reflected in the fluctuations of the particle position. This feature comes about by the growth in the standard deviation of the particles position. The Theorem in Section 5.1 is the rationale for Corrsin's conjecture.

5.3.2 LARGE DISPLACEMENT CONDITION ON THE APPLICABILITY OF CORRSIN'S CONJECTURE

The large time condition on the applicability of Corrsin's conjecture can be appreciated using the results of the Theorem and the examples in Section 5.1. The examples clearly show the inapplicability of Corrsin's conjecture at early times (see Figure 5.1 and 5.2). In the expressions for the coefficient of correlation between a particles position and velocity (5.9) the Lagrangian temporal correlation scale c_1 may be replaced by the spatial correlation scale l divided by the mean velocity v . This yields

$$\left(\frac{l}{2rv}\right)^{1/2}$$

as an estimate for the cross-correlation coefficient between a particles position and velocity. Therefore, for the cross-correlation coefficient to be small, say a value of .1, the particle has to travel 200 correlation distances. Corrsin's conjecture is inapplicable to the to the 'developing dispersion' problem as done in a numerical iterative exercise by Neuman and Zhang [1990].

5.3.3 NONLINEAR FORMULATION FOR MACRODISPERSIVITIES USING CORRSIN'S CONJECTURE

A description for a mean concentration field of the form

$$\frac{\partial \bar{c}}{\partial t} + v \frac{\partial \bar{c}}{\partial x_1} - v(\alpha_{ij} + A_{ij}) \frac{\partial^2 \bar{c}}{\partial x_i \partial x_j} = 0 \quad (5.16)$$

implies that the spatial second moment of the mean concentration follows

$$\frac{1}{2} \frac{d R_i^2(t)}{dt} = (A_{ii} + \alpha_{ii})v \quad (5.17)$$

The mean concentration may also be interpreted as being proportional to the pdf of a particle in the velocity field

$$\bar{c}(\mathbf{x}, \tau) = \frac{M}{n} \Psi_{\mathbf{x}}(\tau; 0) \quad (5.18)$$

Now looking for a constant large displacement macrodispersivity, the pdf of a particle consistent with the mean concentration equation (5.16) may be expressed as

$$\Psi_{\mathbf{x}}(\tau; 0) = \prod_{i=1}^3 \frac{\exp\left[-\frac{(x_i - v\delta_{i1}\tau)^2}{4(A_{ii} + \alpha_{ii})v\tau}\right]}{\sqrt{4\pi(A_{ii} + \alpha_{ii})v\tau}} \quad (5.19)$$

The local dispersion contribution to the rate of change of the mean squared position of a particle in (5.13) is argued as an additive Brownian motion component to the particles position vector, with the strength of the Brownian motion *fitted* to yield the laboratory measured local dispersivities. Substituting the new formulation for the Lagrangian velocity covariance function (5.15) into the expressions gives for the temporal rate of change of the mean squared displacement (5.13) gives

$$A_{ii} = \lim_{t \rightarrow \infty} \frac{1}{v} \int_0^t \int_{-\infty}^{+\infty} R_{v_i v_i}(\mathbf{x}(\tau; \mathbf{0})) \psi_{\mathbf{x}} d\mathbf{x} d\tau \quad (5.20)$$

This is equivalent to the expression for macrodispersivities given in Gelhar [1987], Equation 4.6, with local dispersivities replaced with a sum of local dispersivities and macrodispersivities. It follows from Gelhar [1987] that (5.20) for large displacements is

$$A_{ii} = \int_{-\infty}^{+\infty} \frac{S_{v_i v_i}(\mathbf{k}) d\mathbf{k}}{[ik_1 + (A_{11} + \alpha_{11})k_1^2 + (A_{22} + \alpha_{22})k_2^2 + (A_{33} + \alpha_{33})k_3^2]v^2} \quad (5.21)$$

Equation (5.21) is a nonlinear formulation for the asymptotic macrodispersivities, incorporating a 'higher order' conversion from Eulerian statistics to Lagrangian statistics, via Corrsin's [1962] conjecture, the rationale for which is provided in Section 5.1.

5.4 NONLINEAR COMPUTATION OF MACRODISPERSIVITIES

The computation of the macrodispersivity integral (5.21) will yield nonlinear algebraic equations which can be solved to compute the macrodispersivities. Previous evaluations of the integrals of this type in Gelhar and Axness [1983] are made under the assumption that the local dispersivities are much smaller than the correlation scale or that the local dispersivities are isotropic. Since the nonlinear formulation amounts to replacing a local dispersivity by a sum of local dispersivity and macrodispersivity, both of these assumptions do not hold.

5.4.1 ISOTROPIC CASE

For the isotropic exponential spectrum, exact evaluations of the integral (5.21) are shown in Appendix-VI (replacing the local dispersivities replaced by a sum of local and macrodispersivities). The result is a pair of analytical nonlinear (albeit complicated) expressions from which macrodispersivities may be evaluated. No numerical integration is required and little effort is required in solving the algebraic equations by machine. The results are shown in Figure 5.3 and 5.4. The subscript L refers to results presented in Gelhar and Axness [1983], *i.e.*,

$$A_{11}^L = \sigma_f^2 \lambda \gamma^2 \quad (5.22a)$$

$$A_{22}^L = \frac{\sigma_f^2 \alpha_L}{15\gamma^2} \left(1 + \frac{4\alpha_T}{\alpha_L} \right) \quad (5.22b)$$

The subscript NL refers to the macrodispersivities computed here by a nonlinear formulation incorporating Corrsin's conjecture. The longitudinal macrodispersivity is unchanged in Figure 5.3. This can be easily understood from the evaluation of longitudinal macrodispersivity integral (in Appendix VI). The longitudinal macrodispersivity is quite insensitive to local dispersion, consequently when it is replaced by a macrodispersion plus a local dispersion in the nonlinear formulation, it changes very little,

$$\frac{A_{11}^{NL}}{A_{11}^L} \equiv 1 \quad (5.23)$$

Of course that is not the case with the transverse macrodispersivity. As a first cut guess, the nonlinear formulation involves substituting a local dispersivity by a macrodispersivity in the expression (5.22b) adopted from Gelhar and Axness [1983]. Neglecting the portion

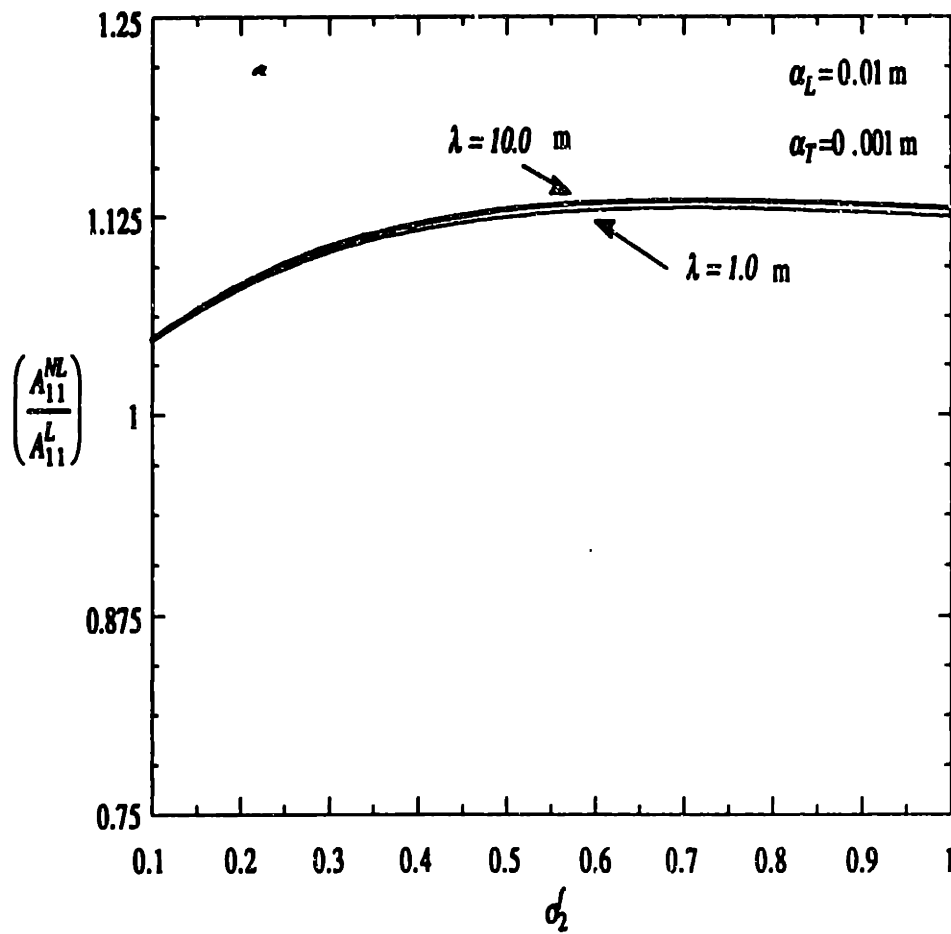


Figure 5.3

Nonlinear computation of longitudinal macrodispersivity
in isotropic medium.

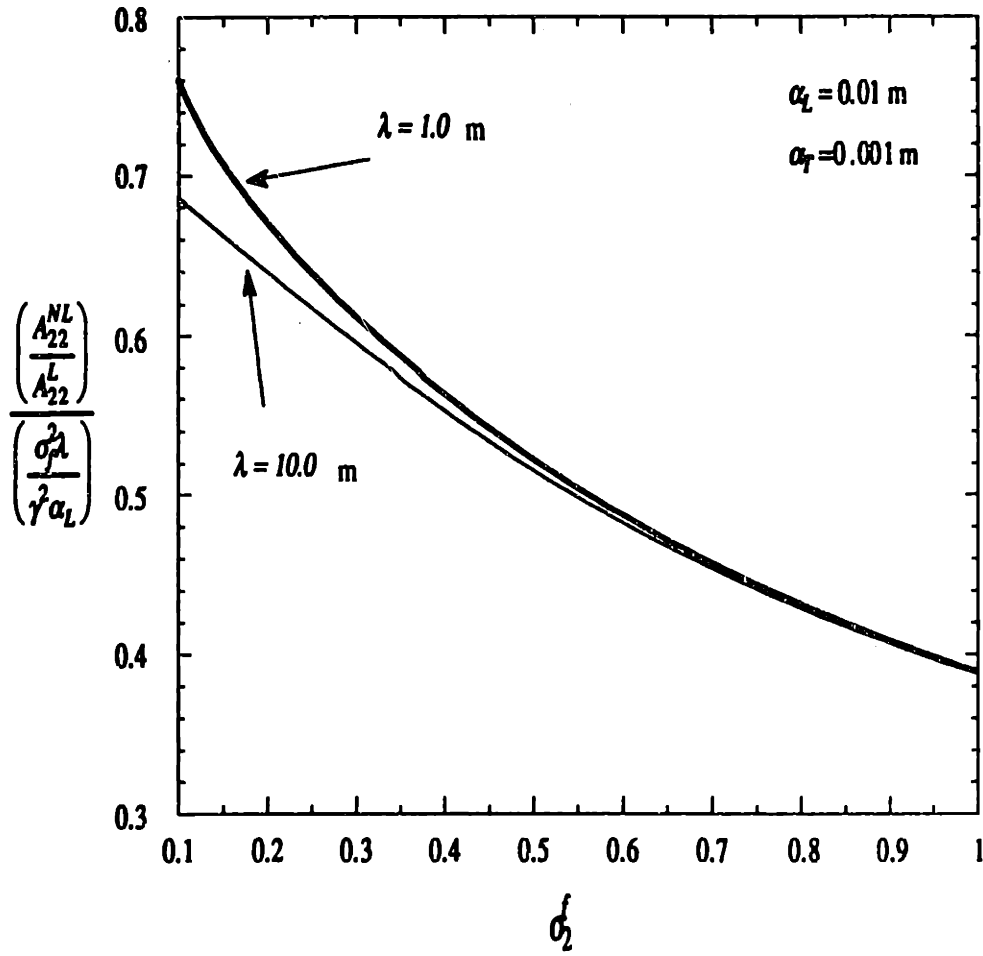


Figure 5.4
Nonlinear computation of transverse macrodispersivity
in isotropic medium.

in the brackets in the expression for transverse macrodispersivity (5.22b), it may be expected that

$$\frac{A_{22}^{NL}}{A_{22}^L} = O\left(\frac{\sigma_f^2 \lambda}{\gamma^2 \alpha_L}\right) \quad (5.24)$$

This is borne out in the detailed evaluation shown in the Figure 5.4. Note that (5.24) implies a dependence of the transverse macrodispersivity on the fourth power of the $\ln K$ standard deviation multiplied by the correlation scale. Dagan [1988] (his Section 6, last paragraph) first presented such a result, without discussing the rationale for Corrsin's [1962] conjecture and the large time conditions on its approximate applicability. Field observation show larger transverse macrodispersivities than predicted by a linear theory. However, comparisons with field experiments require performing this exercise for anisotropic heterogeneous porous media.

5.4.1 ANISOTROPIC CASE

Examining the results of Gelhar and Axness [1983] on macrodispersivities in anisotropic imperfectly layered medium with small ratios of vertical to horizontal correlation scales ε , one finds that the transverse horizontal macrodispersivity is ε^2 times the transverse vertical (equations (43) and (44), Gelhar and Axness [1983]). This is argued to be a fundamental property of the velocity correlation structure. Consider the transverse horizontal and vertical velocity spectra

$$S_{v_2 v_2}(\mathbf{k}) = \frac{v^2}{\gamma^2} \left(\frac{k_1 k_2}{k^2} \right)^2 S_f(\mathbf{k}) \quad (5.25a)$$

$$S_{v_3 v_3}(\mathbf{k}) = \frac{v^2}{\gamma^2} \left(\frac{k_1 k_3}{k^2} \right)^2 S_{ff}(\mathbf{k}) \quad (5.25b)$$

Substituting nondimensional wave numbers

$$u_i = k_i \lambda_i$$

and

$$\varepsilon = \lambda_3 / \lambda_1 = \lambda_3 / \lambda_2$$

For small ε ,

$$S_{v_2 v_2}(\mathbf{u}) = \frac{v^2}{\gamma^2} \left(\frac{\varepsilon^2 u_1 u_2}{\varepsilon^2 (u_1^2 + u_2^2) + u_3^2} \right)^2 S_{ff}(\mathbf{u}) \approx \varepsilon^4 \frac{v^2}{\gamma^2} \frac{u_1^2 u_2^2}{u_3^4} S_{ff}(\mathbf{u}) \quad (5.26a)$$

and

$$S_{v_3 v_3}(\mathbf{u}) = \frac{v^2}{\gamma^2} \left(\frac{\varepsilon u_1 u_3}{\varepsilon^2 (u_1^2 + u_2^2) + u_3^2} \right)^2 S_{ff}(\mathbf{u}) \approx \varepsilon^2 \frac{v^2}{\gamma^2} \frac{u_1^2}{u_3^2} S_{ff}(\mathbf{u}) \quad (5.26b)$$

Since the velocity spectrum is the only difference in the expressions for transverse horizontal and vertical dispersivities, this shows that the transverse horizontal dispersivity will be of the order of ε^2 multiplied by the transverse vertical dispersivity for $\varepsilon \ll 1$. This is what has been found previously by Gelhar and Axness [1983]. Therefore, for highly layered aquifers, a nonlinear evaluation of the macrodispersivities by (5.21) will also result in the transverse vertical macrodispersivity being larger than the transverse horizontal one. This is orthogonal to observations (Rajaram and Gelhar [1990]; Garabedian *et al.* [1991]), thereby ruling out such a higher order effect as an explanation for field scale transverse macrodispersivities. In contrast, Zhang and Neuman [1990]

came to the conclusion that such a higher order effect is 'consistent' with field observations in their two dimensional 'depth averaged' model that prevented them from considering the fundamental theoretical feature of vertical dispersivities being larger than horizontal ones in layered anisotropic soils under steady flow conditions. This finding further supports flow unsteadiness, as analyzed by Rehfeldt and Gelhar [1987], is an important mechanism controlling transverse macrodispersivities in highly layered anisotropic heterogeneous aquifers.

CHAPTER 6

SUMMARY OF FINDINGS

1. Macrodispersive transport mechanism for the concentration variance field.

Without introducing any new assumptions beyond those made in analyzing the mean concentration, it was shown, for the hypothetical zero local dispersion case, that the correlation between squared concentration perturbations and velocity perturbations is a Fickian macrodispersive flux term for the concentration variance, in Equation (2.23). Dagan's [1982] and [1990], zero local dispersion model of concentration variance was shown to implicitly contain this transport mechanism for the concentration variance, Equation (2.26)-(2.27). Csanady [1973] hypothesized this transport mechanism for the concentration variance field. The derivation demonstrates the important role this term plays in transporting fluctuations and therefore the inappropriateness of dropping it, and yet retaining in the variance equation, the transport of fluctuations due to local dispersion, as is implied in Graham and McLaughlin [1989], Vomvoris and Gelhar [1990], and Li and McLaughlin [1991]. The effect of dropping this transport mechanism on the concentration variance is precisely the same as dropping the macrodispersive transport mechanism in the mean concentration equation.

2. Unbounded increase in the coefficient of variation (the ratio of the concentration standard deviation and the mean concentration) for the hypothetical zero local dispersion case.

For the hypothetical zero local dispersion case, the simple fact that both the concentration and the squared concentration are governed by the same hyperbolic operator (Equation (2.11) and (2.19)) makes the results found for the concentration

(Equation (2.15) and (2.18)) directly extendible to squared concentration (Equation (2.23), (2.24) and (2.25)). This fact has not been explicitly acknowledged or exploited in existing literature. Rubin [1991] has performed non diffusive 'particle simulations' to compute the mean and variance of the concentration field, which exhibit an unbounded increase with time of the ratio of the concentration standard deviation to the mean (*i.e.*, the coefficient of variation keeps increasing with time for the hypothetical zero local dispersion case). Simple analytical expressions derived here in Equations (3.43)-(3.45) reveal the sensitivities of the concentration coefficient of variation excluding local dispersion, and show an increase in the coefficient of variation with time, and larger coefficient of variations for smaller initial plume dimensions. They also yield a finite concentration variance for any finite initial dimensions of the plume, for the zero local dispersion case. The zero local dispersion case, as analyzed here, is shown to be in complete agreement with Dagan's [1982] and [1990] analysis of the hypothetical zero local dispersion case. Recognizing the simplicity of the hypothetical zero local dispersion case and the feature of ever increasing coefficient of variations with time, efforts into understanding concentration variance should be focused on how local dispersion modifies this unboundedly increasing coefficient of variation.

3. The dissipation of mean squared concentration fluctuations, *i.e.*, concentration variance, due to local dispersion.

The only sink term in the exact variance equation (2.9a) shows that the rate of destruction of concentration fluctuations by local dispersion is inversely proportional to the square of the scale that characterizes the spatial derivatives of the concentration perturbation field. On assuming the small separation behavior of the concentration covariance function to be stationary, the sink term is a first order decay term with the decay coefficient inversely proportional to the squared concentration microscale (Equations (2.32)-(2.34)). The singular importance of including local dispersion on the

concentration variance can be directly seen by the entirely different behavior of the large time solution for the concentration variance on including local dispersion (Section 3.2 contrasted with Section 3.3) and assuming some non-infinite concentration microscale. The application of the zero local dispersion case in finding concentration variance (*e.g.*, Dagan [1982] and [1990]) can only be justified for small times, *i.e.*, of the order of the squared concentration microscale divided by the local dispersion coefficient. In considering two dimensional transport in a bounded aquifer, it is rigorously demonstrated that in dropping local dispersion, at the minimum, a first order decay term is dropped for the cross-sectional mean squared concentration deviations from the cross-sectional mean (Appendix-II, Theorem 1). Therefore, in an Eulerian continuum analysis of the concentration field in a heterogeneous aquifer (such as in this work), it is easy to recognize the singular importance of the dissipating action of local dispersion on the large time solution for concentration variance. This importance of fluctuation dissipation functions has long been recognized in a variety of phenomenon, via Eulerian continuum analysis, incorporating local diffusive mechanisms that appear as a Laplacian term in a parabolic conservation statement (mentioned in Section 2.4.1). This singularly important role of diffusion or local dispersion is apparently not easily realized in analysis that seek to follow the trajectory of indivisible particles in a Lagrangian framework, *e.g.*, Dagan [1982], [1990]. It remains to be seen what the particle based analysis in a Lagrangian framework have to offer in describing finer details of the concentration field other than its radius of gyration (square root of spatial second moment).

4. Existence, estimation, and importance of the $\ln K$ microscale.

The exponential correlation function is a description of the $\ln K$ field that results in flow fields with infinite shear, vorticity, and principal strain rates. A testimonial to the opaqueness of numerical simulations on flow and transport is the claim of numerical models to be adequately resolving such pathological velocity fields! Moreover, it is

shown in Chapter 4, that if porous medium indeed had fluctuations in its hydraulic conductivity at scales comparable to the square root of its permeability, the Brinkman extension to Darcy's 'law' would limit the increase in strain rates of the ensuing velocity field. Measurements analyzed in this thesis unambiguously show the upward convexity of the $\ln K$ correlation function and the gross extrapolation involved in fitting an exponential correlation function to existing datasets. This also provides an empirical basis to the REV cartoon, *i.e.*, the assertion that there exists a scale disparity between the first scale at which an REV may be defined and the scale at which REV properties vary.

The importance of the $\ln K$ microscale is evident from the sink term in the variance equation (2.9a). The rate of destruction of fluctuations by local dispersion is proportional to the variance of the derivatives of the concentration perturbation field. For advection dominated transport, it is to be expected that the $\ln K$ microscale strongly determines the sink term. An increase in the $\ln K$ microscale causes an increase in the concentration microscale which decreases the rate of destruction of fluctuations and vice versa (Equation (2.55)). The insensitivity of the spatial second moment to this parameter is a testimonial to the lack of information in the spatial second moment about any measure of attenuation of point contaminant concentrations. The longitudinal spatial second moment is not even sensitive to the exclusion of local dispersion, without which there is absolutely no attenuation of injection concentrations, notwithstanding the usual misleading assertion that "spatial second moments determine dilution".

5. Simple analytical expressions for the concentration variance for a multidimensional impulse input in three dimensionally heterogeneous aquifers, including the singularly important dissipating action of local dispersion.

The variance equation (3.2a), embodying the mechanisms of advective transport, dispersive transport, creation and destruction of variance, was analytically solved for

some explicit large time conditions. The derived expressions (Equations (3.23)-(3.26)) explicitly present the sensitivities of the concentration fluctuations in three dimensional space, to the $\ln K$ description in three dimensional space, the initial plume dimension, the value of local dispersion. Most importantly, the sensitivity to the high wave number component of the $\ln K$ spectrum is such that greater the proportion of high wave number energy, *i.e.*, smaller the $\ln K$ microscale (assumed greater than the local dispersivity), smaller is the variance and the coefficient of variation. This reflects the fact that diffusion mechanisms act more rapidly on fine scale variations than on large scale ones (see Appendix-I), and the $\ln K$ microscale determines the concentration microscale (Equation (2.53)). This is the first explicit exposition of the role of the fine scale structure of the $\ln K$ field in facilitating variance dissipation and is argued to be of critical importance in determining the usefulness or success of effective media modeling of transport in heterogeneous $\ln K$ fields. If the $\ln K$ field were devoid of a rich fine scale structure then the sample path concentration deviations would be larger because the concentration fluctuations would occur at large scales resulting in larger concentration microscales and therefore decreasing the efficacy of local dispersion in getting rid of the variance. The success of macrodispersion based effective models will depend on the amount of *surface area* that advective heterogeneity creates and the rate at which the continuum scale diffusion (local dispersion) can destroy fluctuations. The richness of the $\ln K$ fluctuations on the high wave number end enhances the ability of local dispersion to attenuate concentration levels. Without a continuum scale diffusion mechanism, the high wave number characteristics of the velocity field are of no special significance. This sensitivity is ubiquitous in advection diffusion systems as discussed in Section 2.4.1.

The derived expressions also show the conditions under which the rate of production and destruction of fluctuations balances out each other to yield a linear relationship between concentration variance and the squared gradient of the mean

concentration field (Equation (3.28)). Under these conditions the transport terms in the variance equation are unimportant.

6. Concentration fluctuations in the bromide tracer, Cape Cod, MA.

The coefficient of variation estimated at the center of mass of the bromide tracer was found to decrease with time between 200 and 500 days after injection (Figure 3.6). The hypothetical zero local dispersion case predicts otherwise, and is of absolutely no relevance in interpreting experimental observations of contaminant concentrations (Figures 3.7 and 3.8). The decrease of the coefficient of variation with time is predicted by the theory developed here on including the action of local dispersion (Figure 3.7). While local dispersion may play an insignificant role in determining the longitudinal spatial second moment of the plume, it plays a dramatic role in determining point concentration levels (Figure 3.8).

The concentration data for the Cape Cod bromide tracer shows quite clearly that peak concentrations are not strongly dependent on the plume size, when the plume scale and the correlation scale overlap (Figure 3.8). Therefore, the notion that a refined determination of the spatial second moment of a plume with a scale overlap with the $\ln K$ correlation scale gives a better idea of dilution is false, at least for the Cape Cod bromide data. More alarmingly, the effective dispersivity (even if predicting the right value of the spatial second moment) will result in a substantial underestimation of peak concentrations. An analysis of the concentration variance provides a way to assess these concentrations (Figure 3.8).

7. Bounds on the fluctuation dissipation function in a bounded aquifer demonstrating the singular importance of the interaction of local dispersion and high wave number velocity fluctuations in determining concentration levels in heterogeneous velocity fields.

In Appendix-II, variational calculus yielded rigorous lower bounds on the fluctuation dissipation function that sufficiently demonstrate the importance of the interaction of local dispersion and high wave number velocity fluctuations in determining concentration levels in heterogeneous velocity fields. These bounds support the more general approximate analysis of concentration variance in three-dimensionally heterogeneous aquifers. These bounds sufficiently demonstrate the singular importance of modeling the local flux in numerical models of transport. *A priori*, this singularity imposes the need to have grid Peclet numbers of less than 1 in numerical models. The bounds provide a necessary (and not sufficient) condition to assess the adequacy of numerical approximations in solving the details of solute distribution for variable advection diffusion problems. Currently, there is no performance check for variable advection diffusion problems, and therefore, the claims of being able to *handle* grid Peclet numbers of hundreds for such problems can not be judged.

8. Variational characteristic of G. I. Taylor's [1953] solution.

In Appendix-III, it was shown the G. I. Taylor's [1953] solution for the cross-sectional concentration profile has a variational characteristic. It minimizes the dissipation integral subject to a fixed cross sectional dispersive flux. Equivalently, it maximizes the cross-sectional dispersive flux for a given dissipation integral. This further indicates the important role of the fluctuation dissipation function in determining the details of solute distribution in variable advection-diffusion phenomenon.

9. Proof of asymptotically dying cross correlation coefficient between a correlated stochastic process and its integral.

This fact was proven in Section 5.1, and provides a rationale for Corrsin's [1962] (much stronger) conjecture (which is strictly incorrect) and an appreciation of the large time conditions on its approximate applicability.

10. Analytical nonlinear algebraic equations for a nonlinear computation of macrodispersivities.

In Appendix-VI, the Gelhar and Axness [1983] macrodispersivity integrals for the isotropic exponential $\ln K$ correlation function were exactly analytically evaluated for the case of anisotropic local dispersivities, extending the previous exact evaluations for the case of isotropic local dispersivities. It was found that the longitudinal macrodispersivity is a decreasing function of the ratio of the transverse and longitudinal local dispersivities.

These evaluations also yield nonlinear algebraic expression for macrodispersivities, incorporating Corrsin's [1962] conjecture. The transverse dispersivity shows a correlation scale dependence, not exhibited in the first order theory. The longitudinal dispersivity remains practically unaffected. It is argued that the ratio of the vertical to transverse macrodispersivity will be greater than unity for highly anisotropic soils, and therefore the field observations to the contrary are probably explained by flow unsteadiness [Rehfeldt and Gelhar, 1992].

REFERENCES

- Adams, E. E., and L. W. Gelhar, Field study of dispersion in a heterogeneous aquifer 2. Spatial moment analysis, *Water Resour. Res.*, 28(12):3293-3307, 1992.
- Bakr, A. A., Effect of spatial variations of hydraulic conductivity on groundwater flow, Ph.D. dissertation, N. M. Inst. of Min. and Technol., Socorro, 1976.
- Bakr, A. A., L. W. Gelhar, A. L. Gutjahr, J. R. Macmillan, Stochastic analysis of spatial variability in subsurface flows, 1, Comparison of one- and three-dimensional flows, *Water Resour. Res.*, 14(2): 263-271, 1978.
- Batchelor, G. K., Small-scale variation of convected quantities like temperature in turbulent fluid, Part 1. General discussion and the case of small conductivity, *J. Fluid Mech.* 5:113-133, 1959.
- Beavers and Joseph, Boundary conditions at a naturally permeable wall, *J. Fluid Mech.*, 30, 197-207, 1967.
- Brinkman, H. C., A calculation of the viscous forces exerted by a flowing fluid on a dense swarm of particles, *Appl. Sci. Res. A1*, 27-34, 1947a.
- Brinkman, H. C., On the permeability of media consisting of closely packed porous particles, *Appl. Sci. Res. A1*, 81-86, 1947b.
- Corrsin, S., Theories of turbulent dispersion, in *Mecanique de la turbulence, Colloques Internationaux du centre national de la recherche scientifique*, 108, Marseilles, 1962.
- Csanady, G. T., *Turbulent diffusion in the environment*, D. Reidel publishing company, Dordrecht, Holland, 1973.
- Dagan, G., The generalization of Darcy's law for nonuniform flows, *Water Resour. Res.*, 15(1):1-7, 1979.
- Dagan, G., Stochastic modeling of groundwater flow by unconditional and conditional probabilities, 2. The solute transport, *Water Resour. Res.*, 18: 835-842, 1982.

- Dagan, G., Solute transport in heterogeneous formations, *J. Fluid Mech.*, 145:151-177, 1984.
- Dagan, G., Time-dependent macrodispersion for solute transport in anisotropic heterogeneous aquifers, *Water Resour. Res.*, 24(9):1491-1500, 1988.
- Dagan, G., Transport in heterogeneous formations: Spatial moments, ergodicity, and effective dispersion, *Water Resour. Res.*, 26:1281-1290, 1990.
- Frind, E. O., E. A. Sudicky, S. L. Schellenberg, Micro-scale modeling in the study of plume-evolution in heterogeneous porous media, *Stoch. Hydrol. and Hydraulics*, 1:263-279, 1987.
- Garabedian, S. P., *et al.*, Large scale natural gradient tracer test in sand and gravel, Cape Cod, Massachusetts, 2. Analysis of spatial second moments for a non reactive tracer, *Water Resour. Res.*, 27(5):911-924, 1991.
- Gelhar, L. W., A. L. Gutjahr, R. L. Naff, Reply, *Water Resour. Res.*, 17(6):1739-1740, 1981.
- Gelhar, L. W., and A. L. Gutjahr, Stochastic solutions of the one dimensional convective dispersive equation, Hydrology Research Report No. 11, New Mexico Inst. of Mining and Tech., Socorro, NM, September 1982.
- Gelhar, L. W., and C. L. Axness, Three-dimensional stochastic analysis of macrodispersion in aquifers, *Water Resour. Res.*, 19(1):161-180, 1983.
- Gelhar, L. W., Stochastic analysis of solute transport in saturated and unsaturated porous media, *Advances in transport phenomena in porous media*, J. Bear and M. Y. Corapcioglu, eds., Martinus Nijhoff Publishers:658-700, 1987.
- Graham, W. D., and D. McLaughlin, Stochastic analysis of nonstationary subsurface solute transport, 1, unconditional moments, *Water Resour. Res.*, 25(2):215-232, 1989.
- Gutjahr, A. L., L. W. Gelhar, A. A. Bakr, J. R. Macmillan, Stochastic analysis of spatial variability in subsurface flows, *Water Resour. Res.*, 14(5), 953-959, 1978.
- Howard, L. N., Bounds on flow quantities, *Ann. Rev. Fluid Mech.*, 1972.

- Joseph, D. D., *Stability of fluid motions* (2 vols.), Springer Tracts in Natural Philosophy, vols.27 and 28, Berlin: Springer-Verlag, 1976.
- Leblanc, D. R., *et al.*, Large scale natural gradient tracer test in sand and gravel, Cape Cod, Massachusetts, 1. Experimental design and observed tracer movement, *Water Resour. Res.*, 27(5):911-924, 1991.
- Li, S., and D. McLaughlin, A nonstationary spectral method for solving stochastic groundwater problems: Unconditional analysis, *Water Resour. Res.*, 27(7):1589-1605, 1991.
- Lumley, J. L., On the solution of equations describing small scale deformation. In *Symposia Matematica: Convegno sulla Teoria della Turbolenza al Istituto Nazionale di Alta Matematica*, Academic Press, New York, 1972.
- Malkus, W. V. R., and L. M. Smith, Upper bounds on functions of the dissipation rate in turbulent shear flow, *J. Fluid Mech.*, 208:479-507, 1989.
- Neuman, S. P., and Y-K Zhang, A quasi-linear theory of nonfickian and fickian subsurface dispersion 1. Theoretical analysis with application to isotropic media, *Water Resour. Res.*, 26(5):887-902, 1990.
- Neuman, S. P., Universal scaling of hydraulic conductivities and dispersivities in geologic media, *Water Resour. Res.*, 26(8):1749-1758, 1990.
- Nield, D. A., and A. Bejan, *Convection in porous media*, Springer Verlag New York Inc., 1992.
- Rajaram, H., Scale dependent dispersion in heterogeneous porous media, Sc.D. dissertation, Department of Civil Engineering, M.I.T., 1991.
- Rehfeldt, K. R., and L. W. Gelhar, Stochastic analysis of dispersion in unsteady flow in heterogeneous aquifers, *Water Resour. Res.*, 28(8):2085-2099, 1992.
- Reynolds, O., On the dynamical theory of incompressible viscous fluids and the determination of the criterion, *Phil. Trans. Roy. Soc. A* 186, 123, 1895.

- Richardson, L. F., Atmospheric diffusion shown on a distance-neighbor graph, *Proc. Roy. Soc. A*, 110:709, 1926.
- Ringrose, P., G. Pickup, The effects of reservoir structure on hydrocarbon flow illustrated using a deltaic reservoir analogue in Fife, Scotland, to appear at the AAPG Conference in the Hague, 17th-20th October 1993.
- Rubin, Y., Transport in heterogeneous porous media: Prediction and uncertainty, *Water Resour. Res.*, 27(7):1723-1738, 1991.
- Serrin, J., On the stability of viscous fluid motions, *Arch. Rational Mech. Anal.* 3, 1, 1959.
- Smith, L., and F. W. Schwartz, Mass Transport, 1: A stochastic analysis of microscopic dispersion, *Water Resour. Res.*, 16(2):303-313, 1980.
- Sorokin, V. S., Nonlinear phenomenon in closed flows near critical Reynolds numbers, *J. Appl. Math.*, 25:366-81, 1961.
- Taylor, G. I., Diffusion by continuous movements, *Proc. London Math. Soc.* (2) 20:196-211, 1921.
- Taylor, G. I., Statistical theory of turbulence, Part I, *Proc. Roy. Soc. A*, vol. CLI: 421-444, 1935a.
- Taylor, G. I., Statistical theory of turbulence, Part III, Distribution of dissipation of energy in a pipe over its cross-section, *Proc. Roy. Soc. A*, vol. CLI:455-464, 1935b.
- Taylor, G. I., Dispersion of soluble matter in solvent flowing slowly through a tube, *Proc. Roy. Soc. A*, 219 (1137), 186-203, 1953.
- Taylor, G. I., A model for the boundary condition of a porous material, Part 1. *J. Fluid Mech.* 49, 319-326, 1971
- Tennekes, H., and J. L. Lumley, A first course in turbulence, The M.I.T. Press, 1972.
- Tompson, A. F. B., and L. W. Gelhar, Numerical simulation of solute transport in three-dimensional, randomly heterogeneous porous media, *Water Resour. Res.*, 26(10): 2541-2562, 1990.

- Tennekes, H., and J. L. Lumley, A first course in turbulence, The M.I.T. Press, 1972.
- Vomvoris, E. G., Concentration variability in transport in heterogeneous aquifers: A stochastic analysis, Ph.D. thesis, R. M. Parsons Lab., Dept. of Civil and Environmental Eng., M. I. T., Cambridge, 1986.
- Vomvoris, E. G., and L. W. Gelhar, Stochastic analysis of the concentration variability in a three-dimensional heterogeneous aquifer, *Water Resour. Res.*, 26(10):2591-2602, 1990.
- Winter, C. L., C. M. Newman, S. P. Neuman, A perturbation expansion for diffusion in a random velocity field, *SIAM Journal of Applied Mathematics*, 44(2),411-424, 1984.
- Zhang, Y-K, and S. P. Neuman, A quasi-linear theory of nonfickian and fickian subsurface dispersion 2. Application to anisotropic media and the Borden site, *Water Resour. Res.*, 26(5):903-913, 1990.

APPENDIX-I

ON THE HIGH WAVE NUMBER SENSITIVITY OF FLUCTUATION DISSIPATION PHENOMENON

A trivial one dimensional boundary value problem is presented here to illustrate the high wave number sensitivity of fluctuation dissipation phenomenon.

A-I.1 INITIAL-BOUNDARY VALUE PROBLEM

Consider the simple initial -boundary value problem

$$\text{B.C.} \quad c(0,t) = c(1,t) = 0$$

$$\text{I.C.} \quad c(x,t) = \text{Sin}(2k\pi x) \quad k = 1,2,3,\dots$$

$$\text{P.D.E.} \quad \frac{\partial c}{\partial t} = \omega \frac{\partial^2 c}{\partial x^2} \quad \forall x \in (0,1)$$

Solution:
$$c(x,t) = e^{-\omega(2k\pi)^2 t} \text{Sin}(2k\pi x)$$

Defining,

$$\|f\| \equiv \int_0^1 f dx$$

It follows that

$$\|c^2\| = \frac{1}{2} e^{-2\omega(2k\pi)^2 t}$$

and

$$\frac{d \|c^2\|}{dt} = -2\omega (2k\pi)^2 \|c^2\|$$

Therefore,

$$-\frac{1}{4\omega\pi^2} \frac{d \ln[\|c^2\|]}{dt} = k^2$$

This shows the nature of the high wave number sensitivity of fluctuation dissipation phenomenon. Defining the squared concentration microscale by

$$(\Delta^c)^2 \equiv \frac{\|c^2\|}{\left\|\left(\frac{\partial c}{\partial x}\right)^2\right\|}$$

It follows from the solution that

$$\left\|\left(\frac{\partial c}{\partial x}\right)^2\right\| = (2k\pi)^2 \|c^2\|$$

therefore

$$\frac{d \|c^2\|}{dt} = -\frac{2\omega}{(\Delta^c)^2} \|c^2\|$$

i.e., the rate of dissipation of mean squared concentration fluctuations is equal to twice the diffusion coefficient divided by the squared dimension characterizing the derivatives of the concentration field.

Consideration of fluctuation dissipation and its sensitivity to the spectral description of the spatially variable hydraulic conductivity is argued in Chapters 2 and 3 to be importantly controlling the level of concentration fluctuations in three dimensionally heterogeneous aquifers.

APPENDIX-II

TRANSPORT IN HETEROGENEOUS AQUIFERS: ON THE CRITICAL ROLE OF LOCAL DISPERSION

In a bounded two-dimensional aquifer of height H , the cross-sectional mean squared concentration fluctuations from the cross-sectional mean are analyzed. The mean squared concentration fluctuation equation has a dissipation term, which is a product of the local dispersion coefficient and the mean of the squared concentration fluctuation derivatives. The mean of the squared transverse derivatives of the concentration fluctuations is shown to be greater than or equal to $(\pi/H)^2$ multiplied by the mean squared concentration fluctuations. Therefore, the mean squared concentration fluctuations, as a singular consequence of the action of local dispersion, is destroyed at a rate greater than or equal to a first order decay process with a decay coefficient of $2D_T(\pi/H)^2$, D_T being the transverse local dispersion coefficient. For a specified cross-sectional dispersive flux, the minimum of the mean squared transverse derivatives exhibits a wave number squared dependence. These bounds on the fluctuation dissipation function demonstrate that the interaction of the local dispersion process and the high wave number component velocity fluctuations plays a critical role in determining solute concentration levels in heterogeneous aquifers.

A-II.1 INTRODUCTION

In the absence of exact solutions for the details of the concentration distribution for even the most elementary spatially variable advection-diffusion problems, the construction of tractable solutions of various quantities of interest (e.g., spatial second moments, mean concentration, mean squared concentration fluctuations) is inevitably

accompanied by approximations (*i.e.*, dropping of terms, linearization, localization, closures *etc.*). Different approximations leading to different results can sometimes be difficult to reconcile. A glaring example of this is on the role of the local dispersion process in determining the strength of the concentration fluctuations. Dagan [1990] drops local dispersion altogether in his analysis of concentration variance. In the analysis in Chapter 2 and 3, the simplicity of the hypothetical, hyperbolic, zero local dispersion case is acknowledged (the analysis of the zero local dispersion case is in complete agreement with Dagan's [1990] analysis of that case), but it is argued for the parabolic transport problem with a positive local dispersion coefficient, the large time solution for the concentration variance is singularly influenced by the dissipating action of local dispersion. In the approximate analysis in three dimensionally heterogeneous porous medium, the coefficient of variation (the square root of the mean squared concentration fluctuations divided by the mean concentration) initially increases with time, and then decreases with time at large times. This decrease in the coefficient of variation is singularly due to the action of local dispersion. On excluding local dispersion, the coefficient of variation increases unboundedly with time, as is implied by Dagan's work [1990]. In empirical support of the analysis in Chapter 2 and 3, the data of rapidly decreasing peak sampled concentration levels at the Cape-Cod, MA, bromide tracer (Figure 3.8), and an estimate the coefficient of variation, which is found to be decreasing with time between 200 and 500 days (Figure 3.6), is presented.

Further, extensively and intensively characterized sites and tracer tests are needed to create a set of observations on concentration levels (peak concentrations) and estimated coefficient of variations, to sort out these diametrically opposing theoretical results. Numerical simulations that demonstrate that their results are not drowned in numerical dispersion, and are capable of reproducing the details of transport in rich velocity spectrum and modeling the local dispersive flux are nontrivial. We might have to wait a couple of decades for a computer large (and fast) enough to be able to model the local

dispersive flux for a field scale problem, by having a grid Peclet number less than one (without which any claim to be modeling the local dispersive flux is untenable) for local dispersivities of the order of less than a centimeter. While work in these two areas may shed light on the role of local dispersion in determining the concentration variance, a more immediate consensus on the role of local dispersion in dissipating concentration fluctuations is desirable. Needless to say that assessment of contamination exposure levels at a point will /should dramatically differ if the coefficient of variation is 1 as opposed to 100! Currently, there is no agreement even over the sign of the rate of change of the coefficient of variation with the analysis in Chapter 2 and 3 predicting it to be negative at large times (as a consequence of local dispersion) and Dagan's [1990] results implying that it is always positive!

In light of this divergence, the approach taken here is to only present results (including bounds on functions) that can be deduced without any approximations in the analysis for the simple case of a bounded two dimensional aquifer, with the solute undergoing spatially variable advection and a local dispersive flux with a constant local dispersion coefficient. Averages are computed over the height of the aquifer. The *exact* equation for the concentration mean squared fluctuation is constructed. Rigorous lower bounds on the concentration variance dissipation term (due to local dispersion) are found. To make the case that local dispersion can be dropped altogether in analyzing mean squared fluctuations at large times, it is necessary (not sufficient) that the lower bounds on the dissipation function be of no significant consequence at large times. Lower bounds on the dissipation function enable a delineation of the minimum possible effect of the dissipating action of local dispersion on the concentration variance. If this minimum action of local dispersion is insignificant, then it will be concluded that the importance of local dispersion is not shown by this analysis. If this minimum action of local dispersion is significant, then its importance in controlling concentration fluctuations will be considered sufficiently established.

A-II.2 ACTION OF LOCAL DISPERSION IN FLUCTUATION DISSIPATION

Define

$$\bar{g} = \frac{1}{H} \int_0^H g \, dy$$

Consider flow in the two dimensional bounded aquifer in Figure A-II.1

$$x \text{ velocity: } \bar{V} + v, \quad \bar{v} = 0$$

$$y \text{ velocity: } w, \quad \bar{w} = 0 \text{ and } w(x, 0) = w(x, H) = 0$$

$$\frac{\partial v}{\partial x} + \frac{\partial w}{\partial y} = 0$$

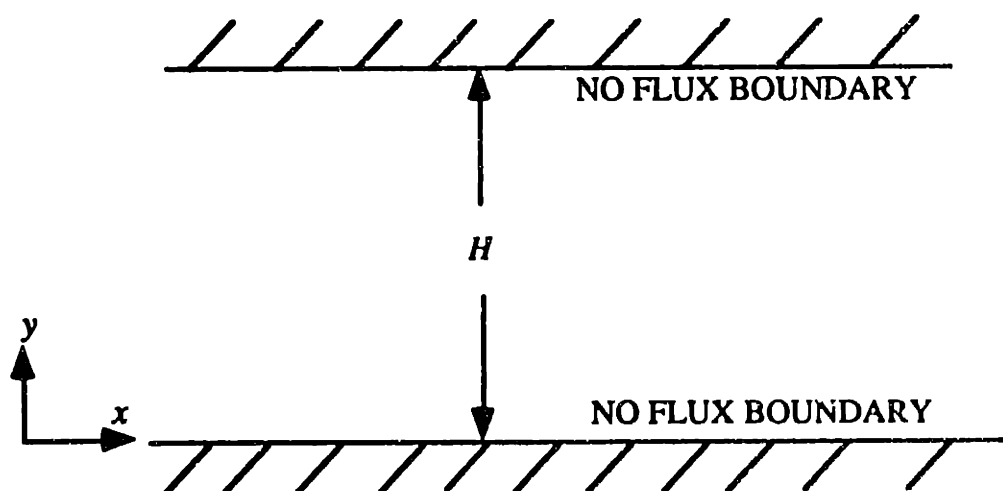


Figure A-II.1

Bounded aquifer.

The solute transport equation along with the auxiliary conditions is

$$\frac{\partial C}{\partial t} + \bar{v} \frac{\partial C}{\partial x} + \frac{\partial vC}{\partial x} + \frac{\partial wC}{\partial y} - D_L \frac{\partial^2 C}{\partial x^2} - D_T \frac{\partial^2 C}{\partial y^2} = 0 \quad (\text{A-II.1})$$

$$C(x, y, t) \Big|_{t=0} = \bar{c}(x, y)$$

$$\begin{aligned} |x| \rightarrow \infty \quad C &\rightarrow 0 \\ \frac{\partial C}{\partial y} \Big|_{y=0} &= \frac{\partial C}{\partial y} \Big|_{y=H} = 0 \end{aligned} \quad (\text{A-II.2})$$

In (A-II.1) D_L and D_T are the longitudinal and transverse local dispersion coefficients. Taking averages of each term in (A-II.1), over the aquifer height, yields the equation for the cross-sectional mean concentration

$$\frac{\partial \bar{C}}{\partial t} + \bar{v} \frac{\partial \bar{C}}{\partial x} + \frac{\partial \bar{v}\bar{C}}{\partial x} - D_L \frac{\partial^2 \bar{C}}{\partial x^2} = 0 \quad (\text{A-II.3})$$

Subtracting the mean equation (A-II.3) from the original transport (A-II.1) equation gives the equation for the concentration perturbation

$$c = C - \bar{C}$$

The equation for the mean squared concentration fluctuations, *i.e.*, concentration variance

$$\sigma_c^2 \equiv \frac{1}{H} \int_0^H c^2 dy$$

is obtained by multiplying the concentration perturbation equation by another concentration perturbation and taking cross-sectional averages to get

$$\frac{1}{2} \left[\frac{\partial \sigma_c^2}{\partial t} + \bar{v} \frac{\partial \sigma_c^2}{\partial x} - D_L \frac{\partial^2 \sigma_c^2}{\partial x^2} + \frac{\partial \overline{vc^2}}{\partial x} \right] = -\bar{vc} \frac{\partial \bar{c}}{\partial x} - \left[D_L \overline{\left(\frac{\partial c}{\partial x} \right)^2} + D_T \overline{\left(\frac{\partial c}{\partial y} \right)^2} \right] \quad (\text{A-II.4})$$

The fluctuation dissipation function

$$d(x,t) = \left[D_L \overline{\left(\frac{\partial c}{\partial x} \right)^2} + D_T \overline{\left(\frac{\partial c}{\partial y} \right)^2} \right] \quad (\text{A-II.5})$$

represents the action of local dispersion in destroying the concentration variance.

Defining

$$\|g\| = \int_{-\infty}^{+\infty} g \, dx$$

a global measure of the concentration fluctuation is governed by

$$\frac{1}{2} \frac{d \| \sigma_c^2 \|}{dt} = \| -\bar{vc} \frac{\partial \bar{c}}{\partial x} \| - \| \left[D_L \overline{\left(\frac{\partial c}{\partial x} \right)^2} + D_T \overline{\left(\frac{\partial c}{\partial y} \right)^2} \right] \| \quad (\text{A-II.6})$$

obtained by integrating the concentration variance equation (A-II.4). In the zero local dispersion case, as D_L and D_T are set to zero, the fluctuation dissipation function (A-II.5) is dropped from (A-II.4) and (A-II.6).

A-II.3 LOWER BOUNDS ON THE FLUCTUATION DISSIPATION FUNCTION

THEOREM 1

There exists $\Delta c_{max} > 0$ such that

$$\overline{\left(\frac{\partial c}{\partial y}\right)^2} \geq \frac{\sigma_c^2}{(\Delta_{max}^c)^2} \quad (\text{A-II.7})$$

PROOF:

The minimum of

$$\int_0^H \left(\frac{\partial c}{\partial y}\right)^2 dy$$

among continuously differentiable functions c is sought, subject to the constraints

$$\int_0^H c^2 dy = E \quad \text{and} \quad \int_0^H c dy = 0$$

and the no flux boundary conditions at $y = 0$ and H . Defining $c' = dc/dy$, the Euler-Lagrange equation for this isoperimetric problem is

$$\frac{\partial f}{\partial c} - \frac{d}{dy} \left(\frac{\partial f}{\partial c'} \right) = 0 \quad (\text{A-II.8})$$

with

$$f = c^2 + \lambda_1 c + \lambda_2 c^2$$

The unknown multipliers are to be determined through the constraints. This yields

$$\lambda_1 + 2\lambda_2 c - 2c'' = 0$$

which is easily solved for the minimizing c ,

$$c = \sqrt{\frac{2E}{H}} \text{Cos}\left(\frac{\pi y}{H}\right) \quad (\text{A-II.9})$$

It follows

$$\int_0^H \left(\frac{\partial c}{\partial y}\right)^2 dy \geq \frac{\int_0^H c^2 dy}{(H/\pi)^2} \quad (\text{A-II.10})$$

Therefore

$$\Delta_{max}^c = (H/\pi) \quad (\text{A-II.11})$$

LEMMA 1

$$\frac{1}{2} \frac{d \|\sigma_c^2\|}{dt} \leq \left\| -vc \frac{\partial \bar{c}}{\partial x} \right\| - \frac{D_T}{(H/\pi)^2} \|\sigma_c^2\| \quad (\text{A-II.12a})$$

This easily follows from Equations (A-II.6), (A-II.7), (A-II.11) and implies

$$\|\sigma_c^2\| \leq \int_0^t \left\| -2vc \frac{\partial \bar{c}}{\partial x} \right\| \exp\left[-\frac{2D_T}{(H/\pi)^2}(t-\tau)\right] d\tau \quad (\text{A-II.12b})$$

It is certainly not being suggested that the minimizing concentration profile (A-II.9) is the answer to the solute transport problem. In fact, nothing about the specifics of

the velocity field was utilized in deriving the bounds (A-II.7), (A-II.12). The exact solution to the transport equation (or any other, obeying the boundary conditions) can only result in there being greater dissipation than the minimum estimated here. The minimizing concentration has been found from among the manifold of possible solutions to the transport problem (the concentration perturbation obeys the boundary conditions and integrates out to zero over the cross-section). The minimizing profile provides a lower bound on the fluctuation dissipation function. In finding this lower bound it has been proven that the mean of the squared concentration fluctuation is being destroyed by the action of local dispersion at a rate greater than or equal to $2D_T/(H/\pi)^2$ multiplied by the mean squared concentration fluctuations (A-II.12a,b). In dropping local dispersion, at the very least, this first order decay term is dropped. Asymptotically, the results after dropping local dispersion will therefore be drastically different from those incorporating this minimal dissipating effect of local dispersion.

THEOREM 2

$$\overline{\left(\frac{\partial c}{\partial y}\right)^2} \geq \theta^2 (\overline{cv})^2 \quad (\text{A-II.13a})$$

where

$$\theta^2 = \frac{H \int_0^H \left[\int_0^y v(y_1) dy_1 \right]^2 dy}{\left[\int_0^H v(y) dy \int_0^y dy_1 \int_0^{y_1} v(y_2) dy_2 \right]^2} \quad (\text{A-II.13b})$$

PROOF:

The minimum of

$$\int_0^H \left(\frac{\partial c}{\partial y}\right)^2 dy$$

is sought, subject to the constraints

$$\int_0^H cv \, dy = F \quad \text{and} \quad \int_0^H c \, dy = 0$$

and the no flux boundary conditions. The Euler-Lagrange equation for this minimization is equation (A-II.8) with

$$f = c^2 + \lambda_1 c + \lambda_2 cv$$

This gives

$$\lambda_1 + \lambda_2 v - 2c'' = 0$$

which is easily solved to get the minimizing vertical concentration profile

$$c(y) = F \frac{\left[\int_0^y dy_1 \int_0^{y_1} v(y_2) dy_2 - \frac{1}{H} \int_0^H dy \int_0^y dy_1 \int_0^{y_1} v(y_2) dy_2 \right]}{\int_0^H v(y) dy \int_0^y dy_1 \int_0^{y_1} v(y_2) dy_2} \quad (\text{A-II.14})$$

from which follows the bound (A-II.13). In general, θ^2 is a function of x . Its minimum value over the values of x may be found if the two-dimensional variation of the velocity field is specified.

LEMMA 2

For unidirectional velocity varying in y , it follows from Equation (A-II.13) and (A-II.6)

$$\frac{1}{2} \frac{d \|\sigma_c^2\|}{dt} \leq \left\| -\bar{v}c \frac{\partial \bar{C}}{\partial x} \right\| - D_T \theta^2 \|\bar{c}\bar{v}\|^2 \quad (\text{A-II.15})$$

Once again, it is not being suggested that the minimizing concentration profile (A-II.14) is the solution to the transport problem. It is only constructed to find a lower bound on the fluctuation dissipation function in terms of the horizontal dispersive flux. For unidirectional flow, it turns out that Taylor [1953] type approximations (in a coordinate system moving along the mean velocity, drop the local acceleration, longitudinal diffusion, and the transverse variations of the longitudinal derivatives of the concentration) yields this dissipation minimizing concentration profile (A-II.14), as shown in Appendix-III.

HIGH WAVE NUMBER SENSITIVITY OF θ^2

Consider the velocity

$$v(y) = \psi \bar{V} \sin(2k\pi y/H)$$

It is easily shown from (A-II.13) that

$$\theta^2 = \left(\frac{8}{3}\right) \frac{k^2}{(H/\pi)^2 (\psi \bar{V})^2} \quad (\text{A-II.16})$$

The minimum of the dissipation function, given a cross-sectional dispersive flux, increases as the square of the velocity wave number.

Consider another velocity function, with a low wave number and a high wave number with different weights

$$v(y) = \bar{V} [\psi_1 \text{Sin}(2k\pi y/H) + \psi_2 \text{Sin}(8k\pi y/H)]$$

For this

$$\theta^2 = 128 \frac{k^2}{(H/\pi)^2 \bar{V}^2 (48\psi_1^2 + 16\psi_1\psi_2 + 3\psi_2^2)} \quad (\text{A-II.17})$$

Note that in (A-II.17), for a specified mean squared fluctuation of the velocity field,

$$\overline{v^2} = \bar{V}^2 \frac{\psi_1^2 + \psi_2^2}{2}$$

the greater the proportion of fluctuations at the higher wave number, the greater is the value of θ^2 (in the denominator, in (A-II.17), the low wave number velocity fluctuations have a greater weight), as shown in Figure A-II.2.

The lower bounds on the fluctuation dissipation function, (A-II.7) and (A-II.13), show that the large time solution for the concentration variance will be singularly influenced by the action of local dispersion. However, despite this fluctuation dissipating action of local dispersion, for a non zero value of the dispersive flux

$$\overline{cv}$$

at a cross-section, even if solute were initially introduced uniformly over the height of the aquifer, the cross-sectional concentration profile cannot be *completely homogenized*:

THEOREM 3

$$\sigma_c^2 \geq \frac{(\overline{cv})^2}{\overline{v^2}} \quad (\text{A-II.18})$$

PROOF:

This is Schwarz's inequality.

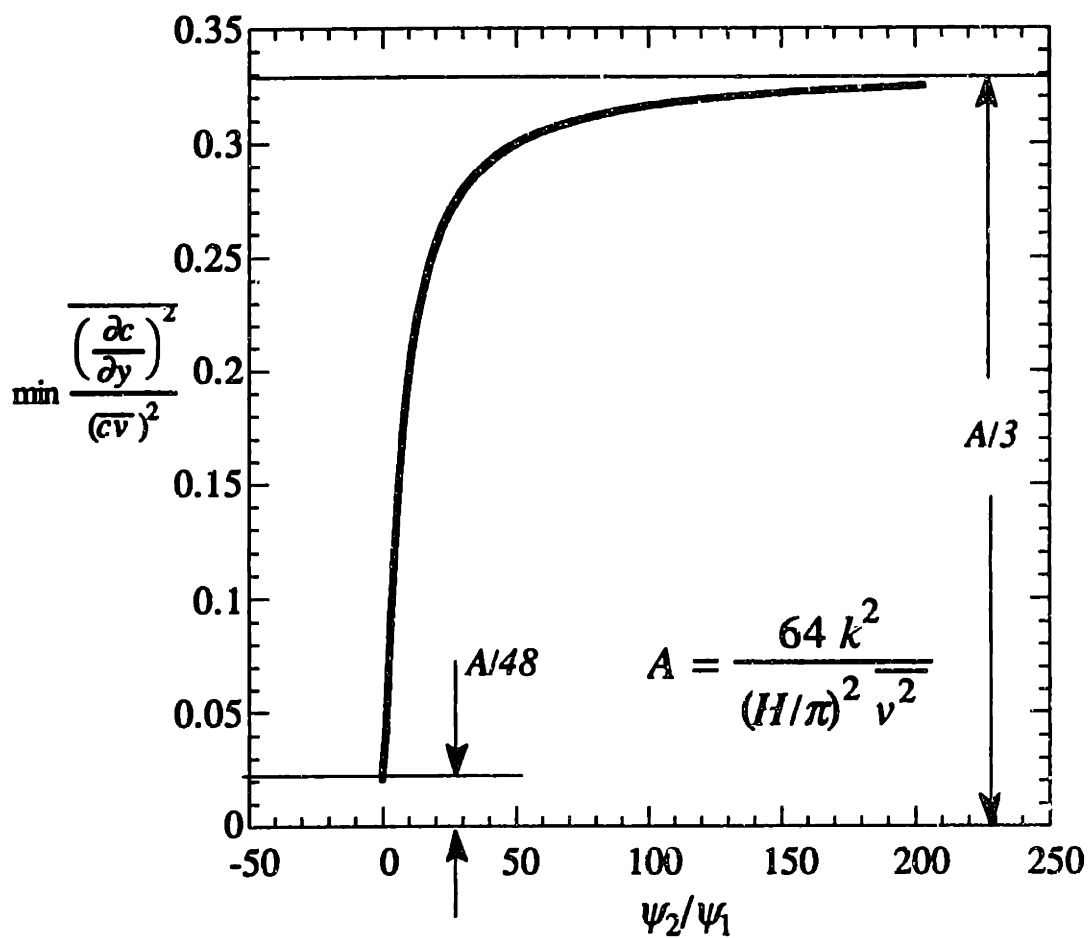


Figure A-II.2

High wave number sensitivity of fluctuation dissipation function.

A-II.4. SUMMARY

1. In dropping local dispersion while analyzing mean squared concentration fluctuations, at the very minimum, a first order decay term is dropped. For any positive local dispersion coefficient, such a dissipation term can be expected to result in dramatically decreased concentration fluctuations at large times, compared to the case in which the dissipating action of local dispersion is dropped altogether.

2. For a specified cross-sectional dispersive flux, the minimum dissipation function is proportional to the squared dispersive flux, with the constant of proportionality having a high wave number sensitivity. For a given mean squared longitudinal velocity fluctuations, the velocity function with a greater proportion of high wave number fluctuations, results in a greater minimum dissipation function.

3. As long as there is a non zero cross-sectional dispersive flux, the concentration profile cannot be completely homogenized along a cross-section.

APPENDIX-III

CROSS-SECTIONAL CONCENTRATION PROFILE IN RECTILINEAR DUCTS:

A VARIATIONAL CHARACTERISTIC OF G. I. TAYLOR'S SOLUTION

The cross-sectional concentration profile that minimizes the dissipation integral for a specified dispersive flux, in unidirectional flows inside a rectilinear duct, is shown to be the same as Taylor's [1953] solution.

A-III.1. MINIMUM DISSIPATION CROSS SECTIONAL CONCENTRATION PROFILE

The minimum of the dissipation integral

$$\int_0^H \left(\frac{dc}{dy} \right)^2 dy \quad (\text{A-III.1})$$

with respect to continuously differentiable functions $c(y)$ is sought. The extremizing function is subject to the constraint of a specified dispersive flux

$$\int_0^H c(y)v(y) dy = F \quad (\text{A-III.2})$$

and

$$\int_0^H c(y)dy = 0, \quad \frac{dc}{dy} \Big|_{y=0} = \frac{dc}{dy} \Big|_{y=H} = 0 \quad (\text{A-III.3})$$

The velocity $v(y)$ integrates to zero over the cross section, shown below in Figure A-III.1.

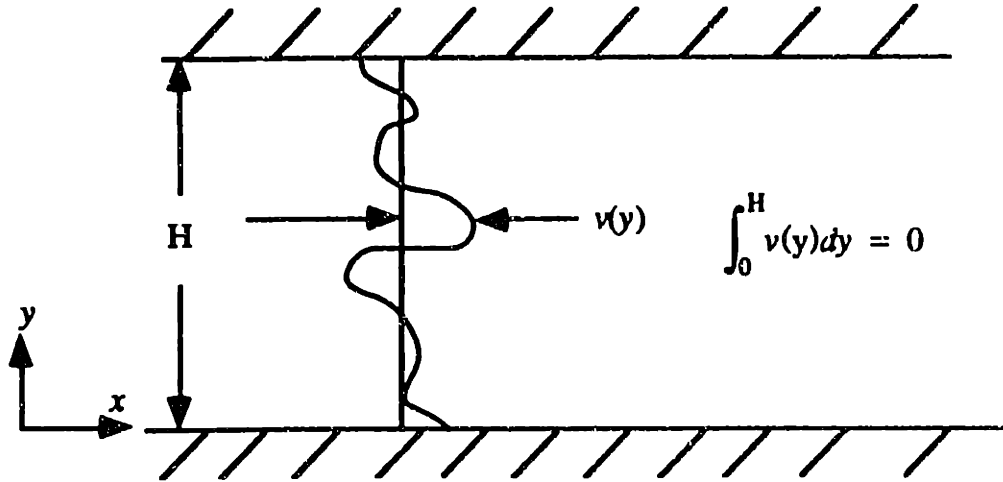


Figure A-III.1

Unidirectional flow in a rectilinear duct.

Defining $c' = dc/dy$, the Euler-Lagrange equation for this extremization is

$$\frac{\partial f}{\partial c} - \frac{d}{dy} \left(\frac{\partial f}{\partial c'} \right) = 0, \quad f = c'^2 + \lambda_1 c + \lambda_2 c v \quad (\text{A-III.4})$$

The undetermined multipliers λ_1 and λ_2 are to be found through the constraints (A-III.2) and (A-III.3). It follows from (A-III.4) that the extremizing function obeys

$$\lambda_1 + \lambda_2 v - 2c'' = 0 \quad (\text{A-III.5})$$

The solution of (A-III.5), subject to constraints (A-III.2) and (A-III.3), is

$$c(y) = F \frac{\left[\int_0^y dy_1 \int_0^{y_1} v(y_2) dy_2 - \frac{1}{H} \int_0^H dy \int_0^y dy_1 \int_0^{y_1} v(y_2) dy_2 \right]}{\int_0^H v(y) dy \int_0^y dy_1 \int_0^{y_1} v(y_2) dy_2} \quad (\text{A-III.6})$$

The dissipation integral (A-III.1), subject to (A-III.2) and (A-III.3), may be made unboundedly large. Therefore, (A-III.6) is the minimizing solution (and not the maximizing one).

A-III.2. TAYLOR'S CONCENTRATION PROFILE

Consider solute transport in the rectilinear duct in Figure A-III.1. The solute concentration C , in a coordinate system moving along with the mean drift, is governed by

$$\frac{\partial C}{\partial t} + v(y) \frac{\partial C}{\partial x} - D \left(\frac{\partial^2 C}{\partial x^2} + \frac{\partial^2 C}{\partial y^2} \right) = 0 \quad (\text{A-III.7})$$

In (A-III.7), $v(y)$ is a zero mean function, and D is the molecular diffusion coefficient. Solving a similar problem in a tube, Taylor [1953], for the large time condition $t \gg H^2/D$, drops the local rate of change and longitudinal diffusion terms

$$\frac{\partial C}{\partial t}, \quad \frac{\partial^2 C}{\partial x^2}$$

and replaces

$$\frac{\partial C}{\partial x} \quad \text{by} \quad \frac{\partial C}{\partial x}$$

where

$$\bar{C} = \frac{1}{H} \int_0^H C(x,y,t) dy, \quad c = C - \bar{C}$$

These approximations yield

$$v(y) \frac{\partial \bar{C}}{\partial x} - D \frac{\partial^2 c}{\partial y^2} = 0 \quad (\text{A-III.8})$$

Subject to the no flux boundary conditions, the solution to (A-III.8) is precisely the minimum dissipation concentration profile (A-III.6). Additionally, Taylor's analysis yields the cross-sectional dispersive flux

$$F \equiv \int_0^H c(y)v(y) dy = \frac{1}{D} \frac{\partial \bar{C}}{\partial x} \left[\int_0^H v(y) dy \int_0^y dy_1 \int_0^{y_1} v(y_2) dy_2 \right] \quad (\text{A-III.9})$$

A-III.3 MINIMUM DISSIPATION CROSS-SECTIONAL PROFILE IN A TUBE

Consider Taylor's [1953] specific problem of solute transport in a tube, where the Poiseuillian velocity deviations from the mean drift $u_0/2$ are

$$v(r) = \frac{u_0}{2} \left(1 - 2 \frac{r^2}{a^2} \right)$$

where a is the tube radius, and r is the distance from the center in a cross-section. The continuously differentiable function $c(r)$ (assuming the concentration to be independent of angular position) which minimizes the dissipation integral

$$\int_0^a \left(\frac{\partial c}{\partial r} \right)^2 r dr$$

subject to a specified dispersive flux

$$\int_0^a c v r dr = \frac{F}{2\pi}$$

and

$$\int_0^a c r dr = 0, \quad \frac{\partial c}{\partial r} \Big|_{r=0} = \frac{\partial c}{\partial r} \Big|_{r=a} = 0$$

is sought. The Euler-Lagrange equation

$$\lambda_1 r + \lambda_2 v r - \frac{d}{dr} \left(2r \frac{dc}{dr} \right) = 0$$

yields the minimum dissipation concentration profile

$$c(r) = \frac{24 F}{\pi a^2 u_0} \left[\frac{1}{3} - \left(\frac{r}{a} \right)^2 + \frac{1}{2} \left(\frac{r}{a} \right)^4 \right] \quad (\text{A-III.10})$$

The minimum dissipation profile (A-III.10), shown in Figure A-III.2, is the same as Taylor's [1953] solution (equations 20-23).

A-III.4 CONCLUSION

Taylor's [1953] solution for the cross-sectional concentration profile is the smoothest profile that can sustain a specified cross-sectional dispersive flux, *i.e.*, it

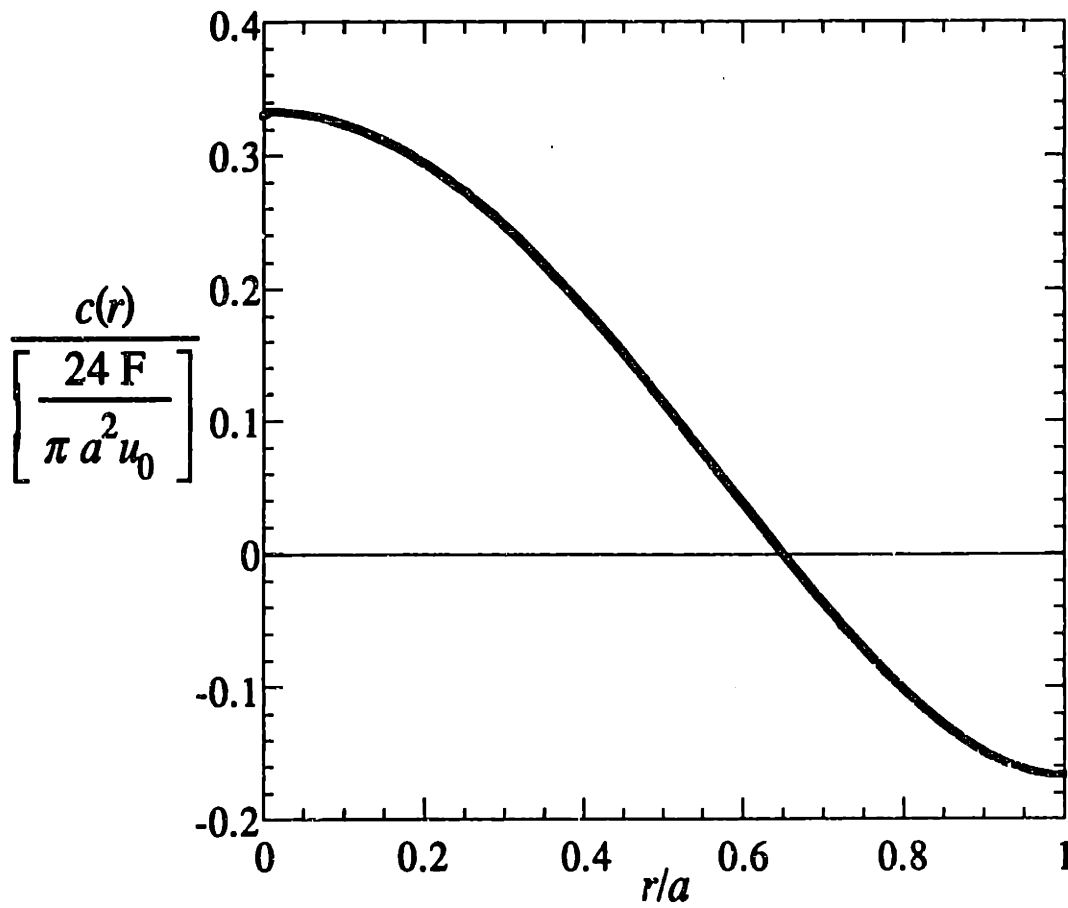


Figure A-III.2

Minimum dissipation cross-sectional concentration profile.

minimizes the cross-sectional integral of the squared transverse concentration derivatives (the dissipation integral), for a specified cross-sectional dispersive flux. Equivalently, Taylor's solution maximizes the cross-sectional dispersive flux for a given value of the dissipation integral.

APPENDIX-IV

STOCHASTIC DESCRIPTION OF THE HETEROGENEOUS HYDRAULIC CONDUCTIVITY AND VELOCITY CONTINUUM

If ϕ is the hydraulic head, conservation of fluid mass dictates

$$\frac{\partial^2 \phi}{\partial x_i^2} + \frac{\partial \ln [K(\mathbf{x})]}{\partial x_i} \cdot \frac{\partial \phi}{\partial x_i} = 0 \quad (\text{A-IV.1})$$

Decomposing $\ln K$ into its mean and perturbation

$$\ln [K(\mathbf{x})] = \ln [K_g] + f \quad (\text{A-IV.2})$$

where K_g , the exponential of the expected value of $\ln K$, is assumed to be a constant. The second order statistics of f , the $\ln K$ perturbation, are also assumed to be translation invariant. For the case of a unidirectional mean hydraulic gradient

$$J = - E \left[\frac{\partial \phi}{\partial x_1} \right]$$

the effective hydraulic conductivity $K_{eff} = \gamma K_g$, relates the mean velocity in the x_1 direction to the hydraulic gradient by $v = (K_{eff} J) / n$, n being the porosity of the medium. Gelhar & Axness [1983] give expressions for γ . For small values of the $\ln K$ standard deviation, the value of γ is slightly greater than one. The spectrum of the divergence free-three dimensional velocity perturbations is related to the $\ln K$ spectrum S_{ff} by

$$S_{v_i v_j}(k) = \frac{v^2}{\gamma^2} \left(\delta_{i1} - \frac{k_i k_1}{k^2} \right) \left(\delta_{j1} - \frac{k_j k_1}{k^2} \right) S_{ff}(k) \quad (\text{A-IV.3})$$

[Bakr *et al.*, 1978; Gelhar & Axness, 1983]

A-IV.1 $\ln K$ SPECTRUM FOR A HETEROGENEOUS POROUS CONTINUUM

The solution of the flow problem relies on a 'small perturbation' assumption on the coefficients in (A-IV.1), *i.e.*, the spatial partial derivatives of the $\ln K$ field. The continuum scale properties like hydraulic permeability and local dispersivities can only be effective on a finite local support. These facts make the exponential spectrum (that yields infinite spatial derivatives of $\ln K$) an unattractive description of a heterogeneous porous continuum. The exponential spectrum and Darcy's law result in a velocity field with infinite characteristic strain rates, *i.e.*, infinite principal strain rates and infinite vorticity! At high frequencies (contained in the exponential spectrum), momentum transfer in the fluid phase as embedded in the Darcy-Brinkman flow equation, provides an important smoothing mechanism, in highly nonuniform porous medium (discussed by Dagan [1979], and Nield and Bejan [1992]). In Chapter 4 is presented the velocity spectrum, incorporation the Darcy-Brinkman 'law'. For currently available datasets of $\ln K$, the exponential spectrum is a gross extrapolation on the high wave number end.

In evaluating the concentration microscale in Section 2.4, it is explicitly assumed that the $\ln K$ microscale is larger than the local dispersivities. A fundamental feature of fluctuation dissipation is the wave number squared dependence of the dissipation rate. To be able to vary the proportion of energies that appear at low wave numbers and high wave numbers in a relatively simple fashion, a spectrum is chosen with a high wave number cutoff. A Gaussian $\ln K$ correlation function that yields a finite $\ln K$ microscale could also

have been chosen, but the ratio of the $\ln K$ microscale to the correlation scale implied by it is a constant (about 1), hence the effect of varying this ratio on the fluctuation dissipation phenomenon can not be explored. Of course, for a site specific problem, a statistical characterization of the site specific spectrum will be needed.

A-IV.2 $\ln K$ SPECTRUM

$$S_{ff}(\mathbf{k}) = \begin{cases} \frac{\sigma_f^2}{4\pi \Gamma(r_m)} l_1 l_2 l_3 \frac{u^2}{(1+u^2)^3} & , u^2 \leq r_m^2 \\ 0 & , u^2 > r_m^2 \end{cases} \quad (\text{A-IV.4})$$

$$u^2 = k_1^2 l_1^2 + k_2^2 l_2^2 + k_3^2 l_3^2$$

$$\Gamma(r_m) = \int_0^{r_m} \frac{r^4}{(1+r^2)^3} dr = \frac{r_m}{4(1+r_m^2)^2} - \frac{5r_m}{8(1+r_m^2)} + \frac{3}{8} \tan^{-1}(r_m)$$

$$\sigma_f^2 \equiv E[f^2] = \int_{-\infty}^{+\infty} S_{ff}(\mathbf{k}) d\mathbf{k} \quad (\text{A-IV.5})$$

is the variance of $\ln K$. The variance of the derivatives of $\ln K$ fluctuations is given by

$$\frac{\sigma_f^2}{(\Delta f_i)^2} \equiv E \left[\left(\frac{\partial f}{\partial x_i} \right)^2 \right] = \int_{-\infty}^{+\infty} k_i^2 S_{ff}(\mathbf{k}) d\mathbf{k} \quad (\text{no sum on } i) \quad (\text{A-IV.6})$$

where Δf_i the 'microscale' of the $\ln K$ field in the i th direction represents the scale of fluctuations that characterizes the derivatives of the $\ln K$ field. r_m is a nondimensional high wave number cutoff. As r_m becomes larger, the low wave number energy in the spectrum decreases, high wave number energy increases, as shown in Figure A-IV.1a,b. The correlation lengths l_i determine the scale corresponding to the location of the peak of

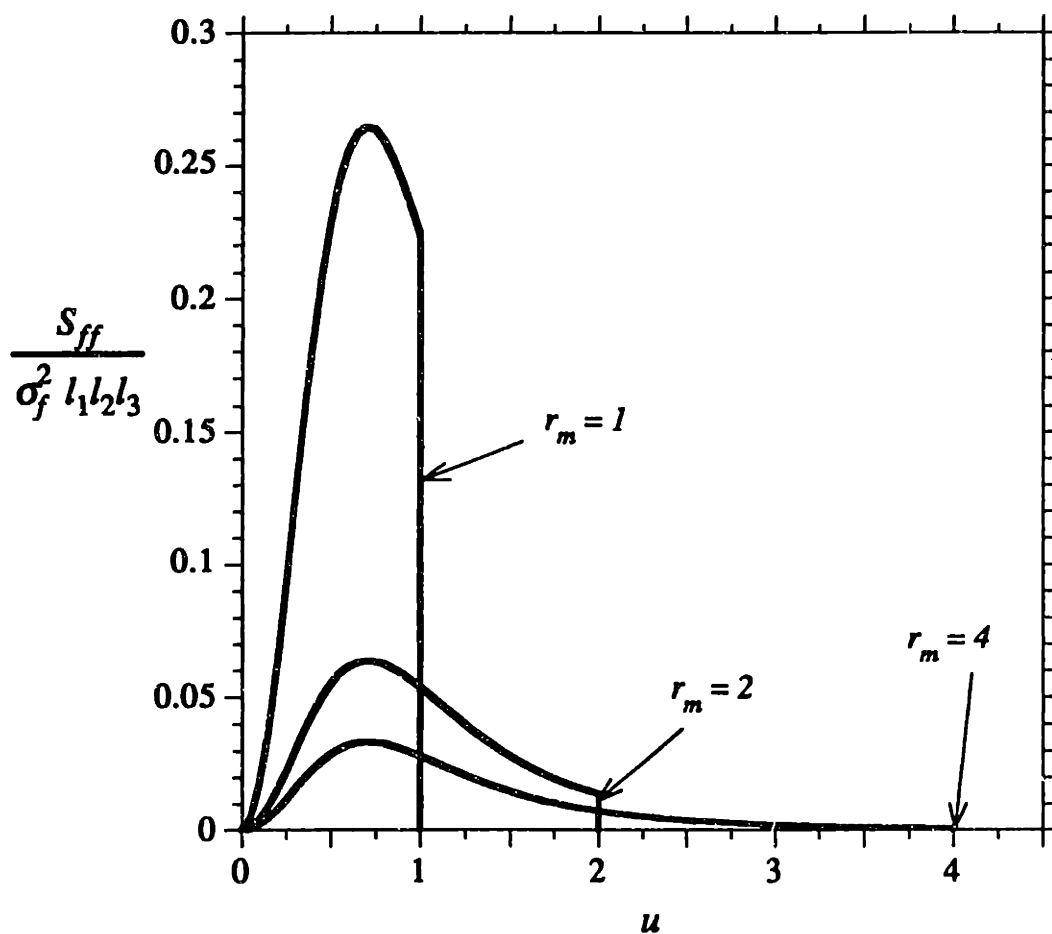


Figure A-IV.1a

Distribution of spectral energy over non-dimensional wave number.

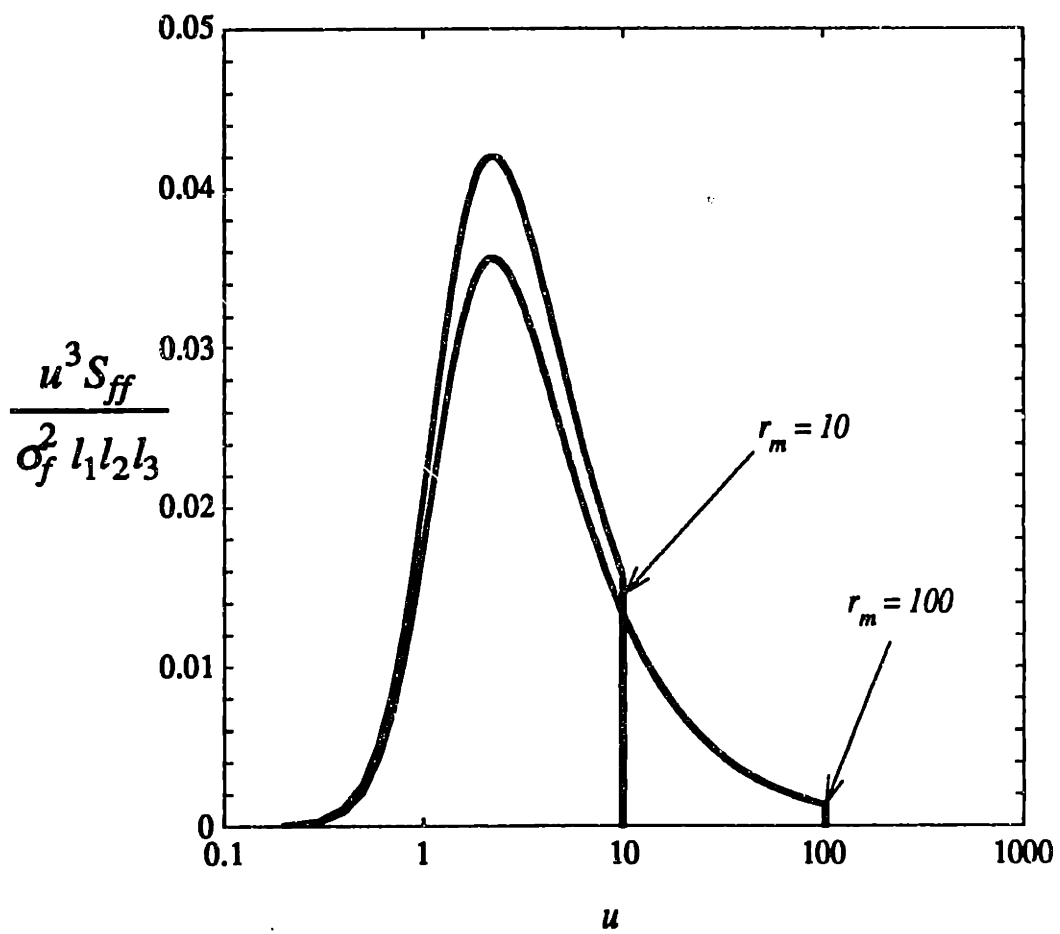


Figure A-IV.1b

Distribution of spectral energy over nondimensional wave number.

the spectrum (Figure A-IV.1a). The scale l_i/r_m is the smallest scale of fluctuations being entertained. It follows from equations (A-IV.4) and (A-IV.6) that r_m , Δf_i , and l_i are linked

$$\frac{\Delta f_i}{l_i} = \sqrt{3 \frac{\Gamma(r_m)}{\Omega(r_m)}} \quad (\text{no sum on } i) \quad (\text{A-IV.7})$$

$$\Omega(r_m) = \int_0^{r_m} \frac{r^6}{(1+r^2)^3} dr = r_m - \frac{r_m}{4(1+r_m^2)^2} + \frac{9r_m}{8(1+r_m^2)} - \frac{15}{8} \tan^{-1}(r_m)$$

(See Figure A-IV.3) For the value of $\Delta f_i/l_i$ to be .2, the cutoff corresponds to a scale that is about a hundredth of the correlation scale l_i .

A-IV.2 VELOCITY FIELD AND ITS CHARACTERISTIC PRINCIPAL STRAIN RATE

$$\sigma_{v_i}^2 \equiv E[v_i^2] = \int_{-\infty}^{+\infty} S_{v_i v_i}(\mathbf{k}) d\mathbf{k} \quad (\text{A-IV.8})$$

The squared characteristic velocity principal strain rate is

$$\frac{\sigma_{v_i}^2}{(\Delta f_i^{v_i})^2} \equiv E\left[\left(\frac{\partial v_i}{\partial x_i}\right)^2\right] = \int_{-\infty}^{+\infty} k_i^2 S_{v_i v_i}(\mathbf{k}) d\mathbf{k} \quad (\text{no sum on } i) \quad (\text{A-IV.9})$$

It follows from (A-IV.3), (A-IV.8) and (A-IV.9) that

$$\frac{\sigma_{v_i}}{v} = \frac{\mu_i}{\gamma} \quad (\text{A-IV.10})$$

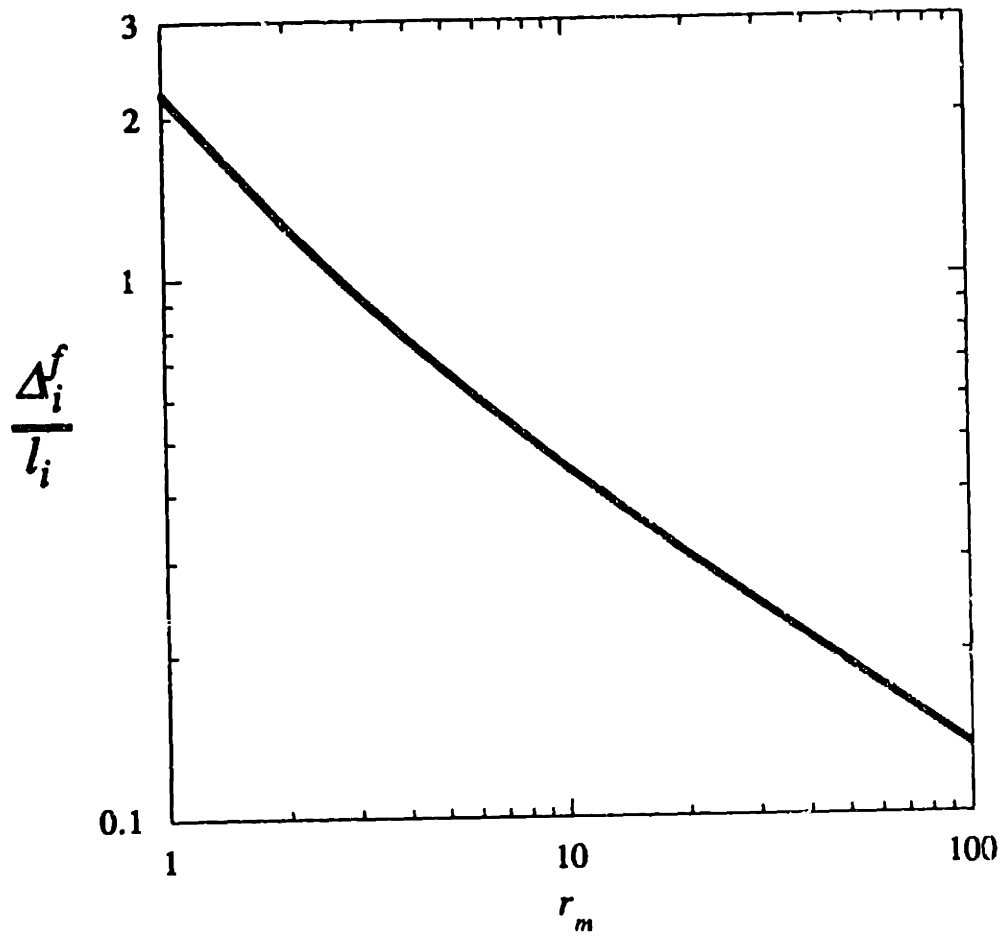


Figure A-IV.2

Ratio of $\ln K$ microscale and correlation scale.

$$\frac{\frac{\sigma_{v_i}}{\nu \Delta_i^{v_i}}}{\frac{\sigma_f}{\Delta_i^f}} = \frac{\beta_i}{\gamma} \quad (\text{A-IV.11})$$

where μ_i and β_i are constants. Unless the $\ln K$ microscale is known, nothing can be said about the characteristic strain rate of the velocity field (A-IV.11). Presuming the $\ln K$ microscale to be zero results in infinite accelerations in the flow field, which is a reflection of the breakdown of Darcy's 'law' in describing the flow field, as discussed in Chapter 4.

ISOTROPIC $\ln K$:

$$l_1 = l_2 = l_3 = l \quad \text{and} \quad \Delta_1^f = \Delta_2^f = \Delta_3^f = \Delta^f$$

Performing integration in spherical coordinates

$$\frac{\mu_1}{\gamma} = \sqrt{\frac{8}{15}}, \quad \frac{\mu_2}{\gamma} = \frac{\mu_3}{\gamma} = \sqrt{\frac{1}{15}} \quad (\text{A-IV.12})$$

$$\frac{\beta_1}{\gamma} = \sqrt{\frac{8}{35}}, \quad \frac{\beta_2}{\gamma} = \frac{\beta_3}{\gamma} = \sqrt{\frac{3}{35}} \quad (\text{A-IV.13})$$

LAYERED ANISOTROPIC $\ln K$:

$$l_1 = l_2 = l_h, \quad l_3 = l_v \quad \text{and} \quad \Delta_1^f = \Delta_2^f = \Delta_h^f, \quad \Delta_3^f = \Delta_v^f$$

$$\frac{l_h}{\Delta f_h} = \frac{l_v}{\Delta f_v}$$

The integration over the two angles in spherical coordinate is performed numerically to get velocity characteristics in Figures A-IV.3-4.

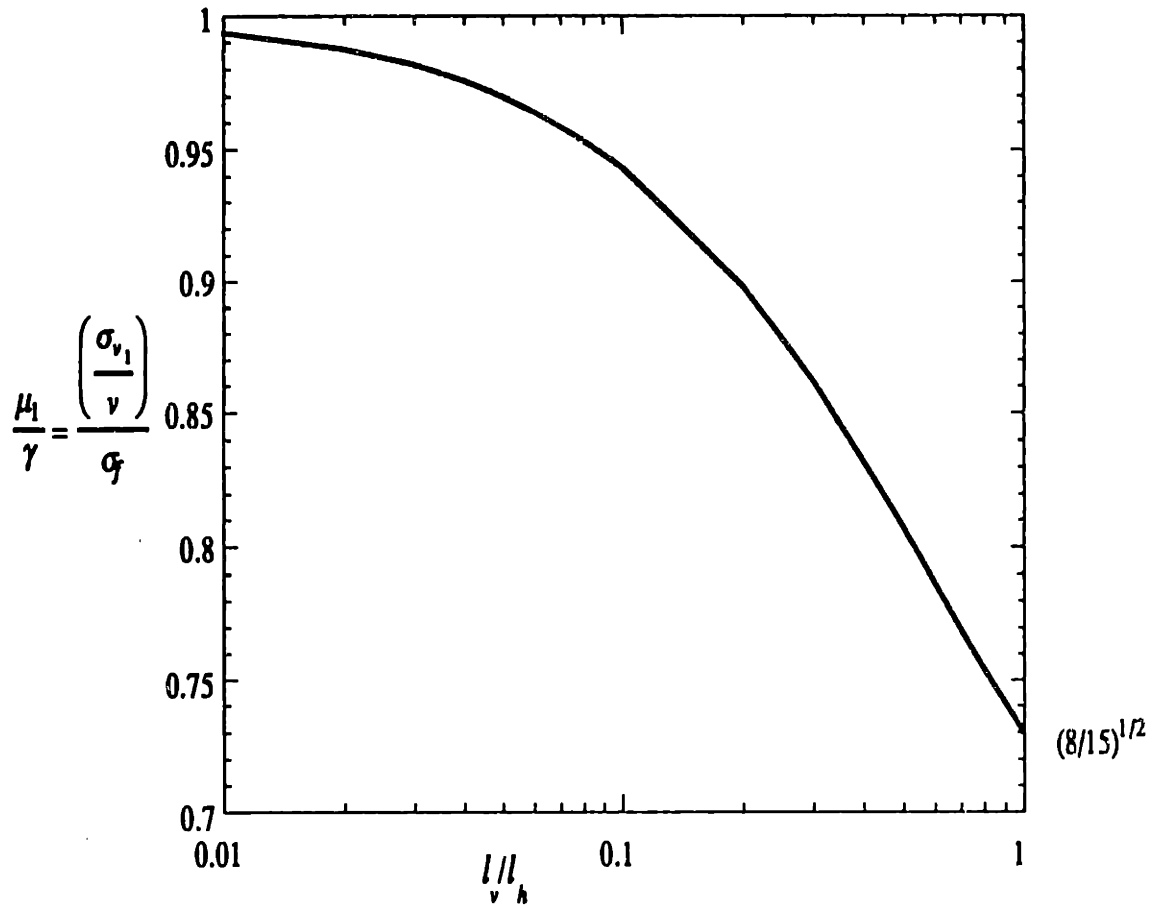


Figure A-IV.3a
Standard deviation of the velocity field.

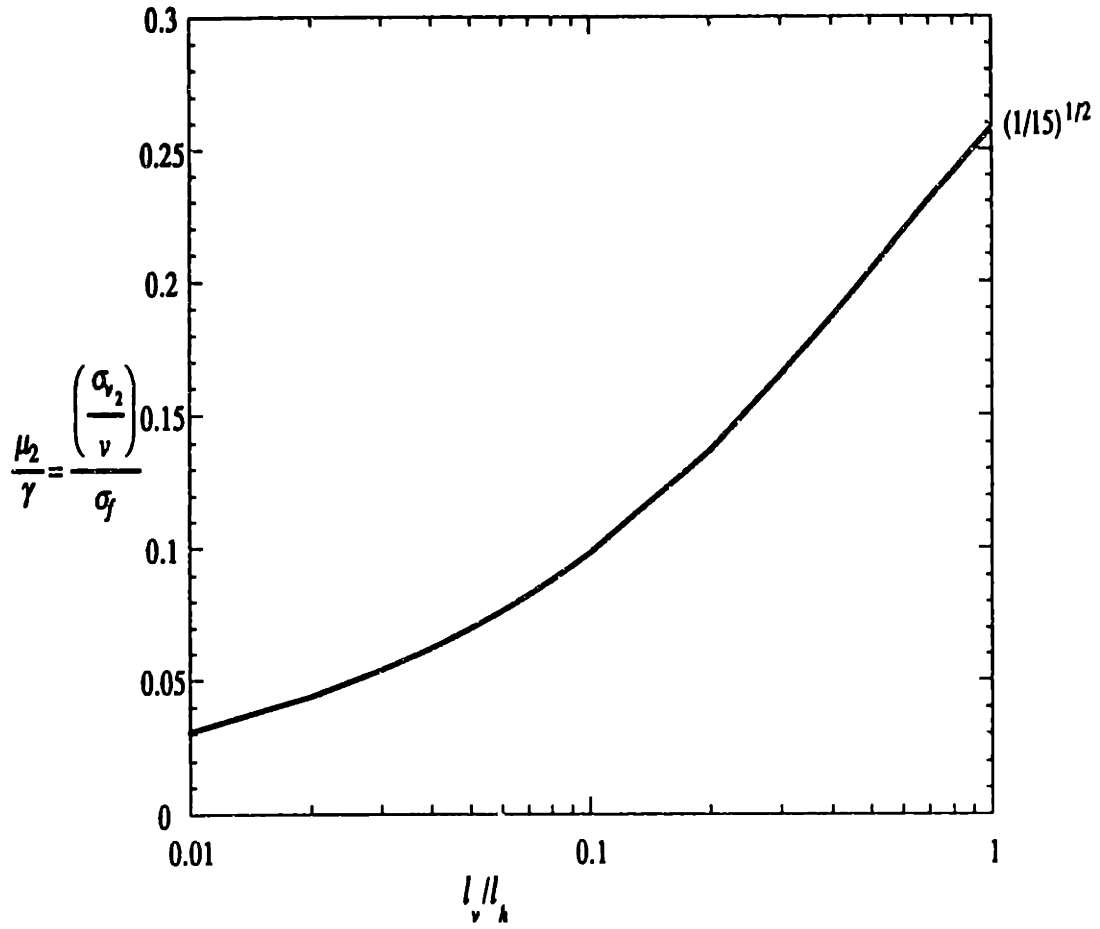


Figure A-IV.3b

Standard deviation of the velocity field.

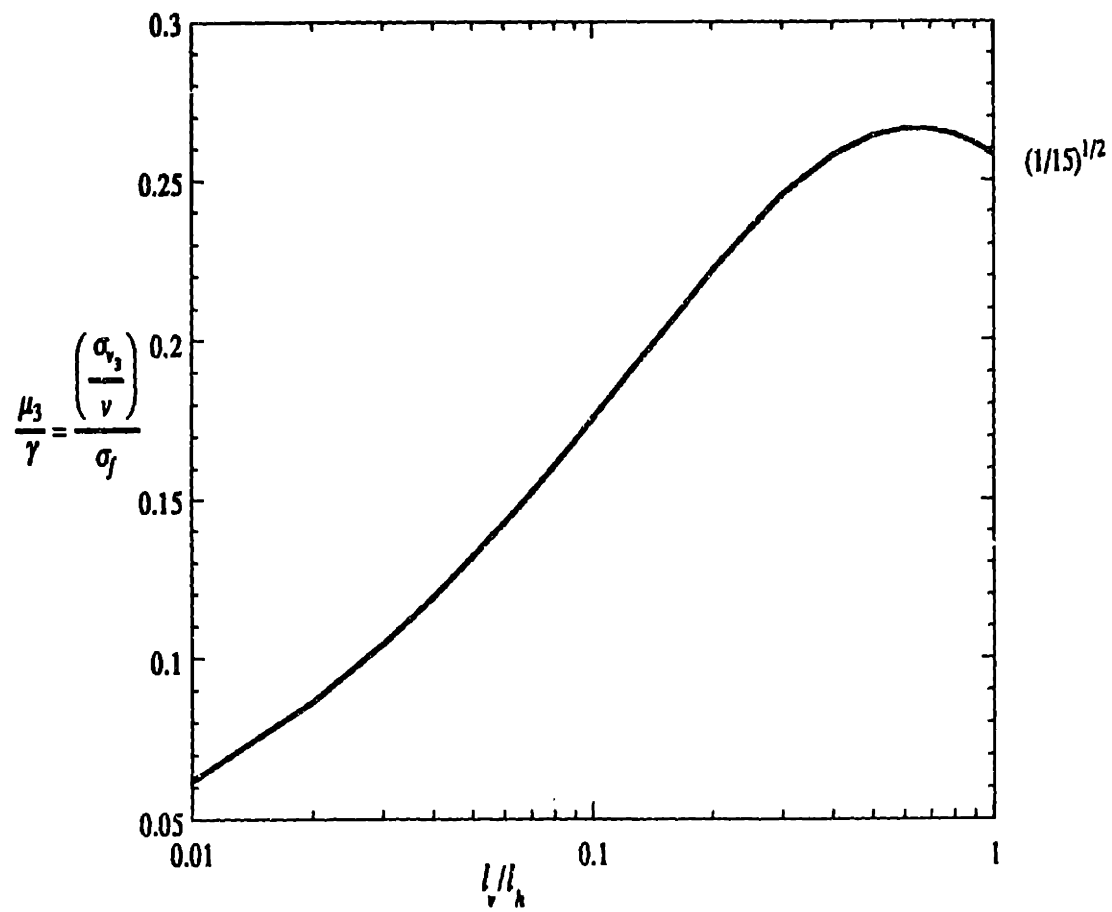


Figure A-IV.3c
Standard deviation of the velocity field.

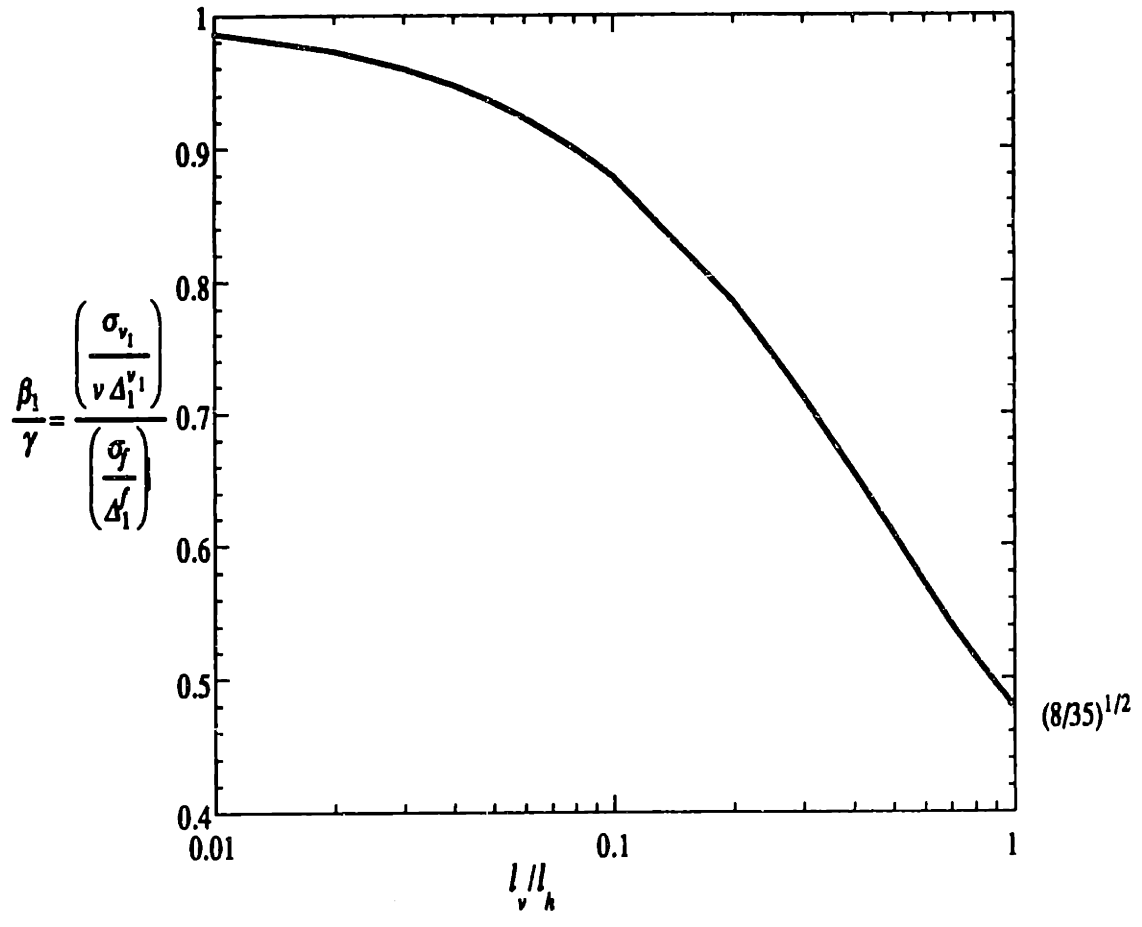


Figure A-IV.4a

Characteristic principal strain rate of velocity field.

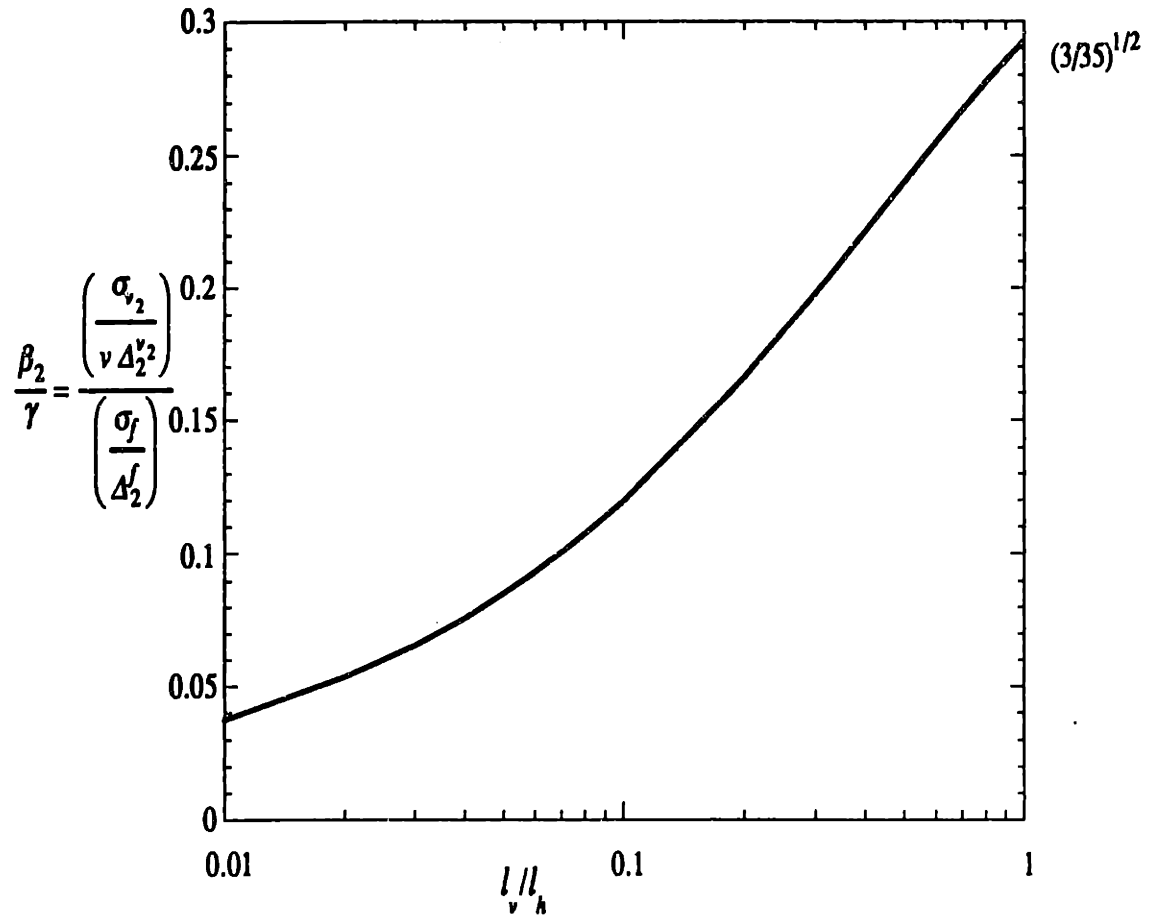


Figure A-IV.4b

Characteristic principal strain rate of velocity field.

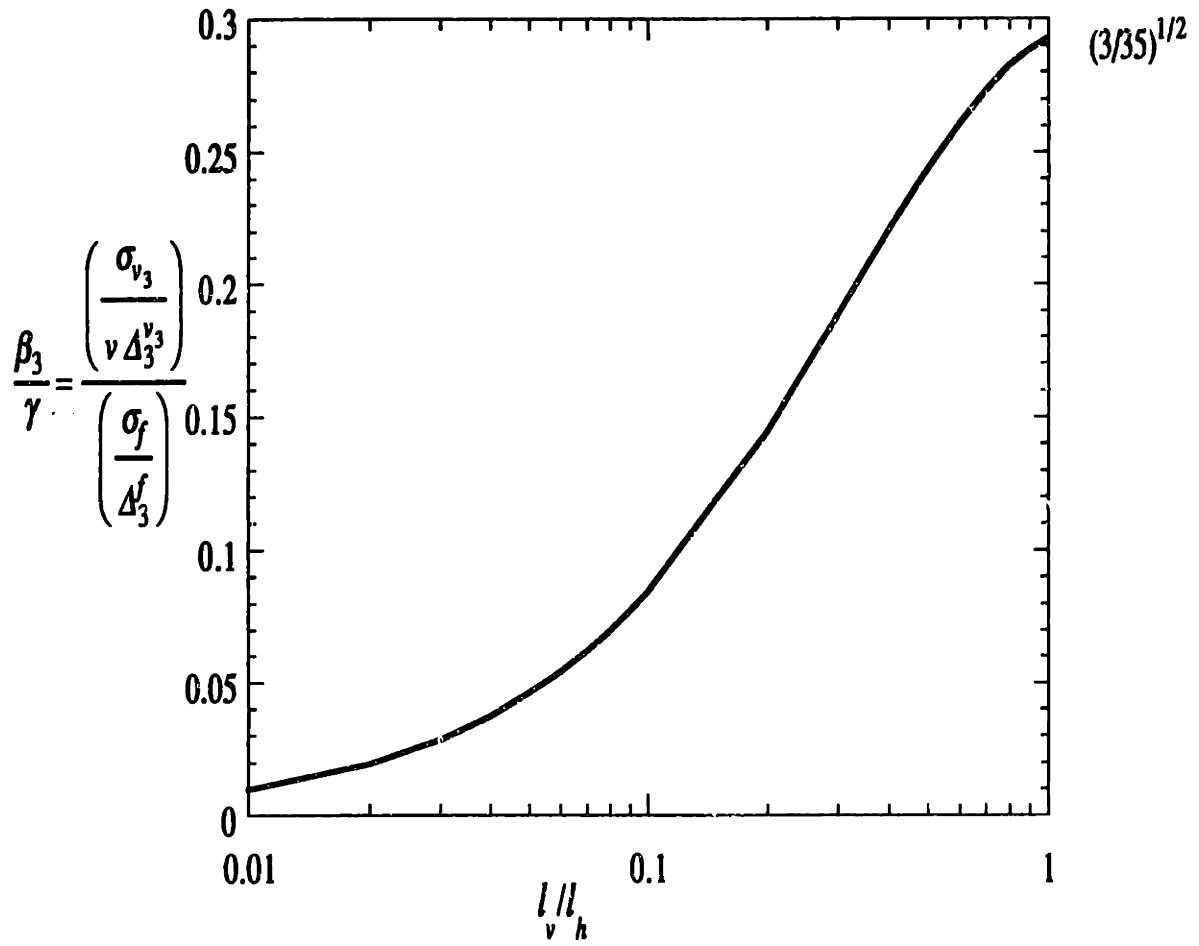


Figure A-IV.4c

Characteristic principal strain rate of velocity field.

APPENDIX-V

CHARACTERISTIC VORTICITY OF THE FLOW FIELD

The characteristic vorticity of the flow field in a three dimensionally heterogeneous aquifer with the $\ln K$ spectral description presented in Appendix-IV, is presented here for the isotropic case.

A-V.1 VORTICITY

The vorticity of the flow field is defined as

$$\omega = \nabla \times v$$

i.e.,

$$\omega = \left(\frac{\partial v_3}{\partial x_2} - \frac{\partial v_2}{\partial x_3} \right) i + \left(\frac{\partial v_1}{\partial x_3} - \frac{\partial v_3}{\partial x_1} \right) j + \left(\frac{\partial v_2}{\partial x_1} - \frac{\partial v_1}{\partial x_2} \right) k$$

From the spectral description of the velocity partial derivatives in Appendix-IV, we have the spectral description of the partial derivatives of the velocity field;

$$S \frac{\partial v_i}{\partial x_j} \frac{\partial v_l}{\partial x_j}(\mathbf{k}) = \frac{v^2}{\gamma^2} k_j^2 \left(\delta_{il} - \frac{k_i k_l}{k^2} \right)^2 S_{ff}(\mathbf{k})$$

A-V.1 RELATIONSHIP OF THE CHARACTERISTIC VORTICITY WITH THE HYDRAULIC CONDUCTIVITY

The mean squared components of the vorticity were computed for the isotropic case to get

$$\sigma_{\omega_i} = \sqrt{E[\omega_i^2]} = \frac{\nu}{\gamma} \frac{\sigma_f}{\Delta^f}, i=2,3$$

$$\sigma_{\omega_1} = 0$$

It can also be shown that any two distinct components of the vorticity are uncorrelated, *i.e.*,

$$E[\omega_i \omega_j] = 0, \quad 1 \leq i \neq j \leq 3$$

APPENDIX- VI

MACRODISPERSIVITY INTEGRALS FOR STATISTICALLY ISOTROPIC MEDIA WITH ANISOTROPIC LOCAL DISPERSIVITIES

The integral relating macrodispersivities to the hydraulic conductivity spectrum presented in Gelhar and Axness [1983] is evaluated for isotropic media with anisotropic local dispersivities. The exact evaluation of this integral enables an exploration of the sensitivity of macrodispersivities to κ , the ratio of the transverse to longitudinal local dispersivity. This evaluation also yields algebraic nonlinear expressions for the macrodispersivities incorporating Corrsin's [1962] conjecture, in Chapter 5.

A-VI.1 MACRODISPERSIVITY INTEGRALS

The macrodispersivity is given by

$$A_{ii} = \int_{-\infty}^{+\infty} \frac{(\delta_{i1} - k_1 k_i / k^2) [\alpha_L k_1^2 + \alpha_T (k_2^2 + k_3^2)] S_{ff}(\mathbf{k})}{\gamma^2 \{k_1^2 + [\alpha_L k_1^2 + \alpha_T (k_2^2 + k_3^2)]^2\}} d\mathbf{k} \quad (\text{A-VI.1})$$

$i = 1, 2, 3$ (Equation (29), Gelhar and Axness [1983]). For the exponential isotropic spectrum of $\ln K$

$$S_{ff}(\mathbf{k}) = \frac{\sigma_f^2 \lambda^3}{\pi^2 (1 + \lambda^2 k^2)^2}$$

Gelhar and Axness [1983] give

$$\gamma = 1 + \sigma_f^2 / 6$$

Substituting the spectrum into the macrodispersivity integral gives

$$\frac{A_{ii}}{\frac{\sigma_f^2 \lambda}{\gamma^2}} = \frac{1}{\pi^2} \int_{-\infty}^{+\infty} \frac{(\delta_{i1} - u_i u_1 / u^2)^2 [\epsilon_L u_1^2 + \epsilon_T (u_2^2 + u_3^2)]}{\{u_1^2 + [\epsilon_L u_1^2 + \epsilon_T (u_2^2 + u_3^2)]^2\} (1 + u^2)^2} du \quad (\text{A-VI.2})$$

where

$$\epsilon_L = \alpha_L / \lambda, \quad \epsilon_T = \alpha_T / \lambda$$

and

$$u_i = k_i / \lambda$$

are the nondimensionalized wave numbers.

A-VI.2 EVALUATION OF MACRODISPERSIVITY INTEGRALS

Making the transformation into spherical coordinates

$$u_1 = r \cos(\theta), \quad u_2 = r \sin(\theta) \cos(\phi), \quad u_3 = r \sin(\theta) \sin(\phi)$$

$$du = r^2 \sin(\theta) dr d\theta d\phi$$

the ϕ integral is trivially achieved. Using

$$\int_0^\infty \frac{r^2 dr}{(1 + p^2 r^2)(1 + r^2)^2} = \frac{\pi}{4(1 + p)^2}$$

the r integral is achieved. Substituting $t = \cos(\theta)$, the theta integration becomes

$$\frac{A_{11}}{\frac{\sigma_f^2 \lambda}{\gamma^2}} = \frac{1}{2} [\epsilon_T I_0 + (\epsilon_L - 3\epsilon_T) I_2 + (3\epsilon_T - 2\epsilon_L) I_4 + (\epsilon_L - \epsilon_T) I_6] \quad (\text{A-VI.3a})$$

and

$$\frac{A_{22}}{\frac{\sigma_f^2 \lambda}{\gamma^2}} = \frac{1}{4} [\epsilon_T I_2 + (\epsilon_L - 2\epsilon_T) I_4 + (\epsilon_T - \epsilon_L) I_6] \quad (\text{A-VI.3b})$$

where

$$I_n = \int_{-1}^{+1} \frac{t^n}{(at^2 + bt + c)^2} dt$$

$$a = \epsilon_L - \epsilon_T, b = 1, c = \epsilon_T$$

For $y = b^2 - 4ac > 0$ we have

$$\varpi = \frac{1}{\sqrt{y}} \left[\ln \left| \frac{2a + b - \sqrt{y}}{2a + b + \sqrt{y}} \right| - \ln \left| \frac{-2a + b - \sqrt{y}}{-2a + b + \sqrt{y}} \right| \right]$$

$$I_0 = \frac{1}{y} \left[\frac{b - 2a}{a - b + c} - \frac{b + 2a}{a + b + c} \right] - \frac{2a}{y} \varpi$$

$$I_1 = \frac{1}{y} \left[\frac{2c + b}{a + b + c} - \frac{2c - b}{a - b + c} \right] + \frac{b}{y} \varpi$$

$$I_2 = \frac{1}{ay} \left[\frac{bc - (b^2 - 2ac)}{a - b + c} - \frac{bc + (b^2 - 2ac)}{a + b + c} \right] - \frac{2c}{y} \varpi$$

$$I_3 = \frac{1}{2a^2} [\ln |a + b + c| - \ln |a - b + c|] - \frac{b}{2a^2} \varpi - \frac{c}{a} I_1 - \frac{b}{a} I_2$$

$$I_4 = \frac{1}{a} \left[\frac{1}{a+b+c} + \frac{1}{a-b+c} \right] - \frac{3c}{a} I_2 - \frac{2b}{a} I_3$$

$$I_5 = \frac{1}{2a} \left[\frac{1}{a+b+c} - \frac{1}{a-b+c} \right] - \frac{2c}{a} I_3 - \frac{3b}{2a} I_4$$

$$I_6 = \frac{1}{3a} \left[\frac{1}{a+b+c} + \frac{1}{a-b+c} \right] - \frac{5c}{3a} I_4 - \frac{4b}{3a} I_5$$

The macrodispersivity integral (A-VI.1) has therefore been exactly analytically evaluated for anisotropic local dispersivities. The isotropic local dispersion version of this is presented in Gelhar and Axness [1983], Equation (38a,b). Figure A-VI.1 and A-VI.2 presents the computed macrodispersivities. The longitudinal macrodispersivity is a decreasing function of the ratio of κ , the transverse to longitudinal local dispersivity. For realistic values of the ratio of longitudinal to dispersivity to correlation scale, the transverse macrodispersivity is an increasing function of the ratio of the transverse to longitudinal local dispersivity. In the figures, the case $\kappa = 1.0$ corresponds to Gelhar and Axness [1983], Equation (38a,b).

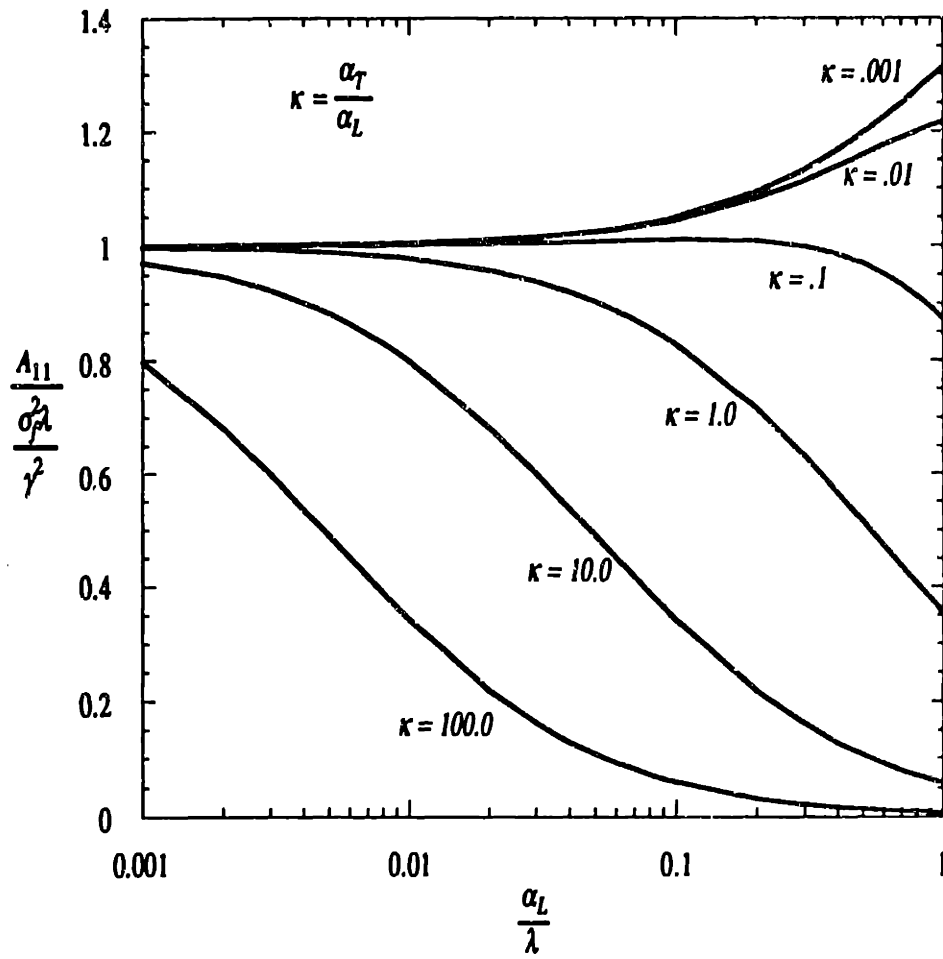


Figure A-VI.1
 Longitudinal macrodispersivity.

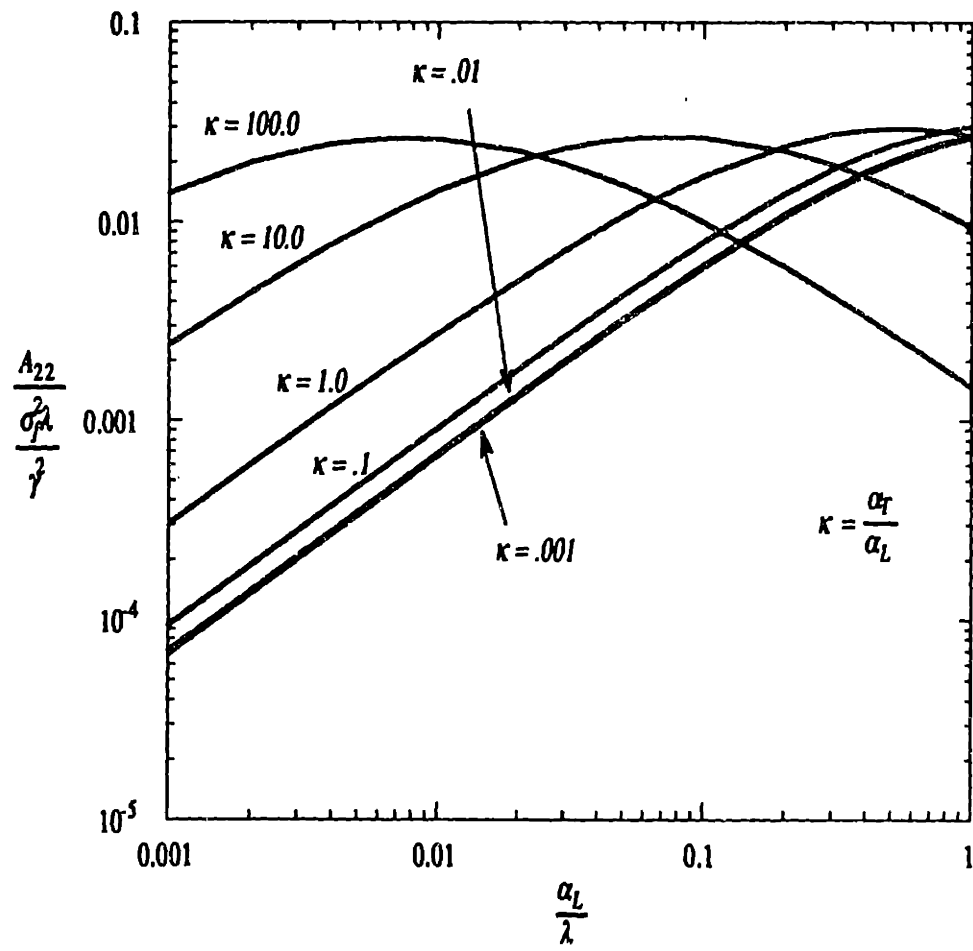


Figure A-VI.2
 Transverse macrodispersivity.